IMPROVEMENT OF THE QUALITY OF RECYCLED FINE AGGREGATES BY MICROBIAL INDUCED CALCIUM CARBONATE PRECIPITATION

GERİ DÖNÜŞTÜRÜLMÜŞ İNCE AGREGALARIN ÖZELLİKLERİNİN MİKROBİYAL KALSİYUM KARBONAT ÇÖKELMESİ İLE İYİLEŞTİRİLMESİ

EKİN ARIKAN

ASSOC. PROF. DR. YUSUF ÇAĞATAY ERŞAN

Supervisor

Submitted to

Graduate School of Science and Engineering of Hacettepe University as a Partial Fulfillment to the Requirements for the Award of the Degree of Master of Science in Environmental Engineering

2024

To my beloved family …

ABSTRACT

IMPROVEMENT OF THE QUALITY OF RECYCLED FINE AGGREGATES BY MICROBIAL INDUCED CALCIUM CARBONATE PRECIPITATION

Ekin ARIKAN

Master of Science, Department of Environmental Engineering

Supervisor: Assoc. Prof. Dr. Yusuf Çağatay ERŞAN

June 2024, 133 pages

The limited availability of natural resources, combined with the expanding construction industry and the resulting construction and demolition waste (CDW), has become a major global concern, and has led to the search for sustainable approaches in the construction industry. In recent years, research on green construction practices has gained substantial momentum and among the most popular of these researches is the enhancement of the quality of recycled aggregates from CDW for use in new concrete production. Microbial induced calcium carbonate precipitation method (MICP) has been investigated by researchers as a biobased approach to improve the surface properties of recycled coarse aggregates. However, studies on the improvement of recycled fine aggregates are scarce. Considering the significant fraction of recycled aggregates consists of fine aggregates, it is necessary to develop approaches for improvement of recycled fine aggregates facilitating their integration into the circular economy.

The thesis study aimed to improve the properties of recycled fine concrete aggregates (fRCA) through MICP, incorporating both urea hydrolysis and nitrate reduction metabolic pathways. The effects of the MICP treatment on surface and mechanical properties of fRCA were investigated by utilizing two different types of fRCA.

Following the application of MICP to six different size fractions of fRCA, a decrease in water absorption across all aggregates sizes was observed, accompanied by an increase in weight. The MICP method was further optimized for the enhancement of fRCA sand mixes. In this method, bacterial activity was confirmed by urea hydrolysis. Bacteria could hydrolyse 20 g of the urea in the biomineralization media demonstrating the 82% urea hydrolysis efficiency. The method resulted in precipitation of deposition of $CaCO_3$ on aggregates' surface, which was quantified as 4.6% weight increase in the MICP-treated fRCA sand mix. Same optimized treatment led to 3.8% weight increase in commercially available fRCA sand mix. In this setup, the bacterial activity was confirmed by 39% nitrate reduction and 88% urea hydrolysis.

Finally, the study achieved significant improvements in the mechanical properties of mortar specimens with MICP applied fRCA. The 28-day compressive strength and flexural strength of mortar specimens with MICP treated fRCA increased by up to 95% and 75%, respectively, compared to mortar containing untreated fRCA. It was supported by SEM, EDX and FTIR analyzes that the increase in the strength quality of the mortars was due to microbial $CaCO_3$ precipitates.

Keywords: recycled fine concrete aggregates (fRCA); biomineralization; urea hydrolysis; nitrate reduction; green concrete; circular economy.

ÖZET

GERİ DÖNÜŞTÜRÜLMÜŞ İNCE AGREGALARIN ÖZELLİKLERİNİN MİKROBİYAL KALSİYUM KARBONAT ÇÖKELMESİ İLE İYİLEŞTİRİLMESİ

Ekin ARIKAN

Yüksek Lisans, Çevre Mühendisliği Bölümü

Tez Danışmanı: Doç. Dr. Yusuf Çağatay Erşan

Haziran 2024, 133 sayfa

Doğal kaynakların sınırlı mevcudiyeti, büyüyen inşaat sektörü ve oluşan inşaat ve yıkıntı atıklarıyla birlikte önemli bir küresel endişe haline gelmektedir ve bu durum inşaat sektöründe sürdürülebilir yaklaşımların araştırılmasına yol açmıştır. Son yıllarda yeşil inşaat uygulamalarına yönelik araştırmalar önemli bir ivme kazanmıştır ve bu araştırmalar arasında en popüler olanı inşaat ve yıkıntı atıklarından elde edilen geri dönüştürülmüş agregaların kalitesinin iyileştirilerek yeniden beton üretiminde kullanılmasıdır. Mikrobiyal kalsiyum karbonat çökelmesi yöntemi (MICP), araştırmacılar tarafından geri dönüştürülmüş iri agregaların yüzey özelliklerini iyileştirmek için biyobazlı bir yaklaşım olarak araştırılmıştır. Ancak geri dönüştürülmüş ince agregaların iyileştirilmesine yönelik yapılan çalışmalar oldukça azdır. Geri dönüştürülmüş agregaların önemli bir kısmının ince agregalardan oluştuğu göz önüne alındığında, geri dönüştürülmüş ince agregaların döngüsel ekonomiye entegrasyonunu kolaylaştıracak iyileştirme yaklaşımlarının geliştirilmesi gerekmektedir.

Tez çalışmasında geri dönüştürülmüş ince beton agregaların (GDİBA) özelliklerinin hem üre hidrolizi hem de nitrat indirgemesi metabolik yollarını içeren mikrobiyal kaynaklı kalsiyum karbonat çökelmesi ile iyileştirilmesi amaçlanmıştır. İki farklı tipte GDİBA

kullanılarak MICP işleminin GDİBA'nın yüzey ve mekanik özelliklerine etkisi araştırılmıştır.

Altı farklı boyut fraksiyonundaki GDİBA'lara MICP uygulanmasının ardından, tüm agrega boyutlarında ağırlık artışıyla birlikte su emmelerinde azalma gözlemlenmiştir. MICP yöntemi, sonrasında, GDİBA kum karışımlarının geliştirilmesi için optimize edilmiştir. Bu yöntemde bakteriyel aktivite üre hidrolizi ile doğrulanmıştır. Bakteriler, biyomineralizasyon solüsyonundaki 20 g üreyi hidrolize edebilerek %82 üre hidroliz verimliliği göstermiştir. Yöntem, agregaların yüzeyinde $CaCO_3$ çökelmesiyle sonuçlanmıştır ve MICP ile iyileştirilmiş GDİBA kum karışımında %4,6 ağırlık artışı elde edilmiştir. Aynı optimize MICP yöntemi ile ticari olarak temin edilebilen GDİBA kum karışımında %3,8 ağırlık artışı elde edilmiştir. Bu deneyle bakteriyel aktivite, %39 nitrat indirgenmesi ve %88 üre hidrolizi ile doğrulanmıştır.

Son olarak, çalışmada MICP uygulanmış GDİBA içeren harç numunelerinin mekanik özelliklerinde önemli iyileşme elde edilmiştir. MICP ile iyileşmiş GDİBA'lı harç numunelerinin 28 günlük basınç ve eğilme dayanımlarında, iyileşmemiş GDİBA içeren harç numunelerine kıyasla sırasıyla %95 ve %75'e kadar artış elde edilmiştir. Harçların mukavemet kalitesindeki artışın mikrobiyal $CaCO_3$ çökeltilerinden kaynaklandığı SEM, EDX ve FTIR analizleri ile gösterilmiştir.

Anahtar Kelimeler: geri dönüştürülmüş ince beton agregası (GDİBA); biyomineralizasyon; üre hidrolizi; nitrat indirgeme; yeşil beton; döngüsel ekonomi

ACKNOWLEDGEMENT

There are many people I would like to thank within the scope of this thesis, but first and foremost, I would like to express my sincere gratitude to my supervisor Assoc. Prof. Dr. Yusuf Çağatay Erşan for his guidance, patience, motivation and endless support along with his vast knowledge throughout my thesis.

This thesis study was supported by the Scientific and Technological Research Council of Turkiye under grant number 120Y291 and by Hacettepe University Scientific Research Projects Coordination Unit under project number FHD-2022-20394.

I would like to thank my committee members Assoc. Prof. Dr. Halil İbrahim Fedakar, Assoc. Prof. Dr. İlknur Durukan Temuge, Asst. Prof. Dr. Derya Deniz Genç Tokgöz and Asst. Prof. Dr. Rıza Görkem Oskay for their comments and contributions.

I would like to thank professors at Hacettepe Mining Engineering Department and Mustafa Yılmaz for providing me with the opportunity to work in the Hacettepe Mineral Processing Mine laboratory, which I use frequently sieving of recycled aggregates.

I would like to express my thanks to Prof. Dr. Sinan T. Erdoğan for granting me the opportunity to cast in the METU Building Materials Laboratory, and to Cuma Yıldırım and Gülşah Bilici for their invaluable assistance during the mortar casting process.

Special thanks to Ayten Çaputçu for her assistance in procuring the commercial recycled aggregates used in my thesis.

Additionally, I would like to thank Prof. Dr. Ali İhsan Karayiğit and Asst. Prof. Dr. Rıza Görkem Oskay from the Hacettepe Geological Engineering Department for their support in providing me with the opportunity to use their laboratories whenever needed. I would also like to thank Merve Sönmez for her help during my analyzes at Hacettepe Construction Laboratory and our professors for allowing us to use the laboratory.

Lastly, I would like to express my deepest appreciation to my family and friends for their unwavering support, patience, and understanding throughout this process. I would especially like to express my endless love and gratitude to my mother, father and brother for always supporting me and making me feel their love.

TABLE OF CONTENTS

LIST OF FIGURES

LIST OF TABLES

ABBREVIATIONS

CDRA	Construction and demolition recycled aggregates
CDW	Construction and demolition waste
$CDW.L^{-1}$	Cell dry weight per liter
COD	Chemical oxygen demand
cRA	Recycled coarse aggregates
cRCA	Recycled coarse concrete aggregates
c-fRCA	Commercially available recycled fine concrete aggregates
cfRAM	Mortar specimen containing c-fRCA sand mixes instead of standard sand
DO	Dissolved oxygen
EDX	Energy dispersive X-ray
fRA	Recycled fine aggregates
fRCA	Recycled fine concrete aggregates
f-RCA	Recycled fine concrete aggregates obtained freshly crushed concrete
fRAM	Mortar specimen containing f-RCA sand mixes instead of standard sand
FTIR	Fourier transform infrared spectroscopy
GHGs	Greenhouse gases
ITZ	Interfacial transition zone
MICP	Microbial induced calcium carbonate precipitation
MRA	Mixed recycled aggregates
NA	Natural aggregates
NAC	Natural aggregates concrete

NAM	Mortar specimen containing standard sand
PM2.5	Particulate matter have a diameter of less than 2.5 micrometers
RA	Recycled aggregates
RCA	Recycled concrete aggregates
RMA	Recycled masonry aggregates
SBR	Sequential batch reactor
SEM	Scanning electron microscope
TAN	Total ammonia nitrogen
THBB	Turkish Ready Mixed Concrete Association
w/c	Water to cement ratio

1. INTRODUCTION

Concrete has become one of the most extensively used building materials, particularly with the rise of industrialization and urbanization. Natural aggregates (NA) serve as the primary raw material in concrete production, and approximately 40 billion tons of NA are consumed annually [1]. This substantial consumption leads to the depletion of NA, which are non-renewable resources.

The depletion of natural resources has become a significant global problem, affecting many regions worldwide, particularly where the construction sector is rapidly developing and consuming resources excessively [2]. Istanbul is one such place experiencing this issue [3]. Istanbul's construction industry is vital to its economic growth, but the high demand for construction materials, especially aggregates, puts immense pressure on local resources. The city faces limited resources and inefficient aggregate production, which are anticipated to cause major problems in aggregate supply in the future [3]. Additionally, unregulated urbanization poses another significant challenge. As the city expands, aggregate mining activities are restricted, limiting the availability of accessible resources [3]. Therefore, the problems and restrictions in NA production, coupled with the city's increasing needs, are a matter of significant concern.

On the other side, the high demand for NA poses significant environmental concerns. The extraction of these materials often results in habitat destruction, noise pollution, air pollution, water pollution, increased energy consumption, and increased carbon emissions [4]. The extraction, processing, transportation and use of NA account for approximately 7% of total global energy consumption [5]. Air pollution from mining, primarily from dust and CO_2 emissions, contributes to respiratory problems and other health issues in humans, as well as broader atmospheric changes linked to climate change [4–6]. Additionally, aggregates mining can have adverse effects on ecosystems and alter hydrogeological and hydrological systems [4–6]. Given these significant environmental impacts, it is crucial to develop and implement sustainable practices in the extraction and use of NA. Moreover, it is essential to find out environment-friendly alternatives to replace NA in construction sector.

Another serious environmental problem arising from the construction industry is construction and demolition waste (CDW). The CDW has a highest waste stream which

accounts for approximately 30-40% of global waste [7]. The most commonly employed CDW management strategy in Turkey and globally is the disposal of waste in landfills [8]. However, this approach is not sustainable due to the limited availability of landfill space and its adverse environmental impacts [9]. Innovative waste reduction, recycling and reuse strategies are needed instead of traditional landfill use to solve the CDW problem.

Considering the NA shortage, the environmental problems caused by aggregate mining, and the CDW issue, the necessity for a sustainable approach in the construction industry becomes evident. In this context, it is critical to adopt the circular economy model over the linear economy model in the construction sector. The circular economy model emphasizes reducing waste through reuse and recycling and minimizing the use of natural resources by identifying alternative materials [7]. This model fosters a green and sustainable construction industry. Green construction practices have started to be embraced in many countries worldwide, particularly in Europe [1]. Numerous studies are being conducted on the recycling and reuse of CDW as construction materials [1]. Among these studies, green concrete applications are the most prevalent [1]. The green concrete principle is based on replacing at least one of the component in traditional concrete with waste material, making the concrete less harmful to the environment and more sustainable [10]. One of the innovative approaches focus on replacing NA with recycled aggregates (RA) obtained from CDW in concrete production [5]. RA usage as a source for new raw materials in concrete production, can be significantly reduce the dependence of the concrete industry on non-renewable natural resources. This not only conserves natural resources but also mitigates the environmental problems associated with storing CDW. Therefore, green concrete applications can significantly reduce the environmental footprint of the construction industry.

Since RA have weaker properties than NA, they require improvement before being used in concrete [11]. In recent years, researchers have focused on techniques to improve the properties of RA [12]. Common improvement techniques of RA are classified into two categories: removing the mortar adhering to the RA surface and increasing the strength of the mortar adhering to the RA surface [12]. Methods used to remove old mortar generally include heat treatment, mechanical grinding and acid washing [12]. On the other hand, methods such as carbonation, polymer impregnation and nano-material treatment are employed to enhance the strength of the old adhered mortar layer on the RA surface

[13,14]. These related methods face various challenges, such as high energy consumption, long processing times, environmental pollution, inefficiency, and difficulty in practical application [12,14]. These issues have driven the search for new technologies for RA improvement. In this context, microbial induced calcium carbonate precipitation (MICP) technology stands out as an effective and environmentally friendly method for treating RA. The MICP method is biobased and involves the precipitation of calcium carbonate within the pores and on the surface of aggregates as a result of the metabolic activities of bacteria [12]. With its environmental friendliness, low energy consumption and effective improving mechanism, MICP has become a very popular application for RA treatment in recent years [15,16]. This innovative biobased approach makes it possible to introduce RA to the construction industry and economy as secondary raw materials.

Promising positive results have been obtained in studies on RA treatment with MICP in Europe and around the world to date. It has been reported that improvements were achieved in the physical, mechanical, and microstructural properties of RA treated with MICP [15–17]. However, the number of studies on the treatment of RA with biobased methods is still limited. Moreover, most of these studies focus on the treatment of recycled coarse aggregates (cRA) with MICP, with rare research on the improvement of recycled fine aggregates (fRA) using MICP method [15–18]. The effects of the MICP method on fRA and mortar samples have not yet been adequately addressed. Therefore, more studies are needed to investigate the improvement of fRA with MICP technology. Additionally, using non-axenic culture formed by microorganisms with different metabolisms instead of pure culture (axenic culture) during the treatment process may offer advantages in the MICP process. Hence, this study investigated the improvement of the recycled fine concrete aggregates (fRCA) with MICP, a method with a low energy consumption and environmental friendliness, using non-axenic cultures capable of urea hydrolysis and nitrate reduction. The changes formed by MICP in fRCA were examined through surface properties and mortar specimens.

2. LITERATURE REVIEW

2.1. Use of Natural Aggregates in Construction Industry

Natural aggregates (NA), heralded as the world's most valuable non-fuel mineral product, constitute the fundamental raw material of the construction industry [19]. They encompass crushed stone and sand, derived from crushing bedrock or naturally occurring unconsolidated sand and gravel [19]. NA are extensively utilized as components in concrete across diverse built environment and constituting approximately 60-75% of concrete volume [11]. This substantial volume used in concrete results in colossal annual consumption of around 40 billion tons of NA globally [1]. The utilization of aggregates in concrete is based on several foundational reasons. Primarily, aggregates are economically advantages compared to cement, leading to volume expansion in concrete mixtures upon addition of aggregates and consequent cost reductions. Moreover, aggregates incorporation enhances volume stability by mitigating shrinkage and creep in concrete mixture. Additionally, as many deterioration processes primarily affect the cement paste, integrating NA enhances concrete durability, enhancing resistance against loads, moisture, abrasion, and weathering effects [20]. NA have a wide range of applications and are used in all construction works, including the construction and maintenance of streets, highways, railways, bridges, bricks, concrete and tile production, buildings, pavements, water and sewer systems, drainage installations, power plants and dams, playgrounds and other physical infrastructures [19].

2.1.1. Sustainability Issues Related to the Use of NA

Depletion of natural resources and reserve problems create a crisis with increasing urbanization and industrialization. This problem has an even greater impact, especially in countries such as Dubai and Singapore, where the construction industry is rapidly developing and resources are overexploited [2]. The rapid increase in population and urbanization causes the development and expansion of many urban and residential areas close to quarries [21]. This development and expansion causes the current mining activities in these regions to be stopped due to created environmental pollution and adverse conditions. Additional land and environmental use constraints placed on aggregates producers will restrict the availability of aggregates production from quarry sites. Furthermore, the increased use of aggregates will cause rapid depletion of the

reserve base [22]. Importing aggregates is a short-term solution to partially overcome this problem, yet it is not sustainable due to the limitations on carbon footprint of materials and high transportation costs.

It was mentioned in Mining Turkey [23] in 2018 that, especially in recent years, as a result of urbanization in big cities in Turkey, the borders of cities have expanded rapidly and places that were not previously planned as settlements in the zoning plan have entered the zoning plan boundaries. As a result of this situation, aggregates production areas and settlements are located within each other. Increasing amount of public complaints have been reported about the dust pollution, noise and ground shaking occurring in the residential areas around the aggregates mines during the aggregates production activities [23].

In the 2021 report of the Turkish Ready Mixed Concrete Association (THBB), it is stated that there are difficulties in accessing aggregates resources day by day in metropolitan cities in Turkey, especially in Istanbul, and that limited resources and inefficient aggregates production may cause a major problem in our country, where mega projects are planned to be carried out in the coming periods [3].

Turkey's aggregates problem was reported similarly in 2022. It is stated in the report that the main issues that negatively affect the producers in the Marmara Region are problems in the supply of aggregates, regional inadequacy of aggregates quarries and unstable quality. In addition, a short and medium-term risk analysis of the ready mixed concrete sector was made, and while the issue of problems in the supply of aggregates in 2021 was determined in the medium risk group, this problem was determined in the high risk group in 2022 [24].

After the earthquakes that occurred in Kahramanmaraş on February 6, 2023 in Turkey, it was predicted in THBB's report that 100 million tons of additional aggregates will be needed for the reconstruction actvities taking place in the region in the next two years. As shown in Table 2.1, it is estimated that a total of 300 million tons of aggregates will be produced in Turkey in 2022. Considering the need for 100 million tons of additional aggregates, limitations in aggregates supply are expected in some provinces of Turkey [24].

Table 2.1. Turkey's annual NA production [24]

Year	**Aggregates production (million tons)**
2018	450
2019	225
2020	270
2021	300
2022	300 (estimated)

In line with the information in the 2022 Ready Mixed Concrete Report prepared by THBB, insufficiency of aggregates resources, aggregates supply becoming an even bigger problem in other years, and problems in aggregates supply stand out as possible risks expected for the sector in 2023 and following years. It is expected that aggregates will become more important for ready-mixed concrete producers in the coming years [24]. For this reason, it is necessity to ensure the efficient utilization of existing resources in Turkey and to develop new strategies for the sustainable management of these resources with reassessing the regional plan. It is evident that the demand for alternative sustainable aggregates has emerged as a pressing necessity for future construction structures and projects. Therefore, the country must transition from its current linear economic paradigm to a circular economy model that promotes the production and utilization of alternative aggregates.

Mining of NA, on the other hand, have substantial environmental impacts. One of the significance concerns caused by aggregates mining is the removal of natural vegetation, subsoil and topsoil to reach the rock underlying quarries. This removal process causes the extinction of existing species and a substantial loss of biodiversity due to the destruction of aquatic and soil ecology. Aggregates mining can lead to soil erosion, which results in the accumulation of silt and sediments in rivers and downstream streams. The wastes (topsoil and weathered material) produced during the aggregates extraction process are discharged into nearby agricultural areas, empty pits or river beds, causing pollution [4].

Additionally, the extraction of NA causes deterioration of air quality and the formation of greenhouse gases that cause global warming. The drilling, blasting, hydraulic hammering, transportation and crushing process releases significant amounts of dust emission that can endanger human health (Figure 2.1). Another emission caused by aggregates mining is CO_2. Aggregates mining, transportation and handling causes approximately 13-20% of the total CO_2 emissions released in the construction sector [4]. One ton of NA obtained from crushed stone emits about 33 kg of CO_2 equivalent greenhouse gases (GHGs) and one ton of NA obtained from river sand emits about 23 kg of CO_2 equivalent GHGs [5]. Other emissions that pose environmental and health problems in NA production are SO_2 and fine particulate matter (PM2.5). In the production of 1 ton of NA, approximately 1.27 kg SO_2 is released and 0.0023 kg PM2.5 is formed [4].

Furthermore, mining generates noise pollution and ground vibrations from the equipment used and the blasting process, which can damage the surrounding buildings and cause serious problems in human health such as hearing loss and cardiovascular diseases [4]. Moreover, the NA extraction process causes high energy consumption, and approximately 518 MJ of energy is required to obtain one ton of NA from crushed stone and the energy required to obtain one ton of NA from river sand is 341 MJ [5]. So considering the serious problems caused by NA production, the construction sector and aggregates mining need to be evaluated from environmental, social and economic perspectives.

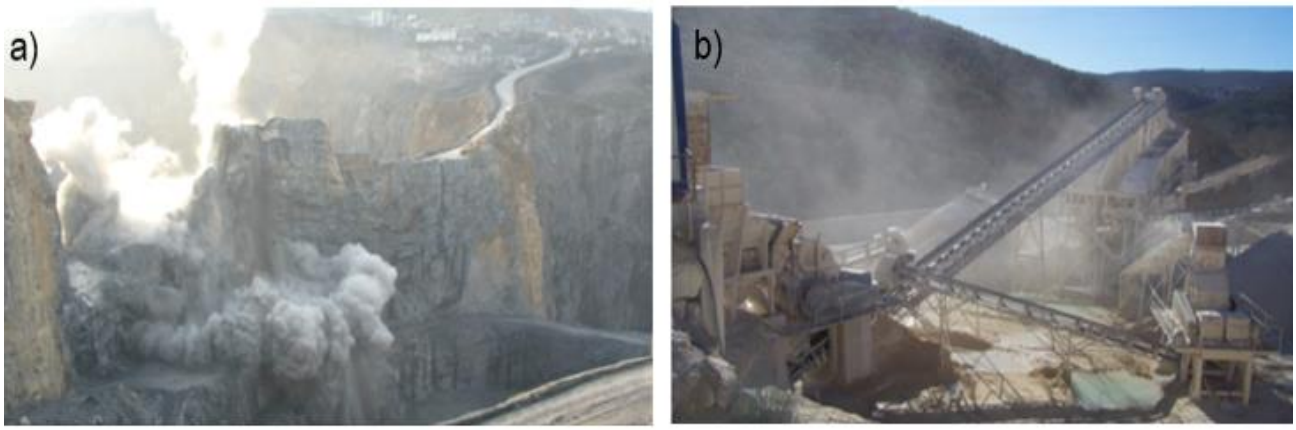

Figure 2.1. Dust emissions from (a) blasting process; (b) mining process area (redrafted after [25])

2.2. Construction and Demolition Waste (CDW)

The continuous and rapid growth of the construction industry leads to the generation of significant amounts of construction and demolition waste. CDW is waste material generated from the construction, extension, maintenance, alteration and demolition of structures, buildings and other infrastructure [26]. It is one of the largest volume waste streams generated in all the world which is representing more than a third of the world's total solid waste [27]. China, the European Union and the United States (USA) are the three largest producers of CDW, and the amount of CDW they generate is about 1130 million tons, 850 million tons and 534 million tons, respectively in 2014 [28–30]. The World Bank predicts that CDW generated in the world will increase to 3.4 billion tons in 2050, which indicates a very serious amount of waste [31]. The waste stream of CDW and its increasing rate every year has make it a global problem for which countries need to develop and implement sustainable solution strategies.

2.2.1. CDW Management in Turkey

The CDW generated in Turkey exceeded 100 million tons in 2014, with a projected increase to approximately 300 million tons by 2023 [32]. Mixed CDW is not easy to dispose of as it contains hazardous substances such as heavy metals, volatile organic compounds, persistent organic compounds and asbestos [33]. As a result of not implementing an environment-friendly waste management plan, CDW negatively affect the balance of the ecosystem. Discharging CDW into forests, streams, valleys and rural areas can cause soil pollution, erosion, contamination of groundwater and surface water, and even fire hazards [34].

The traditional waste management method, which is applied in Turkey and many other countries and is even the most popular, is landfilling. However, landfilling is becoming a relatively primitive way of dealing with waste and it is not an environmentally and economically sustainable solution. CDW occupies very large volumes in landfills, accounting for 25-45% of landfill [35], which shortens the lifespan of landfills. The latter leads to an increase in land prices and the overall cost of the landfilling. In addition, landfilling process has its own environmental drawbacks. For instance, CDW can create harmful chemical leachate and anaerobic processes in landfills can lead to air pollution

and odour problem. These can further contribute to acidification of water resources, increase ecotoxicity and decrease fertility of soil [36].

Landfilling is an unsustainable waste management practice that conflicts with resource efficiency and circular economy principles. With increasing awareness about waste management and the quest for more sustainable practices, a shift away from landfilling towards resource recovery applications has commenced. In recent years, reuse and recycling of CDW has become important in developing and developed countries. CDW mainly consists of concrete, mortar, ceramics, gypsum, brick, asphalt, excavated soil, glass, metal, timber, plastic and the majority are recyclable [37,38]. Recycled and reused CDW provides great advantages in terms of replacing raw materials, enabling cleaner production and ensuring cost-efficiency.

In Turkey, Regulation on the Control of Excavated Soil, Construction and Demolition Waste by Environment and Forest Ministry [39] published in 2004, and it defined criteria for recycled aggregates. It was stated that recycled construction waste fulfilling the defined criteria can be used in the production of new concrete, together or separately with natural materials and it can be used as a filling material for roads, parking lots, pavements, walkways, drainage works, sewer pipes and cable laying. It was also added in the regulation that wastes could be used as a priority in infrastructure and superstructure construction, sports and game facilities, and other filling and recreation works [39].

Construction and demolition waste recycling facilities have recently been established in some provinces in Turkey. In these facilities, a separation process is applied to the collected CDWs, and those suitable for recycling are converted into various materials that can be recycled into the economy and sold. Materials that cannot be recycled are stored in the landfill. Nevertheless, these facilities have not yet reached to enough number and the production of recyclable materials obtained from waste are insufficient. In addition, the usage of these materials obtained from waste in the sectors is not common. Therefore, it is a fact that recycling and reuse of construction and demolition waste is not an adequate practice in Turkey. The CDW generated in Turkey is still stored in landfills or used in limited non-structural applications as road maintenance, filling and drainage material although the regulation [39] was issued in 2004 [40].

In European Union countries, unlike Turkey, CDW recycling and reuse practices are much more common. In the Netherlands, Denmark and Estonia, which have high

recycling rates, sending recyclable and reusable waste to landfills is prohibited [41]. Similarly, Germany, Belgium and Switzerland have a landfill ban for unsorted waste and recyclable materials. Many landfills in the USA also do not accept CDW [42,43]. Hence, in the management of CDW in Turkey, it is necessary to abandon the habit of landfilling, expand the recycling and reuse practices of waste, and adopt a zero waste approach.

2.2.2. Advanced Practices of CDW in the World

The EU Waste Framework Directive set a target for member states to recycle or reuse a minimum of 70% of their CDW by 2020 [44]. In 2021, 14 member states including Germany, the United Kingdom, the Netherlands, Austria, Sweden, Belgium, Denmark, Luxembourg and Japan reached this recycling/reuse target. Among these countries, the Netherland is at the top with 98% CDW recycling and material recovery rate [1]. Some of the methods applied for the recycling of CDW includes the use of wood as a raw material for fiber and board production, the reuse of asphalt materials in roofing or asphalt construction, also the use of asphalt pavement on new pavements and roads, the use of glass in road pavement coatings, the reuse of metals in metal production, and the production of gypsum boards from gypsum [38].

Recycling and reuse of CDW is the subject of much research and practice around the world and in Europe. An emerging approach involves utilizing CDWs as precursors in the generation of new binders known as alkali-activated materials or geopolymers. Along with alkaline activators such as NaOH and KOH; waste concrete, waste ceramics, and waste bricks are the precursors of alkali-activated materials [45,46]. CDWs, which are a potential source of aluminosilicate, can be utilized in the production of geopolymer pastes, geopolymer mortars, and geopolymer concretes by being included in alkali-activated cements [47]. Moreover, waste glass presents an opportunity in usage of concrete production. Its calcium and silicon contents, owed with an amorphous structure, enable waste glass to function as a pozzolanic or even cementitious material [48]. Therefore, waste glass holds promise for partial replacement with aggregates or cements in concrete [49].

Another innovative and high-value recycling practice that has become widespread in recent years involves the use of CDW as aggregates. Fine (<5 mm) and coarse (>5 mm) aggregates obtained by shredding/crushing CDW are called "recycled aggregates". The current trend in the construction sector is to replace the use of virgin materials with the use of alternative construction materials. For this reason, the importance given to recycled aggregates in CDW recycling practices around the world is increasing, and the leading countries that focus on recycled aggregates are England, the Netherlands, Germany and Belgium [1] . The use of recycled aggregates provides many advantages such as decreasing the landfill demand, protecting natural resources and raw materials, reducing energy use and CO_2 emissions, as well as contributing to the overall economy of the country. The researchers also showed that manufacturing recycled aggregates from CDW instead of manufacturing aggregates from crushed stone can reduce net environmental impacts by approximately 49-51% [5].

2.3. Recycled Aggregates and Their Potential Applications

The use of RA in construction sector is an application that has gained great importance in recent years. The main sources of RA are ready-mixed concrete facilities, construction sites, demolition sites of old buildings or demolition waste after natural disasters [50].

The main material types of RA are concrete, masonry and mixed demolition debris. Concrete has the largest portion among these materials with 70%, and the second largest portion is asphalt concrete with 14%. Wooden products make up 7% of recycled aggregates materials, and other products make up 9% [50] .

The stages of the production method of RA briefly include site selection and separation, weighting, fragmentation, crushing in primary and secondary crushers, removal of steel, plastic, wood, paper and soil components, and stocking of fine aggregates and coarse aggregates obtained after washing and grading [50].

The part that needs to be taken into consideration when producing RA is the removal of contaminants such as steel, joint sealants, plastic. Air-sifting or washing can be used to remove light weight materials and electromagnets can be used for items such as steel, ferrous matters. After the main source is separated from these materials, it is treated with washing and air to remove contamination [50].

2.3.1. Sources of Recycled Aggregates

RA are basically divided into four classifications as recycled concrete aggregates, recycled masonry aggregates, mixed recycled aggregates and, construction and demolition recycled aggregates.

Recycled Concrete Aggregates (RCA): Concrete is the most commonly used material in structural applications and included in most recycled aggregates. Recycled aggregates containing a minimum of 90% portland cement-based fractions and aggregates by mass are classified as RCA [51] .

Recycled Masonry Aggregates (RMA): Masonry rubble is a variety of materials resulting from construction and demolition and includes lightweight concrete blocks, mortar plaster, sand-lime bricks, ceramic bricks, blast furnace slag bricks, and burnt clay materials such as roof tiles. The aggregates consisting of at least 90% by mass of all these materials are called RMA [51] .

Mixed Recycled Aggregates (MRA): They are recycled aggregates obtained from the mixture of concrete and masonry rubble, the two main components of CDW. It contains less than 90% portland cement-based parts and aggregates by mass and includes masonry-based materials (lightweight concrete, ceramic bricks, burnt clay materials etc.) [51].

Construction and Demolition Recycled Aggregates (CDRA): In cases where there is insufficient information about the composition and origin of the recycled aggregates and the aggregates content cannot be fully categorized, recycled aggregates is generally referred to as CDRA. RA that do not belong to RMA, RCA, MRA groups and include materials such as asphalt, plastic and glass are in this category. The fact that it contains contamination such as plastic and glass may be due to the fact that the wastes coming from construction and demolition sites are not subjected to any sorting process [51].

2.3.2. Applications of Recycled Aggregates

Popular uses of RA around the world are for pavements, roads and infrastructure construction, and the latest trend is for the production of new concrete and construction materials.

Use of recycled aggregates for pavements, roads and infrastructure construction: Pavements are among the essential and most energy-intensive infrastructure assets. Therefore, utilization of RA from CDW in the construction of pavements, subbases and road bases not only provides a high CDW recycling rate but also creates a market opportunity for RA [26].

The RA can be used in pavement layers, ranging from partial replacement to complete substitution of materials [26]. RA can also be used in the construction of subbase and subgrade levels (capping layer) and can be used as selective fill and bulk fill. Utilization of CDWs in road works and paving has become mandatory in Japan, the Netherlands and Brazil, and high amounts of CDWs are used in paving and road works in these countries [35,52]. RA are also widely used in pavements in the United States and England. The utilization of RA as road base material is also quite common, and the Netherlands uses 95% of crushed concrete waste for this purpose [1].

Applications of recycled aggregates for production of concrete or construction materials: Green building concept is the trending approach to develop projects with less environmental impact, especially when considering the reduction of CDWs. The application in which RCA will be used at the highest quality is new concrete production, and interest in the structural concrete production strategy from RA has increased from all over the world and Europe recently. The use of RA in the production of new concrete offers a promising solution to the problem of eliminating construction and demolition waste, while also reducing the consumption of natural raw materials and energy, minimizing CO_2 emissions and contributing to the country's economy and promoting sustainable development.

Although concrete production with RA is still an area where research continues, it is also a practical reality in ready-mixed concrete production in many countries. Various pilot projects have been implemented in countries such as Germany, Brazil, Portugal, France, the United States and China and promising outcomes of the applications were reported

[26,53–55] Additionally, in Australia, recycled aggregates, both in coarse and fine size, is the most common type of CDW used in new concrete production [1].

The widespread use of RA in the production of new concrete and construction structure reveals the importance of studies investigating the performance and suitability of RA in structural concrete. There are many studies in the literature on concrete production with RA and more research is still ongoing [26].

Another application where RA are used in structural building is concrete blocks. A concrete block represents a type of precast concrete product, comprising a mixture of portland cement, water, gravel and sand. There are various studies on the production of concrete blocks from RA for sustainable development. By reusing CDW aggregates as additives in the production of concrete blocks, not only waste products can be recycled, but also the major problem of clay scarcity can be overcome [26]. In the studies conducted, as a result of replacing natural coarse aggregates and fine aggregates with 25% and 50% of recycled aggregates, there was no negative effect on the compressive strength of the block and brick samples. With up to 100% replacement, concrete paving blocks with a 28-day compressive strength of at least 49 MPa could be obtained. Shrinkage and slip resistance tests of blocks and bricks produced from RA also gave promising results [56].

Other applications: Recycled concrete aggregates (RCA) can be used as raw materials for cement production. The main ingredients of portland cement are limestone ($CaCO_3$), iron oxide (Fe_2O_3), silica (SiO_2) and clay as a source of alumina (Al_2O_3). RCA, particularly old hydrated cement paste and other CDW from cementitious products which containing these ingredients could be used as raw materials to manufacture portland clinker theoretically [57]. RA can be used to produce alkali-activated cements called geopolymers. There are various resarches on the production of geopolymer cement using various CDW such as concrete, tiles, bricks and ceramics [58–60].

It has been shown by research around the world that quality concrete and construction materials can be successfully produced with aggregates recycled from CDW instead of NA, and this green approach constitutes an environmentally friendly practice in CDW

management. The most prominent of these approaches and a trend all over the world is concrete production with RA [26].

2.4. Properties of RA

RA derived from CDW have low physical and mechanical quality compared to NA and have some drawbacks that limit their use as a substitute for NA. The main difference between RA and NA is that there is adhered old cement paste on the recycled aggregates surface as shown in Figure 2.2. The presence of old adhered mortar (cement paste) on RA makes it more porous and inhomogeneous compared to NA [11].

The volume of old adhered mortar can vary between 25-60% of the total volume of RA depending on the size of the aggregates [11]. Crushing process and particle size have an impact on the amount of mortar adhered to the RA. It has been reported in some studies that the mortar layer adhering to the surface of RA with particle sizes between 20-30 mm is 20% [61,62]. In another study, it was reported that RA obtained from waste concrete consists of 35-30% of old mortar and 65-70% of NA by volume [63] . Nagataki et al. [64] showed that increasing the crushing step reduced the old mortar content on RA and increased the density of RA. However, excessive crushing process can cause cracks in the RA, resulting in a decrease in its quality [64].

Figure 2.2. Diagram showing the structure of RA (redrafted after [65])

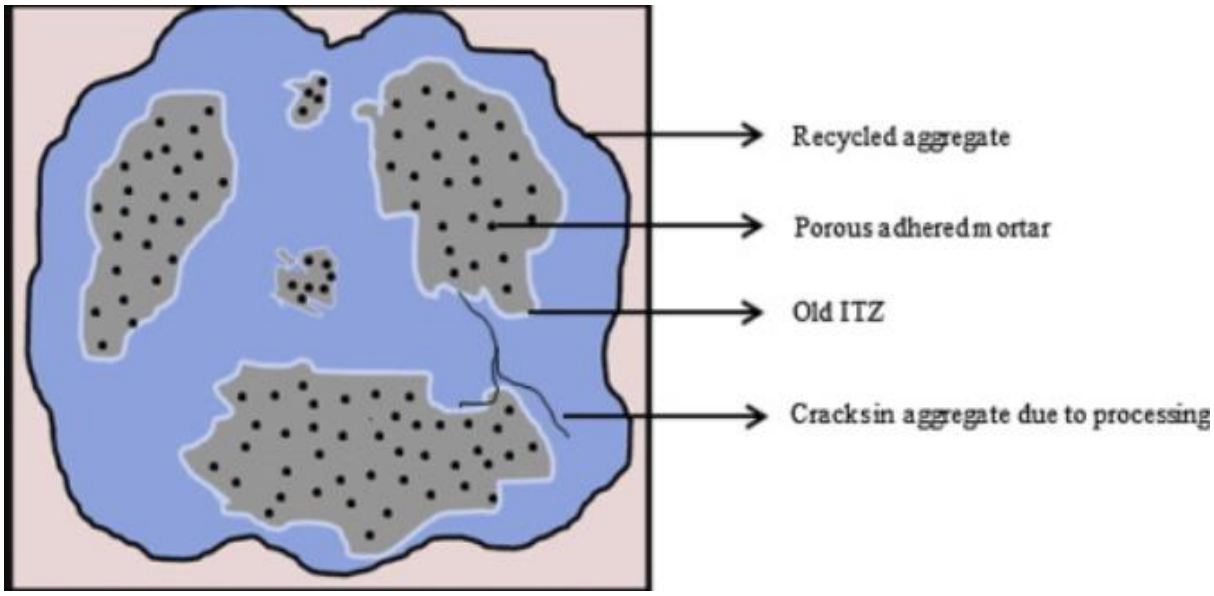

Figure 2.3. Physical properties of RA (redrafted after [11])

The cement paste (old mortar) adhered on the RA creates a rough surface texture on RA and it forms an old interfacial transition zone (ITZ) surrounding the RA (Figure 2.3). The pores in the adhered mortar are very small and the crushing process causes permanent cracks and fissures to form within the aggregates [11]. These cracks cause the recycled aggregates to have weaker properties and can lead to the introduction of detrimental reactive substances like SO_4^{2-} that can interfere with the cement hydration process and compromise durability of the material [66].

Mortar residue adhered to the aggregates affects the density, water absorption and porosity properties of RCA. The density of RA is lower than the NA due to the lower density and specific gravity of cement mortar adhering to the aggregates surface. Although the change in density varies by aggregates, generally RA have a relative density approxemetly 5-10% lower than NA [50]. Residual mortar also causes RA to have different water absorption and porosity properties than NA. As shown in Figure 2.4a, the surface of NA is smooth with low porosity, which causes them to have less water absorption. The mortar layer adhered on the RA has greater porosity, which makes the RA have more and irregular pores and loose particles, as shown in Figure 2.4b, which increases the water absorption capacity of the RA [67]. Water absorption of NA is in the range of 0.5-2% [68]. In contrast, the water absorption of cRA generally change between 2-7% and the water absorption of fRA ranges between 4-13% [50]. Even higher water

absorption may also be observed due to old cement mortar adhering to the aggregates. In general, the water absorption of RA is on average 2.3-4.6 times higher than the upper limit of the water absorption of NA [69]. There is an inverse correlation between the attached mortar and particle size of RA. Specifically, as the aggregates size decreases, the content of attached mortar increases. This behavior is related to processing techniques and as the aggregates gradually crumbles, cement mortar accumulates in the fRA. The fRA generally have lower density and porosity than cRA, but have higher water absorption [65].

Additionally, as RA are recycled several times, they have lower quality than a single time RA. The effect of multiple recycling on aggregates was investigated and it was found that as the number of recycling increased, the content of mortar adhering to the aggregates increased. This affects the water absorption of recycled aggregates, and as the number of recycling increases, the water absorption of recycled aggregates increases [65].

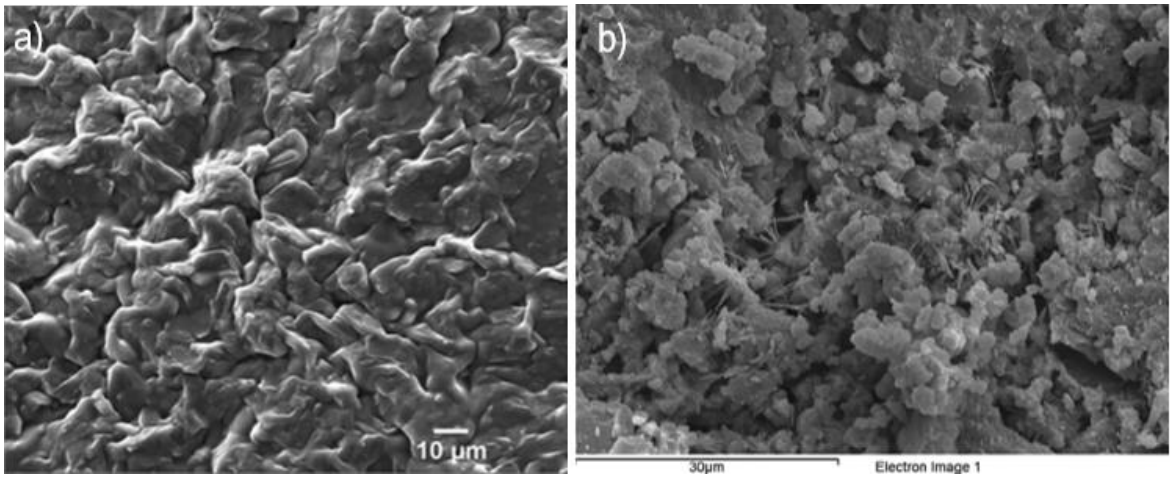

Figure 2.4. SEM image of (a) NA's surface; (b) RA's surface (redrafted after [67])

The crushing index and Los Angeles (L.A.) wear coefficient, which is another feature of the aggregates material and expresses its durability, are higher in RA than in NA. This is because RA contain residual mortar which can easily break off in the ITZ. Residual mortar on the RA breaks when subjected to loading [70]. However in NA, there is no such coating/layer. The weakness of the adhering mortar in RA determines its behavior

in abrasion and crushing tests. Studies indicated that the higher the content of attached mortar, the greater the Los Angeles abrasion and crushing index [65,70].

The use of RA in structural construction has a negative effect on the mechanical properties of the concrete sample, such as the workability of the concrete mixture and concrete strength, due to the weak physical and mechanical properties of RA. For this reason, RA with water absorption rates above 7-10% are not preferred in concrete applications, and recycled fine aggregates without upgraded/strangthened are generally used in limited quantities in concrete mixtures due to their weak properties [65].

2.5. Experimental Studies on the Utilization of RA in Concrete Production

The use of RA in concrete has attracted interest as it is a way to obtain more environmentally friendly concrete, and numerous studies have been conducted on the mechanical properties of recycled aggregates concrete (RAC) [11]. The lower quality of RA than NA causes changes in the mechanical properties of RAC compared to conventional concrete. Tests have shown that the mechanical properties of concrete depend on many parameters such as the water to cement (w/c) ratio of the mixture, the physical properties/quality of the RA, the level of replacement of the RA, and the moisture status of the RA [70,71].

Studies showed that the RA has a remarkable effect on the compressive strength of RAC [72]. It was reported that the compressive strength of RAC differs depending on the percentage of RA to be replaced by NA, using the same w/c ratio [72]. In many studies, the compressive strength of RAC with 100% replacement was obtained up to 30% less than natural aggregates concrete (NAC) [73–75]. However, some studies reported that the compressive strength of 100% replaced RAC may decrease by up to 60-76% compared to conventional concrete [76,77]. These differences in the compressive strength of RAC could be due to the age of the parent concrete from which the RA were derived from [77]. On the other hand, it was shown that if the RA replacement rate was limited to 30%, the decrease in compressive strength of RAC was not very significant [75,78]. Tam et al. [79] modeled the optimum RA replacement level and reported it to be between 25-40%. Additionally, Poon et al. [80] reported that the moisture level of RA also affects the

compressive strength of RAC. Oven-dried samples showed higher strength than surface saturated samples and air dried samples [80].

It is known that there is a decrease in compressive strength as the w/c ratio increases in conventional concrete. For RAC, Li et al. [81] reported that the compressive strength decreased with increasing w/c ratio at all replacement levels except concrete with 50% RA. However, it was also reported that the desired compressive strength is possible by adjusting the w/c ratio [81]. RA are more porous than NA, have higher water absorption capacity, resulting in a decrease in the w/c ratio in the mortar. The slump loss of RAC is higher than NAC, and the required workability is difficult to achieve in RAC [82]. Therefore, RAC requires more water to achieve workability close to that of conventional concrete [83]. Tabsh and Abdelfatah concluded in their study that RAC requires 10% extra water to achieve the same slump as conventional concrete [84]. Researchers also reported that the desired compressive strength in RAC could be achieved by using more cement (up to 10% extra) than normal concrete or adjusting the w/c ratio [85]. On the other hand, some studies reported that the early strength gain rate of RAC (up to 7 days) was higher than NAC [85,86]. This was attributed to the high water absorption capacity of the old mortar as well as the rough texture of the RA, which led to better bonding and interlocking properties between the RA surface and mortar [87]. The replacement ratio of RA might also affect the early strength gain. However, in contrast to early strength gain, the strength gain of RAC from 21 to 28 days was less than NAC [78].

Modulus of elasticity which expresses the hardness of concrete is affected by parameters such as porosity of the aggregates, density of the aggregates, transition zone between the cement matrix and the aggregates, as wel as the amount and the properties of the old mortar present on RA surface. RA content affects the elastic modulus more than the compressive strength. The modulus of elasticity of RAC is less than NAC, and increasing the ratio of replacement of RA reduces the elasticity modulus [78,83]. Previous studies reported up to 45% decrease in modulus of elasticity of the concrete when the NA were completely replaced with RA [78,82,88] which made RAC more brittle. On the other hand, Frondistou-Yannas reported [89] that changes in the w/c ratio of the mix significantly affected the elasticity of the material. His findings indicated that w/c ratio of 0.75 led to as much as 40% decrease in the elastic modulus, while at a lower w/c ratio changes in elastic modulus were insignificant [89,90]. Several studies presented that the effect of RA content on split tensile strength of RAC was less than its effect on

compressive strength [71,82,91,92]. Some researchers examined different percentages of RA replacement in RAC and found that tensile strenght might decrease as much as 10% depending on the RA content [82,92]. It was reported that the split tensile strength and flexural strength were affected by the surface properties, quality of RA and w/c ratio instead of replacement degree of RA [82,93]. It could be possible to achieve the equivalent target strength by modifying the paste content and w/c ratio [94]. In another study conducted by Kou et al., however, it was stated that the split tensile strength of RAC increased in the long term compared to NCA [95]. Several studies also conducted on the flexural strength of RAC, and Topçu and Sengel [96] mentioned that as the percentage of RA in RAC increases, the flexural strength of RAC decreases. Some researchers observed a decrease in the flexural strength of the RAC in the range of 16–23% with different replacement ratio of the RA [93,97]. Additionally, Bairagi et al. [76] reported that differences in the flexural strength of RAC may occur at different w/c ratios.

Studies have indicated that RA exhibit lower properties compared to NA, resulting in concrete with lower mechanical properties when RA is used. Enhancing the quality of RA is paramount to their assessment within the framework of the circular economy model and integration into new product. Therefore, researchers have directed their efforts towards developing processes aimed at improving the quality of RA. Improvement of RA has emerged as a research area with substantial potential for enhancing the sustainability of CDW management and facilitating the construction sector's transition towards a circular economy paradigm.

2.6. RA Improvement Methods

Commonly used approaches and methods for improving the properties of recycled aggregates can be basically classified into two categories. The first category mainly involves the removal of mortar adhering to the surface of RA, while the second category focuses on improving the strength of the adhering mortar on the surface of RA.

2.6.1. Methods for Removing Adhered Mortar

Weak adhered mortar is considered the main factor compromising the quality of RA. Various methods such as mechanical grinding, heat treatment, pre-soaking in water and acid treatment have been investigated to remove adhered mortar from the RA surface [12].

Mechanical Grinding (Ball-Milling): Mechanical grinding is a popular treatment method as it involves a simple procedure to remove attached mortar from the aggregates surface. The attached old mortar is separated from the aggregates using crushing and ball milling. In principle, it is based on the high speed rotating eccentric gear in the grinding mill and the old mortar is pulverized [12]. Mechanical grinding can increase the density of RA and reduce water absorption by removing old mortar remainings. It can also improve the shape of RA due to collision and peeling effects [98].

Thermal Treatment: It consists of heat grinding and selective heat grinding. In the heat grinding method, the RA is heated at about 300 °C to remove moisture from the old attached mortar, rendering it more brittle for subsequent grinding process to separate the mortar layer. In selective heat grinding, microwave is used to heat and weaken the ITZs between NA and old mortar. As the heating temperature increases, the mortar removal more easily, but at temperatures above 500 °C, the properties of RA may be degraded [99].

Pre-soaking in Water: It is the first treatment method for removing adhared mortar. In this method, RA is cleaned by washing with water to remove impurities, loose particles, dust particles, and poorly adhered mortar from the surface. This method just removes loose, weak mortar and most of the adhered mortar (stronger mortar) still remains on the aggregates [100]. Ultrasonic cleaning is also used for the same purpose. The RA is immersed in an ultrasonic bath and its surface is washed with water to remove weak adhered mortar. This process is repeated until clean water is obtained. Katz [101] observed a 7% increase in the compressive strength at 28 days of RAC made from RA improved with ultrasonic bath.

Acid Treatment: Soaking in acid is an effective and traditional approach based on dissolving the cement hydration products in the mortar by acid solution. As a result of the reaction between hydration products and acid, the length and width of the cracks in the old ITZ and the pore size of the mortar can be reduced, and improve the ITZ [102–104]. Sulfuric acid (H_2SO_4), hydrochloric acid (HCl) and phosphoric acid (H_3PO_4) were evaluated as acid solutions and HCl was determined to be the most effective [102]. This method requires safety precautions and requires a final wash with fresh water to clean remaining chemicals in RA [100,105].

2.6.2. Methods for Strengthening Adhered Mortar

Another strategy to upgrade the properties of RA is to strengthen the adhered mortar, and common approaches can be listed as (i) pozzolanic materials application, (ii) polymer emulsion, (iii) immersion in sodium silicate solution, (iv) chemical carbonation and (v) microbial induced carbonate precipitation.

Pozzolanic materials: Addition of pozzolanic materials is an efficient method to reduce the negative properties of RA. Fly ash, volcanic ash, silica fume, blast-furnace slag and nanosilica are pozzolanic materials and can be easily available as they are industrial by-products [105,106]. With this method, a better quality RA is actually obtained compared to the techniques for removing adhered mortar. Pozzolanic materials fill the surface of RA and react with $Ca(OH)_2$ to generate C-S-H gel, which can reduce the porosity of RA and improve ITZs [107–109]. The efficiency of the method depends on the $Ca(OH)_2$ content in the adhering mortar, particle sizes of the mineral materials and the reactivity of the pozzolanic materials. Nano silica with high reactivity and smaller size is more beneficial in improving the RA [110–112].

Polymer Emulsion: Treatment with polymer emulsions is another effective method to reduce the porosity of RA. During polymer emulsion, the RA is kept in the polymer solution, which is usually prepared by adding polymer to water, for a certain period [113]. Two common polymer emulsion is polyvinyl alcohol (PVA) emulsion and silicon-based polymers (silane, siloxane or both). They are water repellent and they can fill the micro-cracks and micro-pores of the old mortar and form a hydrophobic film, thus reduce the water absorption of RA [114].

Sodium Silicate Solution: It is almost similar to the treatment with pozzolanic materials. The pores and cavities of the RA are filled with silicic acid gel precipitated from sodium silicate solution. Additionally, sodium silicate reacts with calcium hydroxide and C-S-H gel is produced, which improves the bond between the adhering mortar and RCA [115,116]. However, excessively high concentration of sodium-silicate solution can deteriorate aggregates quality and damage durability by increasing the risk of alkali-silica reaction [117].

Carbonation: The natural phenomenon in which CO_2 in the atmosphere enters through the micropores of concrete and reacts with $Ca(OH)_2$ to form $CaCO_3$ is called surface carbonation. However, there are some limitations in the natural carbonation process, such

as environmental conditions and process time, and the natural carbonation of a 10-20 mm deep concrete takes approximately 20-80 years [118]. Researchers have investigated the accelerated carbonation process by externally applying CO_2 and pressure, and RA is improved by accelerated carbonation [119,120]. The RA are exposed to CO_2 rich environment to facilitate the carbonation of the hydration products. CO_2 reacts with calcium hydroxide ($Ca(OH)_2$) and calcium silicate hydrate gel (C-S-H) to produce $CaCO_3$, which reduces the porosity of RA and enhances ITZs. This method is efficient for RCA, while for aggregates obtained from other recycled materials, such as brick, the process is inefficient due to the lack of alkaliniy [121,122].

Microbial Induced Calcium Carbonate Precipitation (MICP): Another effective and novel technique applied for improving aggregates properties is MICP. This approach leverages a natural process wherein bacterial cells facilitate the formation of inorganic minerals through their metabolic activities, offering an environmentally friendly solution [17,115] . MICP exploits the bacterial cell wall's negative zeta potential to precipitate $CaCO_3$ on aggregate surfaces. The mechanism of precipitation can vary depending on the type of bacteria, aggregates porosity, and the materials or methods applied [123]. The small size of bacteria allows them to enter micropores that fly ash or cement cannot enter, and this is the main advantage of MICP. Therefore, MICP is also effective for fRA [100]. With MICP, the quality of RCA can be improved by reducing water absorption of old mortar, and the surface properties of concrete can also be improved by reducing permeability [100,124].

2.6.3. Disadvantages of the Current Improvement Methods

The advantages and challenges of the improvement methods of RA described in Sections 2.4.1 and 2.4.2 are summarized in Table 2.2. Mechanical grinding is an effective method for removing old attached mortar from RA surfaces. However, RA particles are damaged due to collision and grinding during the process. Mechanical grinding causes meso-micro cracks and fissures to form on the RA surface, and these cracks and fissures affect the mechanical and durability properties of RAC [125]. Additionally, mechanical grinding requires large investments due to special device requirements and is compelling in terms of high energy consumption. Thermal treatment can reduce the pore size of old mortar and enhance the bond between fresh cement paste and RA. However, thermal treatment may not be useful in large-scale production of improved RA as it time consuming and

causes high energy consumption and CO_2 emission. The method requires also investment due to the equipment used [98]. Pre-soaking in water or ultrasonic cleaning methods cannot remove attached strong mortar to the RA surface and can only remove a minor proportion of loosely attached mortar or dust particles [100,101]. Therefore, this method does not have a significant impact of durability properties of RAC, since the old mortar still remains in the RA. In addition, these methods cause water waste, and contaminated water containing cement dust and other impurities resulting from washing the aggregates requires proper recycling [100]. Using the ultrasonic cleaning method causes additional energy consumption [100].

The acid treatment can be effective for improvement but method has disadvantages such as increased chloride and sulfate interference in the RA, which directly affects the concrete strength, and the process may lead to environmental problems such as the formation of strong acid waste. The high cost of some strong acids may also make this method economically impractical on a large scale [98,100]. The use of pozzolanic material may reduce the workability of RAC because it contains fine particles in the mixture [100]. Nanoparticles cannot reduce the width of old ITZ and, the high cost and difficult dispersion of nano-SiO_2 somewhat limit its large-scale RA development and practical applications [98]. The application of polymer emulsion envelops the surface of RA, leading to a reduction in its porosity and water absorption. However, the hydrophobic film generated from the interaction of silicone-based polymers with calcium silicate hydrate does not contribute to the bonding between the cement paste and aggregates [126]. The polymer emulsion method has several limitations and these are the inability to increase the strength of the old mortar, the inability to make a significant improvement in the mechanical properties of RA, high costs related to the organic polymer solution, and the environmental concerns arising due to the waste liquid solution formed [126]. The sodium silicate solution method is a cost-intensive application and increases the risk of further undesired alkali-silica reaction in concrete [115,117].

MICP and carbonation are the two most effective methods to improve the quality of RA and therefore improve the performance of concrete. Carbonation is a very common phenomenon, but it may not always be a feasible method as it depends on many parameters, such as CO_2 concentration, humidity, RA source history, whether RA contains sufficient hydrated product for reaction with CO_2 [127]. In addition, a special device and time is needed for the process, which brings about economic concerns and difficulty in

large-scale implementation. Of all the methods, MICP provides the best mechanical properties for RAC and can provide up to 40% improvement in compressive strength [115]. Nevertheless, MICP has difficult-to-control test conditions, relatively expensive ingredients such as bacteria, and the method is still under development [115,128].

In improving RA quality, it is necessary to choose the appropriate treatment process by establishing a balance between treatment efficiency, environmental impact and treatment cost. From this perspective of balance, the use of the MICP method for the improvement of RA seems promising and effective.

Table 2.2. Comparison of RA improvement methods [115,126,128]

Treatment methods	**% improvement in compressive strength of RAC at 28 days**	**Disadvantages of methods**
Mechanical grinding	↑ up to 39% [115,126]	• Need special device • Increase energy consumption • Increase CO_2 emission • May cause microcracks in RA after the process
Thermal treatment (microwave heating)	↑ up to 27% [115]	• High energy consumption • CO_2 emission • Time-consuming • Inconvenient on a large scale
Pre-soaking in water	↑ up to 7% [115]	• Time-consuming • Need to dispose of water waste • Removal of attached mortar is hard
Acid treatment	↑ up to19% [115]	• High cost • Increased chloride and sulphate contents • High amount of waste acids

Pozzolanic materials	↑ up to 19% [126]	•Time-consuming •Nanoparticles can not reduce the width of old ITZ
Polymer emulsion	↓ negative effect [126,128]	• Cost-intensive • Need to dispose of liquid waste solution • Inconvenient on a large scale
Sodium silicate solution	↑ up to 15% [126]	• Cost-intensive • Increase the risk of alkali-silica reaction
Carbonation	↑ up to 23% [128]	• Need special device • Cost-intensive • Process depends on vary parameters like CO_2 conc, humidity, RA properties • Time-consuming
MICP	↑ up to 40% [115]	• Cost-intensive • Time-consuming • Difficult to control test conditions

2.6.4. Novel Approach with MICP Method

Research on the incorporation of biological processes into engineering is increasing, and MICP has attracted wide attention as an innovative technique and can be applied in various areas. MICP is a ubiquitous phenomenon in nature and is based on the precipitation of calcium carbonate through basic metabolic activity by bacterial species. Most bacteria can precipitate calcium carbonate if their environment is suitable in terms of pH and temperature, calcium concentrations, nucleation sites and dissolved inorganic carbon [129]. MICP can be accomplished through many different metabolic pathways including photosynthesis, methanogenesis, ureolysis, nitrate reduction (denitrification), ammonification, sulfate reduction [130]. Microbial activities in these pathways increase the amount of dissolved inorganic carbon and pH, thus increasing the carbonate ion

(CO_3^{2-}) concentration in the microenvironment of bacteria. In the presence of Ca^{2+} ion, CO_3^{2-} and Ca^{2+} ions use the bacterial cell as a nucleation site and form insoluble $CaCO_3$, which then precipitates into solid minerals [131]. Commonly reported metabolic pathways that induce $CaCO_3$ precipitation were summarized in Table 2.3.

Table 2.3. The metabolic pathways that produce $CaCO_3$ with their mechanisms and reactions [130,132,133]

Metabolic Pathway	Mechanism and Reaction
Oxygenic photosynthesis	$CO_2 + H_2O \rightarrow H_2CO_3$ $H_2CO_3 \leftrightarrow HCO_3^- + H^+$ $Ca^{2+} + HCO_3^- \rightarrow CaCO_3 + H^+$
Anoxygenic photosynthesis	$CO_2 + 2H_2S + H_2O \rightarrow CH_2O + 2S + 2H_2O$ $2HCO_3^- \leftrightarrow CO_2 + CO_3^{2-} + H_2O$ $CO_3^{2-} + H_2O \leftrightarrow HCO_3^- + OH^-$ $Ca^{2+} + 2HCO_3^- \rightarrow CaCO_3 + CO_2 + H_2O$
Methanotrophy	$CO_2 + 4H_2 \rightarrow CH_4 + 2H_2O$ $CH_4 + SO_4^{2-} \rightarrow HCO_3^- + HS^- + H_2O$ $Ca^{2+} + 2HCO_3^- \rightarrow CaCO_3 + CO_2 + H_2O$
Urea hydrolysis	$CO(NH_2)_2 + H_2O \rightarrow NH_2COOH + NH_3$ $NH_2COOH + H_2O \rightarrow NH_3 + H_2CO_3$ $NH_3 + H_2O \leftrightarrow NH_4^+ + OH^-$ $HCO_3^- + H^+ + 2NH_4^+ + 2OH^- \leftrightarrow CO_3^{2-} + 2NH_4^+ + 2H_2O$ $Ca^{2+} + CO_3^{2-} \rightarrow CaCO_3$
Ammonification	$NH_3 + H_2O \leftrightarrow NH_4^+ + OH^-$ $CO_2 + H_2O \leftrightarrow H_2CO_3$ $H_2CO_3 \leftrightarrow H^+ + HCO_3^-$ $H^+ + HCO_3^- \leftrightarrow CO_3^{2-} + 2H^+$ $CO_3^{2-} + Ca^{2+} \leftrightarrow CaCO_3$

Denitrification	$2HCOO^- + 2NO_3^- + 2H^+ \rightarrow 2CO_2 + 2H_2O + 2NO_2^-$ $HCOO^- + 2NO_2^- + 3H^+ \rightarrow CO_2 + 2NO + 2H_2O$ $HCOO^- + N_2O + H^+ \rightarrow CO_2 + N_2 + H_2O$ $Ca^{2+} + CO_2 + H_2O \rightarrow CaCO_3 + 2H^+$
Sulfate reduction	$CaSO_4 \cdot 2H_2O \rightarrow Ca^{2+} + SO_4^{2-} + 2H_2O$ $2CH_2O + SO_4^{2-} \rightarrow H_2S + 2HCO_3^-$ $Ca^{2+} + 2HCO_3^- \rightarrow CaCO_3 + H_2O + CO_2$

The most commonly used pathway in MICP is ureolysis due to simple mechanism, low cost, high yield of carbonate ions in a short time, and an easy-to-control reaction process [134]. In ureolysis, microorganisms can use urea as an energy source, produce urease with their metabolic activities and catalyze the hydrolysis of urea. As a result of the interaction between NH_3 and H_2CO_3, CO_3^{2-} is formed and the pH around the microbial cells increases (Table 2.3). In the presence of Ca^{2+}, the positively charged ions are attracted by the negative cell wall and adsorbed on the cell surface. As a result, the product of microbial activity, CO_3^{2-}, and the adsorbed Ca^{2+} precipitates as $CaCO_3$ around the bacteria [132].

MICP with ureolysis also has some disadvantages. The ammonium produced as a result of urea hydrolysis in an alkaline environment such as concrete consumes the OH^- ions in the cement and turns into ammonia, which is toxic and causes an unpleasant odor. This may deteriorate the concrete material over the time. Moreover, most ureolytic bacteria produce urease enzyme under aerobic conditions thus they require oxygen for growth and MICP. This means that in the absence of oxygen, most ureolytic bacteria can not induce $CaCO_3$ precipitation [135]. Considering these disadvantages of ureolytic bacteria, alternative microbial mechanisms for MICP have been investigated [136–138]. Denitrification emerges as a convenient alternative mechanism for MICP. In the literature, there are pioneering studies by Kavazanjian et al. [137] that include soil consolidation through denitrification, and studies by Ersan et al. [136,138] in which denitrification is used for MICP and for development of microbial self-healing concrete.

In denitrification, nitrate-reducing bacteria precipitate $CaCO_3$ in solution using NO_3^- as the electron acceptor. Biological reduction of NO_3^- is a heterotrophic process and occurs by bacteria oxidizing organic matter (Table 2.3) Since denitrification can lead to $CaCO_3$ precipitation in the absence of oxygen, it offers significant potential for the strengthening of RA, particularly inducing $CaCO_3$ precipitation at deeper parts of the pores. Additionally, nitrate reducing bacteria can work in the absence of micronutrients and still induce significant amount of $CaCO_3$ precipitation, which can be beneficial for reducing the cost of the RA treatment process [139] .

Urea hydrolysis and denitrification can complement each other as metabolic pathways, and employing both mechanisms concurrently can enhances the MICP process. The coexistence of these metabolisms allows for microbial $CaCO_3$ precipitation to occur both in the presence and absence of oxygen or presence of limited oxygen. Moreover, utilizing both metabolisms in MICP can lead to an increase in microbial precipitated $CaCO_3$ crystals. Theoretically, the use of two metabolisms appears to be advantageous for MICP by providing an increase in CO_3^{2-} ions.

2.6.5. RA Improvement via MICP Method

In MICP based RA improvement studies, coarse aggregates sizes were tested by using ureolytic bacteria, and promising positive results have been obtained in the studies. Grabiec et al. [15] treated RCA with MICP method and they observed an effective reduction in water absorption of cRCA with size between 6-16 mm after MICP with *Sporosarcina pasturii* bacteria. They also reported that RCA in smaller sizes (6 mm-8 mm) are more suitable in terms of microbial precipitation efficiency than larger sizes (12 mm-16 mm) [15]. Wang et al. [18] used spray and immersion treatments with *Bacillus sphaericus* to improve the properties of two different recycled coarse aggregates in the 6.3-20 mm size range. Using the immersion method, they achieved up to a 1% reduction in water absorption for cRCA and up to a 2% reduction for cRMA [18]. The obtained weight increases for cRCA and cRMA were up to 2% and 2.5%, respectively [18]. Moreover, they revealed that MICP had a strengthening effect on the aggregates, resulting in better resistance to fragmentation. They reported a 40% increase in the compressive strength of concrete containing cRCA and a 16% increase for concrete containing cRMA after MICP [18]. Zeng et al. [140] reported that the surface properties of industrial sourced RA with sizes ranging from 10 to 20 mm can be improved, and the microhardness of the

ITZs can be increased using the MICP method. In another study by Singh et al. [141], ureolytic bacteria (*B. megaterium*) and non-ureolytic bacteria (*B. cohnii*) were examined for the treatment of RA. After 14 days of treatment, a 29% specific gravity increase was obtained after treatment with non-ureolytic bacteria and a 30% specific gravity increase with ureolytic bacteria. The decrease in water absorption of RA was 42.9% and 64.3%, respectively. Water absorption reduction and specific gravity increase directly show the effect of mineral precipitation [141].

Qiu et al. [17] studied the surface treatment of RCA with 5-20 mm in size using microbial induced calcium carbonate precipitation, and major difference in RCA microstructure before and after treatment was observed as shown in Figure 2.5. In Figure 2.5b it can be seen that the pores and surface of RCA after MICP treatment were covered with spherical $CaCO_3$ crystals. These crystals particles, precipitated by the MICP process, effectively blocked the microcracks and pores of RCA, leading to a reduction in its water absorption [17].

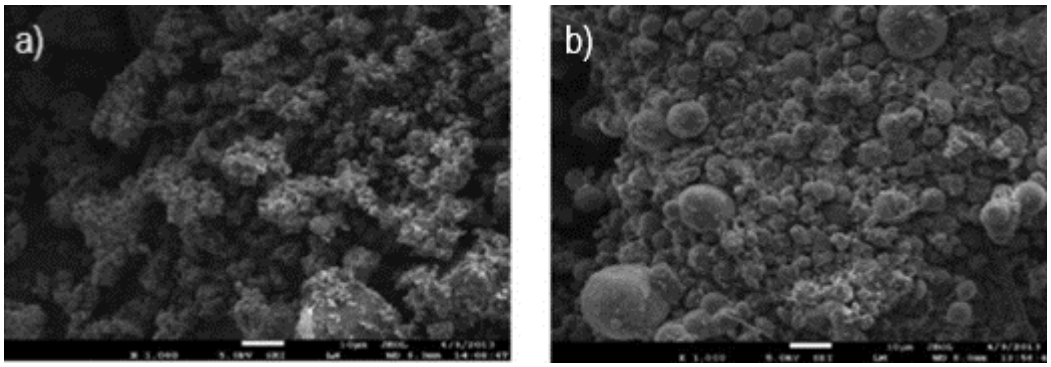

Figure 2 5. Micrograph of (a) RCA without treatment, (b) RCA treated with MICP (redrafted after [17])

Additionally, Qiu et al. [17] investigated the factors influencing MICP on recycled aggregates. In the study, it was stated that the amount of $CaCO_3$ obtained on RCA by the immersion method using *S. pasteurii* reached its highest value when the ambient pH was 9.5 and increased with higher temperature, bacterial concentration and Ca^{2+} concentration [17]. As a result of the research, an increase in weight and a decrease in water absorption were observed in the improved cRCA, and surface modification of RCA by MICP was proven [17].

De Muynck et al. evaluated the effect of $CaCO_3$ precipitation using pure *Bacillus sphaericus* culture and ureolytic mixed culture [142]. The deposition of a calcite layer on the surface of the aggregates resulted in reduced capillary water absorption and reduced gas permeability [142]. It was found that the type of bacterial culture and the composition of the medium had a profound effect on the $CaCO_3$ crystal morphology, and the use of different cultures for improvement causes different results in the water permeability of the poured mortar samples. Mortar samples poured with improved aggregates using pure culture showed a more significant decrease in water permeability compared to mortar samples poured with improved aggregates using mixed ureolytic culture [142]. In another study, which tried to increase the improvement efficiency of aggregates, RCA and MRA were improved by applying two different methods, spray method and immersion method [143]. In both methods, a 2-stage improvement was applied, first with bacterial nutrient solution (10^8 *B. sphaericus* cells/ml) and then with 0.5 M $Ca(NO_3)_2$ biomineralization solution [143]. The immersion method was found to be more efficient in treatment, and a 1.3% reduction in water absorption of RCA was obtained with this method [143]. Compressive strength and elastic modulus increased by 5.0% and 27.4%, respectively, in the twice-improved mixed recycled aggregates [143].

In one of the recent studies on the improvement of RCA by $CaCO_3$ precipitation, three different sizes of recycled mortar aggregates were used which including smaller than 5 mm, between 5-10 mm and between 10-20 mm [144]. For the smallest size of aggregates, reductions of 23% and 12% in water absorption and refractive index were observed, respectively [144]. The compressive strength of the mortar poured by mixing fine (<5 mm) and coarse (5-20 mm) improved RA at a ratio of 1:1.5 was 25% higher than the mortar prepared with unimproved RA at the end of the 28th day [144].

Feng et al. [145] carried out the study on the improvement of recycled fine aggregates with MICP. They investigated the improvement of RA with 0.1 mm-5 mm size by $CaCO_3$ precipitation using *Sporosarcina pasteurii*. The bacterial concentration used in the research was 10^8 cells/ml and the calcium concentration was 0.55 M. Experimental analyzes were carried out at 9.5 pH and 30 °C temperature. A two-stage improvement process was applied, where the aggregates was first immersed in a bacterial media solution for 1 day, followed by immersion in a biomineralization (precipitation) solution for 7 days. After the improvement, the weight of the recycled aggregates increased by 2.5% and the water absorption amount of the aggregates decreased by 27.3%. It was

reported that an 84% increase in the flexural strength and a 14% increase in the compressive strength achieved if the untreated RA in mortar was replaced with improved RA [145]. In the follow-up study on fRA, the optimum microbial $CaCO_3$ precipitation process was tried to be found using the *S. pasteurii* species for RA between 0.1 mm-5 mm [16]. The optimum improvement process was determined to be immersing the aggregates in the bacterial media and biomineralization (precipitation) solution for 1 day, and then repeating this two-stage MICP process three times totally. After applying the optimized improvement process, the weight of the RA increased by 9.4% and water absorption decreased by 45.8% [16]. The flexural strength of mortars poured with improved RA increased by 23.3% and 17.9% at 0.50 water ratio and 0.65 water ratio, respectively [16]. Additionally, Sonmez et al. [146] studied the improvement of fRCA with MICP using non-axenic nitrate-reducing biogranules. In SEM analysis, it was observed that RCA treated with MICP by biogranules had less porous area than untreated RCA, which shows the positive effect of MICP. However, it was noted that the process was not efficient enough [146]. This low efficiency was attributed to the sizes of the nitrate-reducing biogranules, as they were larger than some of the tested aggregates and the pore sizes of all the tested aggregates [146]. This approach could be further improved by using relatively smaller planktonic bacteria instead of biogranules. This study showed that not only ureolytic bacteria but also nitrate-reducing bacteria can be used for MICP process.

2.7. The Goal and the Scope of Thesis

The development of the construction industry has led to major crises, including NA depletion and the production of significant CDW. These challenges have prompted the world to seek sustainable solutions. Research into green applications, focusing on improving RA sourced from CDW for integration into concrete production, is progressively expanding. Researchers have turned to MICP technology, which is novel, environmentally friendly, and effective in improving of RA. However, as seen from the literature, studies have predominantly focused on the improvement of coarse-sized RA with MICP technology. The number of studies on the improvement of fine-sized RA with MICP is almost non-existent. Therefore, it is important to increase research on improvement of fRA with MICP and address uncertainties regarding how the MICP treatment affects the surface properties, microstructure, degree of bonding with the cement matrix, and consequently the strength properties of mortar samples containing fRA. Reducing these uncertainties is crucial for the reuse of fRA, which constitute a

significant fraction of RA, through green practices within the scope of the circular economy model.

Almost all previous studies have focused on urea hydrolysis as the metabolic pathway for improving RA with MICP. A few studies have demonstrated that RA can also be improved using nitrate-reducing biogranules. However, to date, in almost all studies on RA improvement with MICP, researchers have used a single metabolic pathway. To the best of our knowledge, there is no study investigating the simultaneous use of both nitrate reduction and urea hydrolysis pathways for RA improvement through MICP. The integration of these two metabolic pathways offers a significant advantage by enabling the MICP process to occur in both aerobic and anoxic environments. Recent studies have employed non-axenic biogranules and achieved MICP through a single metabolic pathway. Yet, none have investigated the improvement of fRA through MICP using non-axenic culture. The use of non-axenic cultures presents several advantages: it reduces processing costs, increases the practicality and flexibility of application, and allows for the integration of different metabolic pathways.

In Turkey, regardless of the size fraction the number of studies on the treatment of RA with MICP is almost non-existent. Researching of RA improvement processes is crucial for our country to manage the country's natural resources efficiently and to obtain added value by reusing waste in the construction sector within the scope of the zero waste strategy.

Considering all the aforementioned needs, in this thesis, the improvement of fRA properties with MICP was investigated by using non-axenic culture which includes both ureolytic and nitrate reducing bacteria. Within the scope of the thesis, two types of fRCA were used: f-RCA and c-fRCA. Different size groups of f-RCA were improved with MICP and the suitability of the method was checked. Then, the optimized MICP method was determined by obtaining 1350 g sand mixes from f-RCA. After this preliminary study, c-fRCA sand mixes were improved with the optimized method and the surface properties and mortar properties of improved f-RCA and c-fRCA sand mixes were examined.

3. MATERIALS AND METHODS

This thesis was conducted in 3 consequtive parts. The first part involved improving the properties of fRCA of different sizes by the microbial calcium carbonate precipitation method and verifying the suitability of the biobased treatment method. The second part involved improving 1350 g (required amount for 1 L of mortar) of fRCA sand mixes which had particle size distribution as defined in DIN EN 196-1 standard. The fRCA sand mixes treatment process was optimized at this stage and then the optimized treatment process was repeated with commercially available fRCA taken from cement industry. The latter was a preliminary study to confirm quality improvement of fRCA available in construction sector. The third part focused on evaluation of the mechanical properties of mortar specimens prepared by completely replacing standard sand with treated fRCA sand mixes and treated commercially available fRCA sand mixes. Additionally, changes in surface properties and chemical properties of the treated aggregates were also analysed.

3.1. Checking the Suitability of the Improvement Method for fRCA in Different Size Groups

3.1.1. Obtaining and Sizing of fRCA

The fRCA used in this study were obtained by re-crushing the concrete initially poured for testing in the Civil Engineering Department at Hacettepe University and these freshly crushed concrete aggregates were called as “f-RCA”. The f-RCA were grouped according to their sizes by passing them through stainless steel sieves of suitable sizes. Size groups were determined based on the size distribution ranges described for DIN EN 196-1 standard sand. Accordingly, the aggregate size groups were defined as; (i) < 0.075 mm, (ii) 0.150 mm - 0.600 mm, (iii) 0.600 mm - 1.180 mm, (iv) 1.180 mm - 2.360 mm, (v) 2.360 mm - 4.750 mm, and (vi) > 4.750 mm.

The upper size limit for recycled fine aggregates is defined as 5 mm [147]. Therefore, aggregates larger than 4.750 mm were not considered as recycled fine aggregates. Previous studies reporting succesful recycled aggregates improvement via MICP were conducted on coarse aggregates [15,17,18,143] which were larger than 5 mm. Therefore, in this thesis study, cRCA fraction (> 4.750 mm) was included as a control group in method optimization tests. This control group allowed us to confirm the effectiveness of MICP method on cRCA and then further check if the same MICP method can be used for

treatment of fRCA. In this way, the effect of recycled aggregate size could be isolated from the variables in the treatment procedure.

3.1.2. Bacteria Cultivation Procedure

In this thesis study, non-axenic microbial culture that can perform urea hydrolysis and nitrate reduction was used. The inoculum for cultivation of this non-axenic microbial culture was obtained from a sequential batch reactor (SBR) being operated in the scope of the thesis study of Kardogan (2024) for producing biogranules in the Department of Environmental Engineering at Hacettepe University. At the end of an SBR cycle, following settling of the granules a 100 ml sample was taken from the remaining suspension. Taken sample was centrifuged at 3045 g for 10 minutes to obtain bacterial pellets. Each bacterial pellets were incubated with 1 liter of nutrient media given in Table 3.1. Inoculated bottles were placed to a 100 rpm shaker and incubated at 28 °C for 72 hours. The first 24 hours of the batch operation were anoxic (bottles were tightly closed with rubber stoppers) and the following 48 hours the bottles were open to air. At the end of the 72 hours, 90% of the total volume was centrifuged and the bacteria were collected in pellets. The remaining 10% of the volume was fed with fresh nutrient media. This batch operation was repeated by replacing 90% of the content with fresh nutrient media until sufficient amount of bacteria was obtained for the MICP treatment. The bacterial concentration used in MICP treatment of each aggregate size group was 0.5 g CDW.L^{-1}.

Table 3.1. Nutrient media composition

Substrate source	**Concentration (g.L^{-1})**
Urea (CH_4N_2O)	6.00
Yeast Extract	0.20
NaHCOO	10.00
$NaNO_3$	3.00
KH_2PO_4	0.06
$MgSO_4.7H_2O$	0.10

3.1.3. Tests for Treatment of f-RCA in Different Size Groups

Experimental setups were prepared in three groups as water control, abiotic control and microbial treatment to distinguish the effect of MICP from the potential effects of water and the nutrients. Each setup was conducted in triplicates. The weight of the aggregate size groups tested in each setup were given in Table 3.2.

Table 3.2. f-RCA weights used in each setup according to their sizes

Size of aggregate (mm)	**Weight of aggregate (g)**
>4.750	50.00
4.750 - 2.360	50.00
2.360 - 1.180	50.00
1.180 - 0.600	50.00
0.600 - 0.150	5.00
<0.075	5.00

The f-RCA treatment procedure consisted of two stages. The first stage was called “microbial attachment stage” and the second stage was called “biomineralization stage”. Growth media was used in first stage and biomineralization media was used in the second stage. Compositions of the used media were given in Table 3.3. The applied treatment procedure was similar to those used in previous MICP based RA improvement studies [15,16,18,145] . In the microbial attachment stage, each size group were immersed in growth media together with bacteria. During the first 24 hours of this stage, the test containers were tightly closed to prevent air contact and promote anoxic conditions required for biological nitrate reduction. In the following 48 hours of the microbial attachment stage, containers were open allowing air circulation at the headspace. These microaerobic/aerobic conditions were needed for bacteria requiring oxygen for production of urease enzyme. At the end of the first 72 hours, the aggregates were completely separated from the growth media and passed to the biomineralization stage. A vacuum filtration device and 0.45 μm cellulose filter was used to completely separate the aggregates from the growth media. At the end of this process, only the bacteria that had penetrated the pores of the aggregates or adhered to the aggregate surface were passed

to the biomineralization stage. In the biomineralization stage, the aggregates were immersed in a biomineralization media containing both dissolved calcium and essential nutrients under tightly closed conditions (anoxic environment) for 24 hours. Then, the aggregates were separated from the excess media and dried in a ventilated oven at 105 °C.

Table 3.3. Compositions of growth media and biomineralization media

Chemicals	**Growth media ($g.L^{-1}$)**	**Biomineralization media ($g.L^{-1}$)**
Urea	6.00	20.00
Yeast Extract	0.20	-
$Ca(HCOO)_2$	-	6.50
$Ca(NO_3)_2.4H_2O$	-	1.20
NaHCOO	10.00	-
$NaNO_3$	3.00	-
KH_2PO_4	0.06	-
$MgSO_4 \cdot 7H_2O$	0.10	-

Water control setup: The water control setup was prepared to demonstrate any effect of water immersion on the quality characteristics of f-RCA. In this setup, only tap water was used in both the microbial attachment and biomineralization stages.

Abiotic control setup: The purpose of the abiotic control setup was to determine the effect of bacteria-free growth media and biomineralization media on the surface properties of f-RCA. The media to be used in the procedure were sterilized by autoclaving at 1 bar of pressure, 121°C for 20 minutes. Chemicals that were likely to decompose/precipitate during autoclaving process (i.e. urea, KH_2PO_4, $MgSO_4.7H_2O$) were subsequently added to the autoclaved media by filter sterilization (using a 0.22 μm sterile syringe filter). An aggregate improvement procedure was applied using sterile growth media in the microbial attachment stage and sterile biomineralization media in the biomineralization stage.

Microbial treatment setup: In this setup, the effect of microbial activity on f-RCA improvement was demonstrated. In the microbial attachment stage, the aggregates were kept in the growth media containing 0.5 g cell dry weight (CDW).L^{-1} non-axenic culture for 72 hours. In this stage the bacteria adhered to the aggregates and grew on surface/in pores of aggregates (Figure 3.1). Then, the aggregates, which were completely separated from the bacterial growth media, were kept in the biomineralization media for 24 hours.

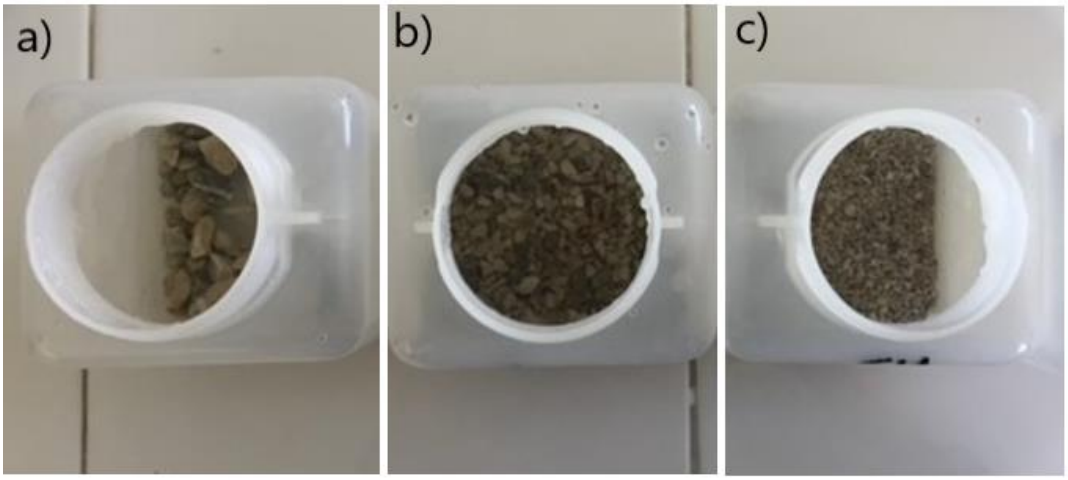

Figure 3.1. Microbial attachment stage at the end of 24 hours for (a) > 4.750 mm, (b) 2.360 mm - 4.750 mm, (c) 1.180 mm - 2.360 mm

3.1.4. Determining the Effect of Improvement on Surface Properties of f-RCA

The change in the properties of the f-RCA after the treatment procedure was evaluated by conducting water absorption and weight increase tests, as described in previous studies in literature [16–18,143,145].

Water Absorption Test

Before the water absorption test, the aggregates were dried in a ventilated oven at 105 °C until the weight change in the last 24 hours became less than 1%. Dried aggregates of all sizes were separately immersed in containers filled with tap water for 24 hours. At the end of 24 hours, each aggregate-water mixture was passed through a 0.45 μm pore filter with a vacuum filtration to remove the excess water. Thus, the saturated surface dry weight of the aggregates could be obtained.

Water absorption values of the f-RCA before and after improvement were calculated according to Equations 3.1 and 3.2.

$$WA_{,before} = \frac{W_3 - W_1}{W_1} \text{x } 100\% \quad \text{(Equation 3.1)}$$

$$WA_{,after} = \frac{W_4 - W_2}{W_2} \times 100\% \quad \text{(Equation 3.2)}$$

$WA_{,before}$ = water absorption of aggregates before treatment (%)

$WA_{,after}$ = water absorption of aggregates after treatment (%)

W_1 = weight of dried aggregate before treatment (g)

W_2 = weight of dried aggregate after treatment (g)

W_3 = saturated surface dry weight of aggregate before treatment (g)

W_4 = saturated surface dry weight of aggregate after treatment (g)

Weight Increase Test

Before and after the MICP treatment process, the f-RCA were dried in a ventilated oven at 105 °C until they reached a constant weight (until the weight change was less than 1% in the last 24 hours), and then, dried aggregates were weighed. Weight increase occurred due to the MICP treatment could be calculated according to Equation 3.3.

$$WI = \frac{W_2 - W_1}{W_1} \times 100\% \quad \text{(Equation 3.3)}$$

WI = weight increase after treatment (%)

W_1 = weight of dried aggregate before treatment (g)

W_2 = weight of dried aggregate after treatment (g)

3.2. Enrichment of Non-axenic Nitrate-Reducing and Urea Hydrolyzing Bacterial Culture

In Hacettepe University Department of Environmental Engineering, a SBR was being operated by Kardogan (2024) for production of nitrate-reducing and urea hydrolyzing biogranules. As biogranule production reactors require certain selective pressure to select between flocs and granules [148] after 3 minutes settling period flocs were discarded from the reactor operated in the study of Kardogan (2024). These discarded flocs were regularly taken as inoculum for enrichment of the non-axenic culture used in this thesis study. The specific nitrate reducing and specific urea consumption activities of the inoculum were given in Table 3.4.

Table 3.4. Specific activities of the inoculum according to feed nutrient

Concentration of feed nutrient	Specific activity of the seed
10 $g.L^{-1}$ urea	125.13 mg $urea.g^{-1}.h^{-1}$ (anoxic condition) 120.62 mg $urea.g^{-1}.h^{-1}$ (microaerobic condition)
0.11 $g.L^{-1}$ NO_3-N	6.72 mg NO_3-$N.g^{-1}.h^{-1}$ (anoxic condition) 1.35 mg NO_3-$N.g^{-1}.h^{-1}$ (microaerobic condition)

Enrichment of the non-axenic culture was further performed in a 1.2 L volume plexiglass (76 cm length, 4.5 cm diameter) cylindrical reactor under sequencing batch reactor operating conditions. The schematic diagram and photograph of the reactor used for cultivation of the non-axenic bacterial culture was given in Figure 3.2.

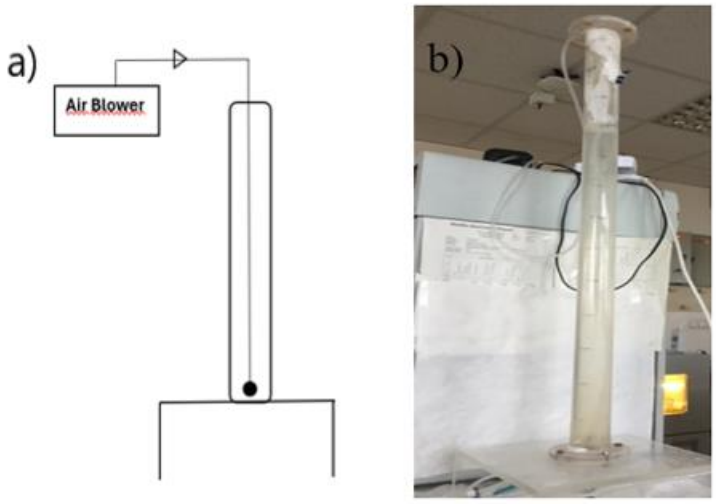

Figure 3.2. Manually operated sequencing batch reactor as (a) schematic diagram, (b) used in laboratory

The SBR was operated in three periods, in total of 72 hours. In the first 24 hours, no air was provided and it was defined as anoxic period. Subsequent period was defined as aerobic period and 4.5 $L.min^{-1}$ air was provided for 47.5 hours. This system allows further enrichment of urea hydrolyzing and nitrate-reducing bacteria. In the absence of dissolved oxygen in the first 24 hours of the operating system, bacteria that can use nitrate as electron acceptor were enriched. In the subsequent aerobic period, dissolved oxygen was the electron acceptor and bacteria that strictly require oxygen for urease production could also be enriched in this period. Aeration was provided in reactor by an air pump and an automatic time controller was used to switch between anoxic and aerobic periods. At the end of the aerobic period, 30 minutes settling period was applied to promote settling of the solids prior to refreshing of the nutrient media. Following the 30 minutes of settling period, 900 mL of the reactor volume was refreshed with fresh nutrient media given in Table 3.5. Sodium formate was occasionally replaced with acetic acid (COD concentration was kept constant at 2.35 $g.L^{-1}$) to promote bacterial growth in the reactor. This manual sequencing batch operation enabled production of the non-axenic culture used in MICP treatment tests.

Table 3.5. Composition of nutrient media used in reactor feeding

Chemical	Concentration ($g.L^{-1}$)
Urea (CH_4N_2O)	6.00
Yeast Extract	0.20
NaHCOO	10.00
$NaNO_3$	3.00
KH_2PO_4	0.06
$MgSO_4.7H_2O$	0.10
C:N ratio	4.76*
*C:N ratio is dimensionless	

Surface of recycled aggregates contain residuals from the cementitious materials which results in alkaline pH environment. The inoculum taken from SBR operated in Kardogan (2024) was already alkali-tolerant as it was enriched at pH values higher than 9. Therefore, in this thesis study, to continue the enrichment of alkali-tolerant bacteria, reactor pH was adjusted to around 9.0 by using NaOH.

3.3. Preparation of Sand Mixes from f-RCA for Mortar Tests

In order to conduct tests on mortar specimens, sand mixes (1350 g) were prepared by using f-RCA. The size distribution of the prepared f-RCA sand mixes were similar to the size distribution described for standard sand in DIN EN 196-1, as given in Table 3.6. The f-RCA used in this part of the study was also obtained by re-crushing the concrete initially poured for testing in the Civil Engineering Department at Hacettepe University.

The relevant size ranges were obtained by passing the f-RCA through stainless steel sieves by following the ASTM C136. The four different size ranges of f-RCA used in preparation of sand mix were shown in Figure 3.3.

Obtained aggregates of four different size ranges were further dried in the ventilated oven at 105 °C until they reached a constant weight. Then, these aggregates were mixed in the ratios specified in Table 3.6 to obtain a sand mix of 1350 grams suitable for casting 1 L of mortar according to EN 196-1 standard (Figure 3.4).

Table 3.6. Size distribution and weight ratio in standard sand and f-RCA sand mixes of 1350 g

DIN EN 196-1 standard sand		**f-RCA sand mix**	
Size range	**Percent weight (%)**	**Size range**	**Percent weight (%)**
2.00 mm – 1.60 mm	7	2.00 mm – 1.00 mm	33
1.60 mm – 1.00 mm	26		
1.00 mm – 0.50 mm	34	1.00 mm – 0.50 mm	34
0.50 mm – 0.16 mm	20	0.50 mm – 0.15 mm	20
0.16 mm – 0.08 mm	13	0.15 mm – 0.075 mm	13

Figure 3.3. The four different size groups of f-RCA used in the sand mix

Figure 3.4. f-RCA sand mixes of each 1350 g

3.4. Test on Urea Hydrolysis of Bacteria Before Treatment Setups of Sand Mixes

Before proceeding with the improvement experiments of the f-RCA sand mixes, a batch test was performed to check the urea hydrolysis activity of bacteria. The media composition used with 0.5 g CDW.L^{-1} was consisted of 2.00 g.L^{-1} urea, 0.20 g.L^{-1} yeast, 3.33 g.L^{-1} NaHCOO, 1.00 g.L^{-1} $NaNO_3$, 0.02 g.L^{-1} KH_2PO_4 and 0.10 g.L^{-1} $MgSO_4 \cdot 7H_2O$. The experimental test was conducted in duplicates. The experimental setups conducted under anoxic condition for 24 hours, and at the end of 24 hours, total ammonia nitrogen (TAN) concentrations were measured in the filtered samples.

3.5. Optimization of Microbial Treatment Process for the f-RCA Sand Mixes

In order to cast 1 L of mortar according to EN 196-1 standard, 1350 g sand is used. Therefore, all the optimization studies were conducted by using the prepared 1350 g f-RCA sand mix. The effective treatment condition was determined by making some changes and optimizations in the aforementioned microbial treatment setup used for separate treatment of each size group.

The treatment of f-RCA mix followed a two-stage process: microbial attachment and biomineralization stages, similar to the aforementioned method described for separate treatment of each size group in f-RCA. In microbial attachment stage, two different initial bacteria concentrations (i) 0.1 g CDW.L^{-1} and (ii) 0.3 g CDW.L^{-1}, were tested to avoid the excess use of bacteria and the best performing one was used in further stages of the thesis.

During the treatment, in microbial attachment stage, f-RCA sand mix was immersed in bacteria containing growth media for 72 hours. Subsequently, aggregates were separated from the growth media, and immersed in biomineralization media for another 24 hours. The schematic diagram of treatment is given in Figure 3.5. Water control and abiotic control setups were used for comparison. For the water control setup, tap water was used as growth and biomineralization media. For the abiotic control setup, treatment was conducted by using bacteria free, but not sterile, growth media and biomineralization media.

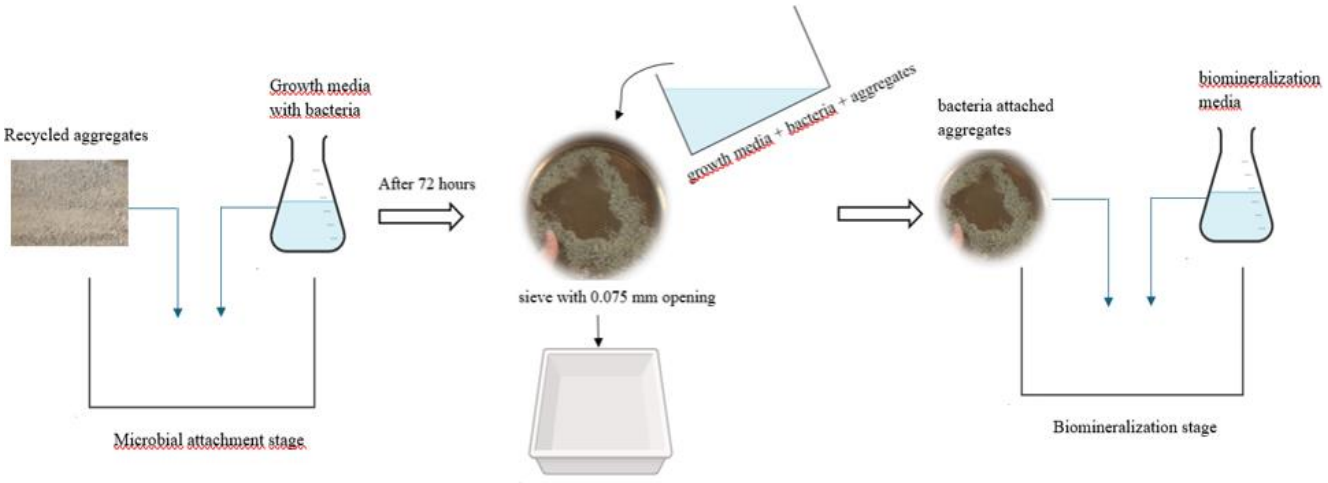

Figure 3.5. Schematic diagram of microbial treatment setup

The f-RCA sand mix (1350 g) was treated in 3 replicates of 450 g at room temperature as shown in Figure 3.6. At each stage (microbial attachment and biomineralization) 3 L of media was used for the treatment of 450 g f-RCA sand mix. Within a few hours of the beginning of both the microbial attachment stage and biomineralization stage, dissolved oxygen was less than 0.2 mg.L^{-1}.

Without any adjustments the pH of the media during microbial attachment stage was around 12.5. This alkaline pH was due to the $Ca(OH)_2$ and CaO content of the used f-RCA [149,150]. Solution pH is important for MICP as it affects microbial activity and $CaCO_3$ solubility. Researchers reported that the pH range in which the urea enzyme is optimally active was between 7.0 - 8.0 [151,152]. In order to standardize the pH conditions in different treatment sequences of 450 g of f-RCA, initial pH of the media used in microbial attachment stage was adjusted to a range between 7.5-8.0 using acetic acid.

Another modification in growth media was the readjustment of the initial nutrient (CH_4N_2O, $NaNO_3$, KH_2PO_4 and NaHCOO) concentrations previously described in Table 3.3 for separate treatment of f-RCA. In order to avoid excess amount of nutrient use, initial urea concentration was decreased from 6.00 $g.L^{-1}$ to 2.00 $g.L^{-1}$, initial NO_3-N concentration was decreased from 0.49 $g.L^{-1}$ to 0.16 $g.L^{-1}$ and initial KH_2PO_4 concentration was decreased from 0.06 $g.L^{-1}$ to 0.02 $g.L^{-1}$ (Table 3.7). As acetic acid was used to adjust pH, dissolved organic carbon became available in the media, thus NaHCOO concentration was also decreased from 10.00 $g.L^{-1}$ to 0.67 $g.L^{-1}$.

In MICP applications, the use of yeast extract as a supplementary nutrient for urea hydrolyzing bacteria is common. Therefore, a separate experiment was conducted to confirm the potential boosting-effect of yeast extract on microbial activity of the non-axenic culture used in this study. Based on the results, to promote the growth, attachment and the activity of bacteria during the MICP treatment of f-RCA sand mix, initial yeast extract concentration in both media was set to 2.0 $g.L^{-1}$. Finally, the NO_3-N concentration, which was lower in the biomineralization media than in the growth media, was increased to 0.26 $g.L^{-1}$ by supplementing with 0.70 $g.L^{-1}$ $NaNO_3$, given that MICP and its improvement predominantly occur during the biomineralization stage. The growth and biomineralization media used in the treatment of f-RCA sand mix were given in Table 3.7.

Figure 3.6. Experimental setup for treatment of f-RCA sand mix

Table 3.7. Differences in growth and biomineralization media used in two different experiments

Chemicals	**Separate treatment of f-RCA size groups**		**f-RCA sand mix treatment**	
	Growth media	**Biomineralization media**	**Growth media**	**Biomineralization media**
Urea (CH_4N_2O)	6.00 $g.L^{-1}$	20.00 $g.L^{-1}$	2.00 $g.L^{-1}$	20.00 $g.L^{-1}$
Yeast Extract	0.20 $g.L^{-1}$	-	2.00 $g.L^{-1}$	2.00 $g.L^{-1}$
$Ca(HCOO)_2$	-	6.50 $g.L^{-1}$	-	6.50 $g.L^{-1}$
$Ca(NO_3)_2.4H_2O$	-	1.20 $g.L^{-1}$	-	1.20 $g.L^{-1}$
NaHCOO	10.00 $g.L^{-1}$	-	0.67 $g.L^{-1}$	-
$NaNO_3$	3.00 $g.L^{-1}$	-	1.00 $g.L^{-1}$	0.70 $g.L^{-1}$
KH_2PO_4	0.06 $g.L^{-1}$	-	0.02 $g.L^{-1}$	-
$MgSO_4 \cdot 7H_2O$	0.10 $g.L^{-1}$	-	0.10 $g.L^{-1}$	-

In a separate batch experiment, the effect of yeast extract on microbial activity was examined by monitoring urea hydrolysis activity. In total, four different yeast extract concentrations; (i) 0.2 $g.L^{-1}$, (ii) 0.5 $g.L^{-1}$, (iii) 1 $g.L^{-1}$, (iv) 2 $g.L^{-1}$ were tested. Each test was conducted in triplicates as shown in Figure 3.7. Initial bacteria concentration in batch tests was set to 0.5 g $CDW.L^{-1}$. The experimental setups were carried out with in 100 mL tightly closed serum bottles with an effective test volume of 50 ml. The used nutrient media in experimental setups contained 2.00 $g.L^{-1}$ urea, 3.33 $g.L^{-1}$ NaHCOO, 1.00 $g.L^{-1}$ $NaNO_3$, 0.02 $g.L^{-1}$ KH_2PO_4, 0.10 $g.L^{-1}$ $MgSO_4 \cdot 7H_2O$ and the yeast extract specific to each test. The experimental setups were carried out under anoxic condition for 24 hours, and at the end of 24 hours, TAN concentrations were measured in the filtered samples.

Figure 3.7. Batch tests for investigating the effect of yeast extract on microbial activity

3.5.1. Microbial Activity Analysis During f-RCA Sand Treatment

During the treatment, samples were taken from growth media at t=0 h, t=24 h and t=72 h, and from biominerilization at t=0 h and t=24 h to monitor the microbial activity of bacteria. Taken samples were filtered through 0.45 µm syringe filters and stored at +4°C for further analyses. TAN and Ca^{2+} were analyzed in samples.

Since TAN production during treatment of f-RCA results from urea hydrolysis, the efficiency of urea hydrolysis was determined by TAN analysis. TAN analyzes were performed according to standard methods coded as 4500-NH3 Step-B, C. The titration

process was carried out using 0.02 N sulfuric acid as a titrant [153]. Ca^{2+} analysis was carried out using the atomic absorption spectroscopy (Perkin Elmer Inc., AAnalyst 800, USA) device in the Environmental Engineering Department of Hacettepe University.

3.6. Tests on Commercially Available fRCA

After the tests on the improvement of f-RCA obtained from Civil Engineering Department of Hacettepe University, the improvement tests of aggregates on a sectoral basis was implemented by procuring fRCA from a ready-mix concrete company that has a large cement and building materials factory in Turkey. Sand mix of 1350 g was prepared from this commercially available fRCA (c-fRCA) by following the procedure described in section 3.3. Prepared c-fRCA sand mix were further treated by following the optimized treatment procedure described in section 3.5 and microbial activity was confirmed by conducting the tests described in section 3.5.1. Additionally, NO_3-N analysis was also performed on the samples to confirm microbial activity. HACH, LCK 340 test kits (5-35 $mg.L^{-1}$ NO_3-N) were used for nitrate analysis.

3.7. Assessment of Mortar Specimens Containing Treated fRCA

This part of the thesis was aimed at understanding the change in the quality of mortar specimen containing treated fRCA. The mortar specimens containing treated f-RCA sand mixes and treated c-fRCA sand mixes were examined separately.

The effect of f-RCA sand was examined by comparing two different groups of mortars: (i) untreated-fRAM and (ii) microbial treated-fRAM. In the untreated-fRAM groups, 1350 g of untreated f-RCA sand mix, tap water and Portland cement were used. In the microbial treated-fRAM groups, 1350 g of f-RCA sand mix which was obtained after microbially treatment, tap water and Portland cement were used. No chemical admixtures were used in any of the fRAM groups. fRAM specimens were prepared in accordance with EN 196-1 standard. Since fRA had relatively higher water absorption [18,154], mortar specimens containing untreated f-RCA sand mixes (untreated-fRAM) poured with w/c ratio of 0.50 were not appropriate to obtain a workable mix. There were also studies in the literature that mortar specimens with w/c ratios different from 0.5:1.0 tested [16]. Therefore, the w/c ratio of the fRAMs were rearranged based on the workability of untreated-fRAM. Untreated-fRAM were prepared with w/c ratios of 0.60, 0.65 and 0.70 and the appropriate w/c ratio to be used in the comparisons was determined as 0.65.

The effect of c-fRCA was quantified by comparing six different groups of mortars: (i) reference 0.50-NAM, (ii) reference 0.65-NAM, (iii) water control-cfRAM, (iv) abiotic control-cfRAM, (v) microbial treated-cfRAM and (vi) untreated-cfRAM. In the preparation of reference NAM groups, 1350 g of DIN EN 196-1 standard sand, tap water and CEM I 42,5 R Portland cement were used. In the untreated cfRAM groups, 1350 g of untreated c-fRCA sand mix, tap water and Portland cement were used. In other cfRAM groups (water control, abiotic control, microbial treated), 1350 g of c-fRCA sand mix which was obtained after a relevant treatment, tap water and Portland cement were used. No chemical admixtures were used in any of the mortar specimens. The compositions of the mortars were summarized in Table 3.8. Mortar specimens were prepared in accordance with EN 196-1 standard and the w/c ratio of mortars were 0.65. In order to clarify the effect of w/c ratio on mechanical properties of reference mortar containing standard sand (NAM), reference mortar tests were conducted at both 0.50 and 0.65 w/c ratios.

Table 3.8. Mortar types and their descriptions

Mortar specimen group	Description
Water control-cfRAM	Mortar mixture prepared with aggregate: cement: water ratio of 3.0: 1.0: 0.65. Mortar components including; 1350 g of water treated c-fRCA sand mix, 450 g of CEM I 42,5 R Portland cement, and 292,5 g of tap water.
Abiotic control-cfRAM	Mortar mixture prepared with aggregate: cement: water ratio of 3.0: 1.0: 0.65. Mortar components including; 1350 g of abiotically treated c-fRCA sand mix, 450 g of CEM I 42,5 R Portland cement, and 292,5 g of tap water.
Microbial treated-cfRAM	Mortar mixture prepared with aggregate: cement: water ratio of 3.0: 1.0: 0.65. Mortar components including; 1350 g of microbially treated c-fRCA sand mix, 450 g of CEM I 42,5 R Portland cement, and 292,5 g of tap water.

Untreated-cfRAM	Mortar mixture prepared with aggregate: cement: water ratio of 3.0: 1.0: 0.65. Mortar components including; 1350 g of untreated c-fRCA sand mix, 450 g of CEM I 42,5 R Portland cement, and 292,5 g of tap water.
Reference 0.65-NAM	Mortar mixture prepared with sand: cement: water ratio of 3.0: 1.0: 0.65. Mortar components including; 1350 g of DIN EN 196-1 standard sand, 450 g of CEM I 42,5 R Portland cement, and 292,5 g of tap water.
Reference 0.50-NAM	Mortar mixture prepared with sand: cement: water ratio of 3.0: 1.0: 0.5. Mortar components including; 1350 g of DIN EN 196-1 standard sand, 450 g of CEM I 42,5 R Portland cement, and 225 g of tap water.

While preparing the all mortar groups, the mixing procedure in accordance with EN 196-1 standard was followed. Casting of fRAMs were carried out using 50 x 50 x 50 mm (cubic) molds and casting of cfRAMs and NAMs were carried out using 40 x 40 x 160 mm (beam) molds as shown in Figure 3.8. The mortars poured into the molds was covered with a wet cloth and cured for 24 hours. At the end of the first 24 hours, the mortars were demoulded and water curing was applied until the test day. During the water cure, the mortars were kept at room temperature. The photograph of water curing for the beam mortar specimens were given in Figure 3.9.

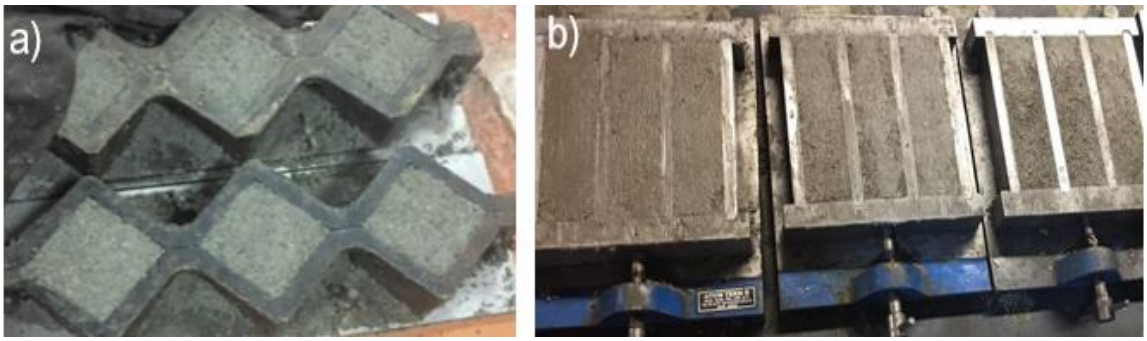

Figure 3.8. Mortar casting with (a) cubic molds and (b) beam molds

Figure 3.9. Water cured beam mortar specimens

Compressive strength tests were conducted on 50 mm cubic specimens in accordance with the ASTM C109 standard after 7 days and 28 days of curing periods. UTC-5700, Turkey compressive strength test machine with a capacity of 100 kN was used. The loading rate in the test was 0.9 $kN.s^{-1}$.

For beam specimens, compressive strength and flexural strength tests were conducted after 3 days, 7 days and 28 days of curing periods. Compression device with a capacity of 300 kN was used in accordance with the ASTM C 349 standard and the loading rate in the test was 0.9 $kN.s^{-1}$. Beam mortar specimens were tested for flexural strength with three-point bending test in accordance with ASTM C 348 standard (Figure 3.10). After the flexural strength test, the beams were divided into two pieces and had a cross-sectional area of 4*4 cm^2, and then the compressive strength test of the two pieces was performed according to ASTM C 349 (Figure 3.10). For each type of beam mortar specimens, two replicates were used for flexural strength testing, and four pieces obtained from beams tested with flexural strength were used for compressive strength testing.

Figure 3.10. Flexural strength test (a) and compressive strength test (b) of beam mortars

3.8. Scanning Electron Microscopy Analysis

Changes in microstructural properties of microbially treated f-RCA sand mix and c-fRCA sand mix were visualized under scanning electron microscope (SEM). Before imaging of each aggregates, random samples were taken from the treated sand mixes. For c-fRCA, randomly taken samples were sieved into 3 sizes: 2.00–1.00 mm, 1.00–0.50 mm and 0.50–0.075 mm. Sample taken from f-RCA mixes and 3 different sizes of c-fRCA were then coated with gold and micrographs of aggregates were obtained with Tescan GAIA3+Oxford XMax 150 EDS (Figure 3.11).

Additionally, the elemental composition of minerals in the treated c-fRCA were mapped applying energy dispersive X-ray spectroscopy (EDS).

Figure 3.11. SEM combined with energy dispersive X-ray spectroscopy

3.9. Fourier Transform Infrared Spectroscopy Analysis

Fourier Transform Infrared Spectroscopy (FTIR) analysis was performed on untreated, abiotically treated and microbially treated c-fRCA sand. Each c-fRCA sand was seperately ground by using a mortar and a pestle to remove surface attached compounds and minerals. The obtained powder (<5 mg) from each c-fRCA sand was further dried in the ventilated oven at 105 °C for 1 hour and then characterized by FTIR (Shimadzu IRSpirit). FTIR spectra were obtained from 20 scans at 4 cm^{-1} resolution for wavenumbers ranging between 600–4000 cm^{-1}.

3.10. Statistical Analysis

The test results were presented as mean and standard deviation values. The results were compared among themselves using one-way ANOVA analysis ($p<0.05$) in SigmaPlot 14.0 software.

4. RESULTS AND DISCUSSION

4.1. Improvement of Different Size Groups of f-RCA via MICP

A two-stage MICP improvement method, including microbial attachment and biomineralization, was applied to f-RCA of six different sizes range. Initially, f-RCA were immersed in a growth media containing 0.5 g CDW.L^{-1} bacteria to provide bacterial growth within the aggregate pores. In the biomineralization stage, calcium, urea, and nitrate were provided to the adhered bacteria to achieve $CaCO_3$ precipitation. The effect of the applied improvement method was evaluated through changes in water absorption and in weight of the f-RCA, as in the literature [15,17].

4.1.1. Variation in Water Absorption of f-RCA Based on Size Groups

Water absorption of f-RCA before and after the microbial treatment were evaluated based on their particle size group as shown in Figure 4.1. Initial water absorption of fine aggregates (<4.750 mm) was higher than the coarse aggregates (>4.750 mm). The aggregates size and the measured water absorption appeared to be inversely proportional (Figure 4.1). The water absorption of the aggregates increased as its size decreased. This result was consistent with studies in the literature indicating that fRA have higher water absorption [154]. Before treatment, the highest water absorption was determined as 21.40±0.62% and belonged to the fRCA with sizes smaller than 0.075 mm, and the lowest water absorption was determined as 4.23±0.07% and belonged to the cRCA with sizes larger than 4.750 mm. Recycled fine aggregates smaller than 0.075 mm are in powder form and this fRA powder are generally considered undesirable materials due to their high water absorption capacity [155]. However, these materials were found to have a filler effect that reduces porosity and contributes to the improvement of mechanical properties of concrete, such as durability and compressive strength, by increasing the density of concrete [156]. Additionally, the use of fRA powder improved hydration capacity and caused lower chloride penetration through capillary action [157]. However, excessive use had the opposite effect; using more than 30% reduced the freeze-thaw resistance of concrete, increased water absorption, and reduced compressive strength of concrete [157–159].

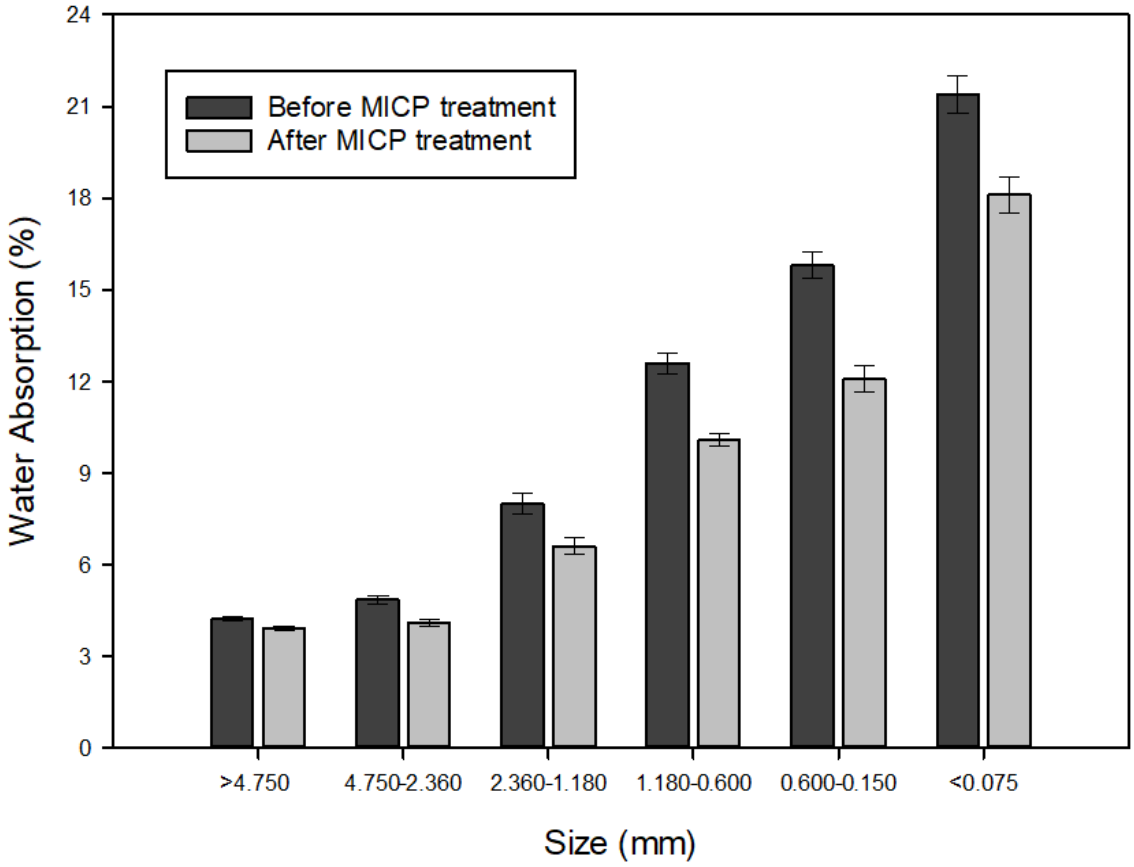

Figure 4.1. Water absorption of f-RCA according to their size before and after MICP treatment

A significant reduction in water absorption of all f-RCA sizes was achieved after microbial treatment setup ($p<0.05$), while no significant improvement was observed in the water absorption of f-RCA after the water control and abiotic control setups. As seen in Figure 4.1, after microbial treatment the least water absorption was 3.92±0.06% which was achieved for aggregates larger than 4.750 mm. Considering the water absorption values before and after the treatment of aggregates larger than 4.750 mm, microbial treatment resulted in 7.33±0.25% decrease in water absorption of the aggregates. This decrease was attributed to the microbial induced $CaCO_3$ precipitation occurred on the surface or in the pores of aggregates.

The decrease in water absorption (%) of aggregates due to the treatment varied according to the aggregate sizes. Reductions in water absorption according to sizes were given in Figure 4.2. The decreases in water absorption of f-RCA due to the treatment were recoreded as 15.34±0.15% in the size range of 4.750 mm - 2.360 mm, 17.40±0.30% in the size range of 2.36 mm - 1.180 mm, 20.00±0.67% in the size range of 1.180 mm - 0.600 mm, 23.53±0.69% for the size range 0.600 mm - 0.150 mm and 15.42±0.80% for sizes <0.075 mm. It was observed that except for the aggregates smaller than 0.075 mm, the decrease in water absorption increased as the aggregate size decreased.

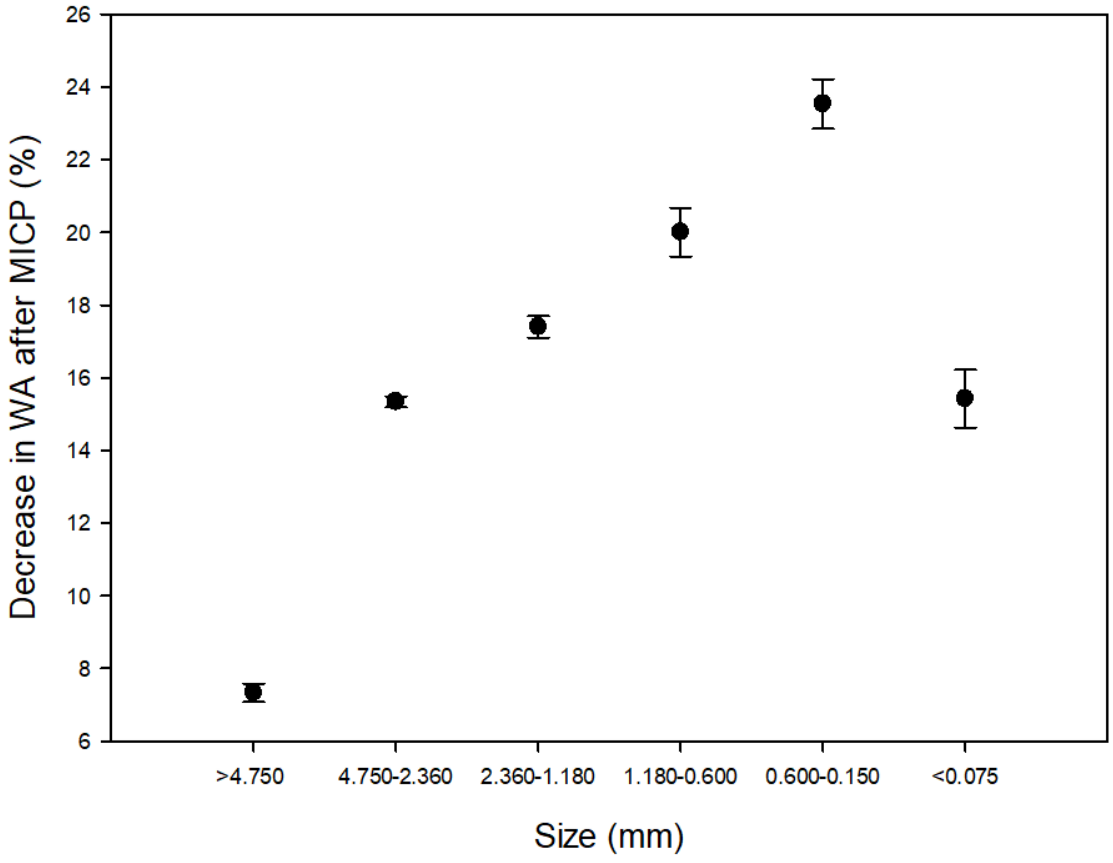

Figure 4.2. Decrease in water absorption (%) according to aggregate dimensions after MICP improvement

While no significant decrease in water absorption could be observed in water control and abiotic control, the fact that this was achieved only after microbial treatment showed that the quality increase in the f-RCA was due to microbial-induced $CaCO_3$ precipitation. $CaCO_3$ formed a barrier by filling/blocking the pores and microcracks on the f-RCA surface, and this barrier caused a decrease in water ingress from pores of aggregates

[17,18]. In previous studies, water absorption of coarse-sized RCA, in size between 6.3-20.0 mm, decreased by about 10% after a 3-day biodeposition treatment [18]. Qiu et al. reported up to 15% decrease in water absorption of cRCA after 3-day MICP treatment [17]. In a study on fRA obtained from wall building materials, the decrease in water absorption of modified fRA varied according to MICP treatment time [145].The decrease in the water absorption of fRA (size between 0.1-5.0 mm) after MICP with 3 days and 7 days was 22.0% and 27.3%, respectively [145]. Although the wider size ranges of the recycled aggregates examined in the previous studies, the decreases in the water absorption obtained in this study were close to those obtained in the literature. The findings obtained in this research support the literature and showed that the MICP process could effectively reduce the water absorption of fRCA.

The limit for water absorption of aggregates used in structural concrete is 5% [85], and BS 8007 standard determines this limit as 3% [160]. According to global legislation, the standards for the use of RCA in concrete production were also summarized in Table 4.1.

Table 4.1. Legislation on the use of RCA in concrete production in the world [161,162]

Country	**Maximum replacement ratio (%)**	**Fraction of RCA**	**Type of concrete**	**Strength Class**	**Water absorption of RCA (%)**
Belgium PTV 406–2003/ NBN B 15–001	50	-	structural	C30/37	9
ItalyNTC-2008	60	coarse	structural	C25/30	-
China GB/T-2573	100	coarse	structural	no limit	3
	100	fine	structural	C40/50	3
Japan JIS-5021/ JIS-5022/ JIS-5023	100	coarse and fine	structural	C45/55	3 for coarse 3.5 for fine
	100	coarse and fine	structural	C35/45	5 for coarse

					7 for fine
	no limit	coarse and fine	non-structural	-	-
Denmark DS 2426/DCA No.34	100	coarse and fine	structural	C40/50	-
Brazil NBR 15116	100	coarse and fine	non-structural	-	-

In Belgium, RCA with water absorption up to 9% can be used in structural concrete of class C30/37 by replacing with 50% of NA. According to Japanese standards, fRCA with water absorption up to 3.5% can fully replace NA in the production of structural concrete of class C45/55. Also, in the production of class C35/45 structural concrete, fRCA with up to 7% water absorption can be entirely used instead of NA. Additionally, Japanese and Brazilian standards permit the use of fRCA as a 100% replacement in non-structural concretes without specifying a limit on the water absorption of RCA. In this case, after MICP treatment, it seems feasible to use f-RCA with a size of 1.180 mm and above in the production of structural concrete. However, the water absorption of smaller-sized f-RCA (especially smaller than 0.600 mm) remains significantly above the permissible limits even after MICP treatment, making them more suitable for use in non-structural concrete production.

4.1.2. Weight Increase in Different Size of f-RCA After Improvement

MICP process was expected to form insoluble calcium carbonate minerals on the aggregate surface. Therefore, after a successful MICP treatment weight increase could be achieved. After the water control treatment and abiotic control treatment, no significant weight increase was obtained in the f-RCA. Contrarily, after MICP treatment, regardless of the sizes, weight increase was observed in all f-RCA. An overview of the weight increase (%) of f-RCA before and after MICP were presented in Figure 4.3.

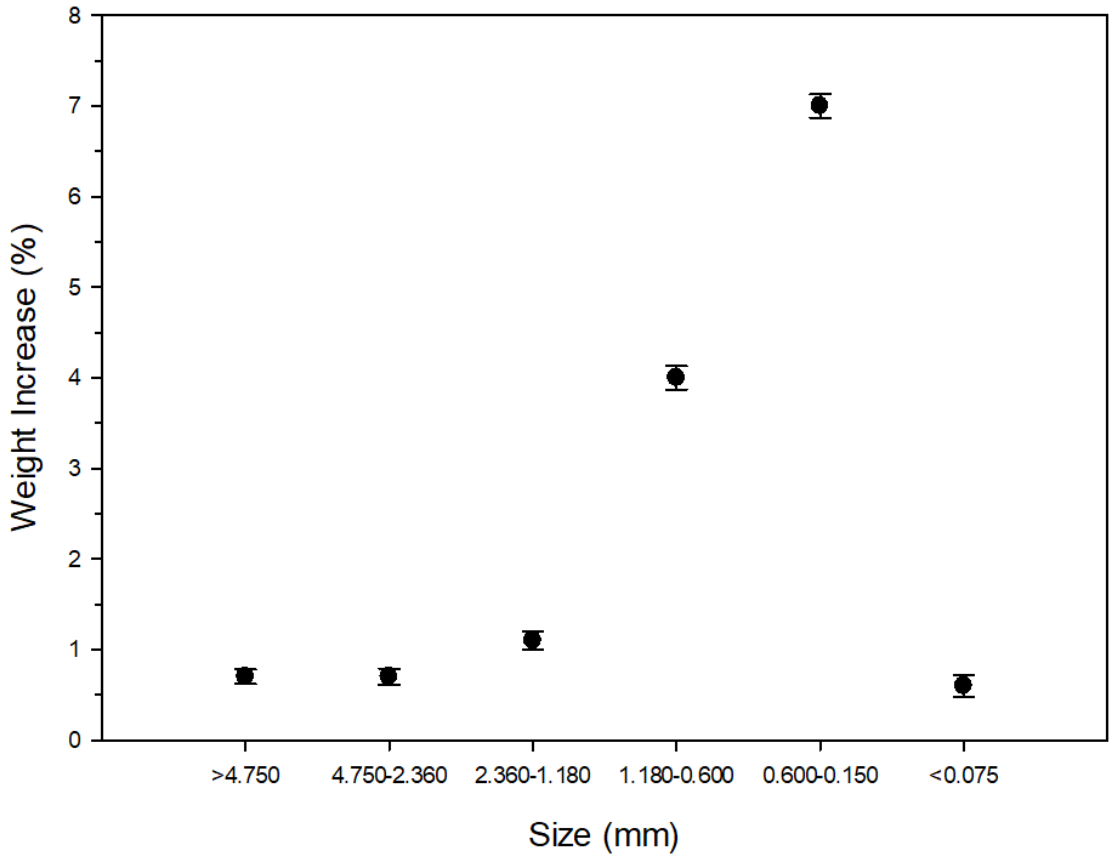

Figure 4.3. Weight increase according to aggregate size after MICP treatment

After the MICP process, the average weight increases resulted in the largest size of the aggregates to the smallest size were 0.7±0.08%, 0.7±0.09%, 1.1±0.10%, 4.0±0.13%, 7.0±0.13%, 0.6±0.12%, respectively. These weight differences obtained after treatment were due to the additional weight of biodeposition ($CaCO_3$ precipitation) occurring on the surface and/or pores of the aggregate. Aggregates smaller than 0.075 mm were very small particles and some mass loss might have occurred in the experimental procedure whilst transferring aggregates between containers, as they stuck to the container surface, spatula and filter paper during vacuum filtration. This may have caused less weight increase in aggregates smaller than 0.075 mm. It should be noted that the weight change was still positive despite the possible mass loss.

A significant decrease in the water absorption of f-RCA and an increase in the weight of the f-RCA after the applied improvement method confirmed the suitability and effectiveness of the method used. The results in this section showed that the MICP method was effective for improving the quality of f-RCA by improving the surface properties of them.

4.2. Effect of Different Yeast Extract Concentrations on Urea Hydrolysis

In MICP applications with urea hydrolyzing bacteria, it is quite common to use yeast extract as a supplementary nutrient [163]. The inclusion of yeast extract in the media could facilitate the proliferation of adsorbed bacteria on/within the aggregates surface, and this could lead to a substantial increase in the amount of precipitated $CaCO_3$ [18]. The aim of this batch test was to examine the potential effect of different yeast extract concentrations on urea hydrolysis activity. In this setup, four different yeast extract concentrations ranging between 0.2-2.0 $g.L^{-1}$ were tested. The bacterial concentration used in each test setup was 0.5 g $CDW.L^{-1}$. Setups were carried out under anoxic conditions for 24 hours, and TAN analyzes were performed at the beginning and end of the test. The TAN concentrations and urea hydrolysis obtained at different initial yeast extract concentrations were given in Figure 4.4.

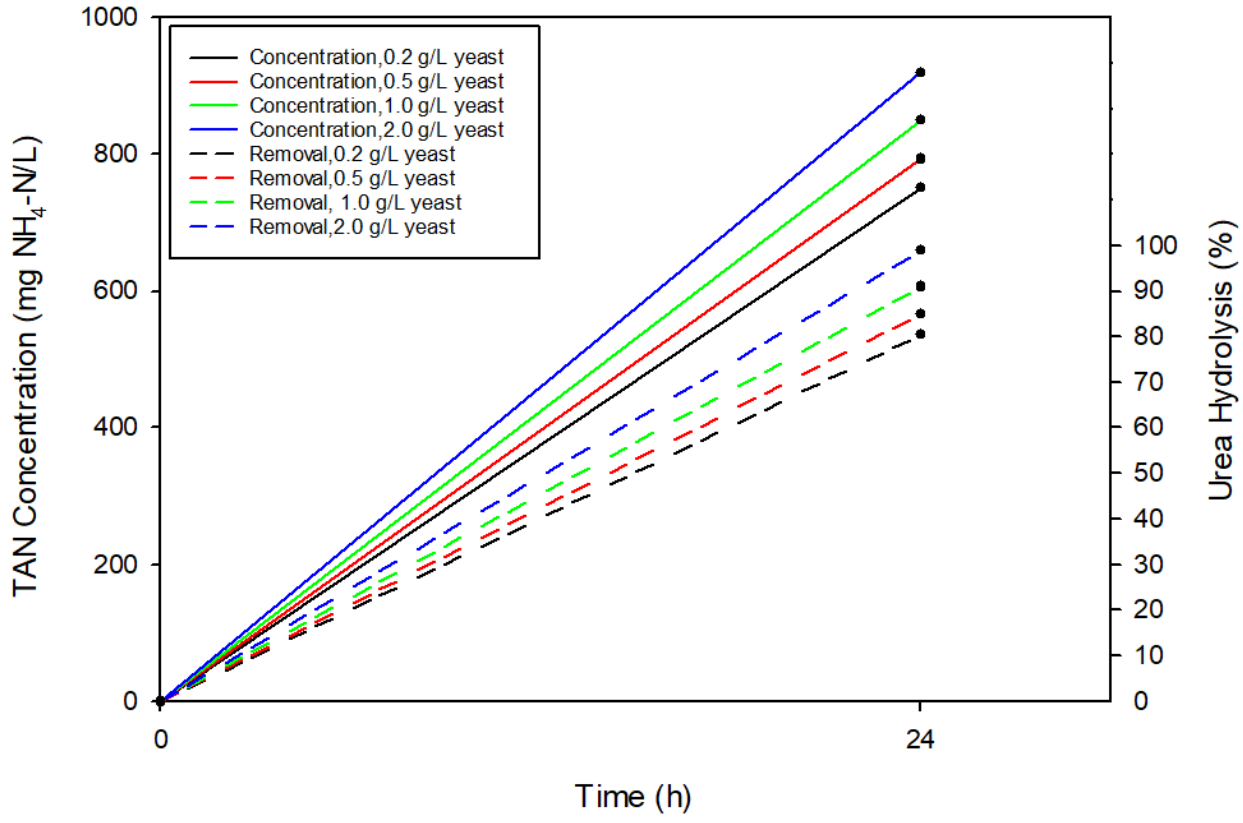

Figure 4.4. TAN concentrations and urea hydrolysis (%) obtained at different yeast concentrations

As yeast extract concentration increased from 0.2 $g.L^{-1}$ to 2.0 $g.L^{-1}$, the achieved TAN concentration increased indicating the positive effect of yeast extract on urea hydrolysis activity. The average TAN concentrations obtained at the end of 24 hours were 751.3±8.1 $mg.L^{-1}$, 793.3±8.1 $mg.L^{-1}$, 849.7±8.4 $mg.L^{-1}$ and 919.3±8.1 $mg.L^{-1}$, respectively, from low yeast extract concentration (0.2 $g.L^{-1}$) to high yeast extract concentration (2.0 $g.L^{-1}$). Initial urea concentration in these tests was 2.0 $g.L^{-1}$ and identical in all batches. Theoretically, the maximum TAN concentration that could occur as a result of 100% urea hydrolysis was 933 $mg.L^{-1}$. The average urea hydrolysis (%) obtained at the end of 24 hours were 80.5±0.9%, 85.0±0.9%, 91.0±0.9% and 98.5±0.9%, respectively, from low yeast extract concentration to high concentration. It was observed that almost all of the urea was consumed at 2.0 $g.L^{-1}$ yeast extract concentration.

4.3. Urea Hydrolysis Performance of Bacteria Before MICP

Urea hydrolysis of non-axenic culture was controlled by performing a batch test with 0.5 g $CDW.L^{-1}$ before MICP of f-RCA sand mix. Initial urea concentration was 2.0 $g.L^{-1}$, and initial yeast extract concentration was 0.2 $g.L^{-1}$. Batch test was performed for 24 hours under anoxic condition. TAN concentration and urea consumption at the end of 24 hours were summarized in the Table 4.2.

Table 4.2. Urea hydrolysis results under anoxic condition at the end of 24 h

Time (h)	TAN concentration (mg NH_4-$N.L^{-1}$)	Urea hydrolysis (%)
0	0 ± 0	0 ± 0
24	763 ± 9.9	81.7 ± 1.1

The initial TAN concentration was measured as 0±0 $mg.L^{-1}$ and the measured TAN concentration at the end of 24 hours increased to 763±9.9 $mg.L^{-1}$. Theoretically, the TAN concentration that could occur as a result of complete urea hydrolysis was 933 $mg.L^{-1}$. TAN results indicated that the urea consumption of bacteria reached to 81.7±1.1% after 24 hours under anoxic conditions. Additionally, the average 763±9.9 $mg.L^{-1}$ TAN concentration obtained in this test was almost similar to the 751.3±8.1 $mg.L^{-1}$ TAN

results obtained with 0.2 $g.L^{-1}$ yeast extract in the test of the effect of yeast extract on urea hydrolysis (Figure 4.4). This showed that the bacteria had a stable urea hydrolysis performance under same conditions.

4.4. Increasing the Quality of f-RCA Sand Mixes with the Optimized Process

After seeing the positive effect of the MICP on the quality of the aggregates in the treatment tests with f-RCA of different sizes, the effective treatment condition of f-RCA sand mixes was determined by making some changes and optimizations in the treatment process.

In the treatment process, 1350 g of f-RCA sand mixes were divided into 3 replicates of 450 g each. For each replicate, 3 liters of growth media with two different initial bacterial concentrations (0.1 and 0.3 g $CDW.L^{-1}$) were used. Biomineralization media was identical in all batches. Microbial activity during treatment was examined based on urea hydrolysis and dissolved calcium concentration results, and the weight changes of RCA sand mixes due to the treatment were compared among each other.

4.4.1. Urea Hydrolysis During Treatments

Urea hydrolysis was assessed by monitoring the change in TAN concentration. To ensure that changes in TAN concentration accurately reflected urea hydrolysis, it was checked that the bacteria did not exhibit nitrification in aerobic conditions or anammox in anaerobic environments.

Changes in TAN concentrations in the microbial attachment stage and biomineralization stage of f-RCA sand mixes during water control treatments, abiotic control treatments, and microbial treatments with both 0.1 g $CDW.L^{-1}$ and 0.3 g $CDW.L^{-1}$ were given in Figure 4.5. Urea hydrolysis (%) during the treatment groups were given in Figure 4.6. It should be noted that in microbial attachment and biomineralization stages the initial urea concentrations were 2.0 $g.L^{-1}$ and 20.0 $g.L^{-1}$, respectively.

During the water treatment of f-RCA sand mixes, no TAN production was observed as expected. Within the abiotic control group, the TAN concentration was 0 $mg.L^{-1}$ at the initial of the microbial attachment stage; however, after 72 hours, TAN concentration of 56.0±0 $mg.L^{-1}$ was recorded and TAN concentration of 88.7±8.1 $mg.L^{-1}$ was observed at the end of biomineralization stage. The treatment process was carried out in a clean conditions, but the growth and biomineralization media and equipment used were not

sterile. This unsterile conditions may have caused some microorganisms to grow during the treatment and resulted in low concentrations of TAN along with urea hydrolysis in abiotic group.

In the microbial treatment, the initial TAN concentration measured at the microbial attachment stage was 0 $mg.L^{-1}$. In tests, theoretically, the maximum TAN concentrations that could occur due to the complete hydrolysis of 2 $g.L^{-1}$ and 20 $g.L^{-1}$ urea is 933 $mg.L^{-1}$ and 9333 $mg.L^{-1}$, respectively. In the treatment test containing 0.1 g $CDW.L^{-1}$, at the end of 24 hours and 72 hours in microbial attachment stage, TAN concentrations of 270.7±16.2 $mg.L^{-1}$ and 328.0±17.4 $mg.L^{-1}$ were recorded, respectively (Figure 4.5). Therefore in this treatment, 29.0±1.7% and 35.1±1.9% of the urea were hydrolyzed at the end of 24 hours and 72 hours, respectively (Figure 4.6).

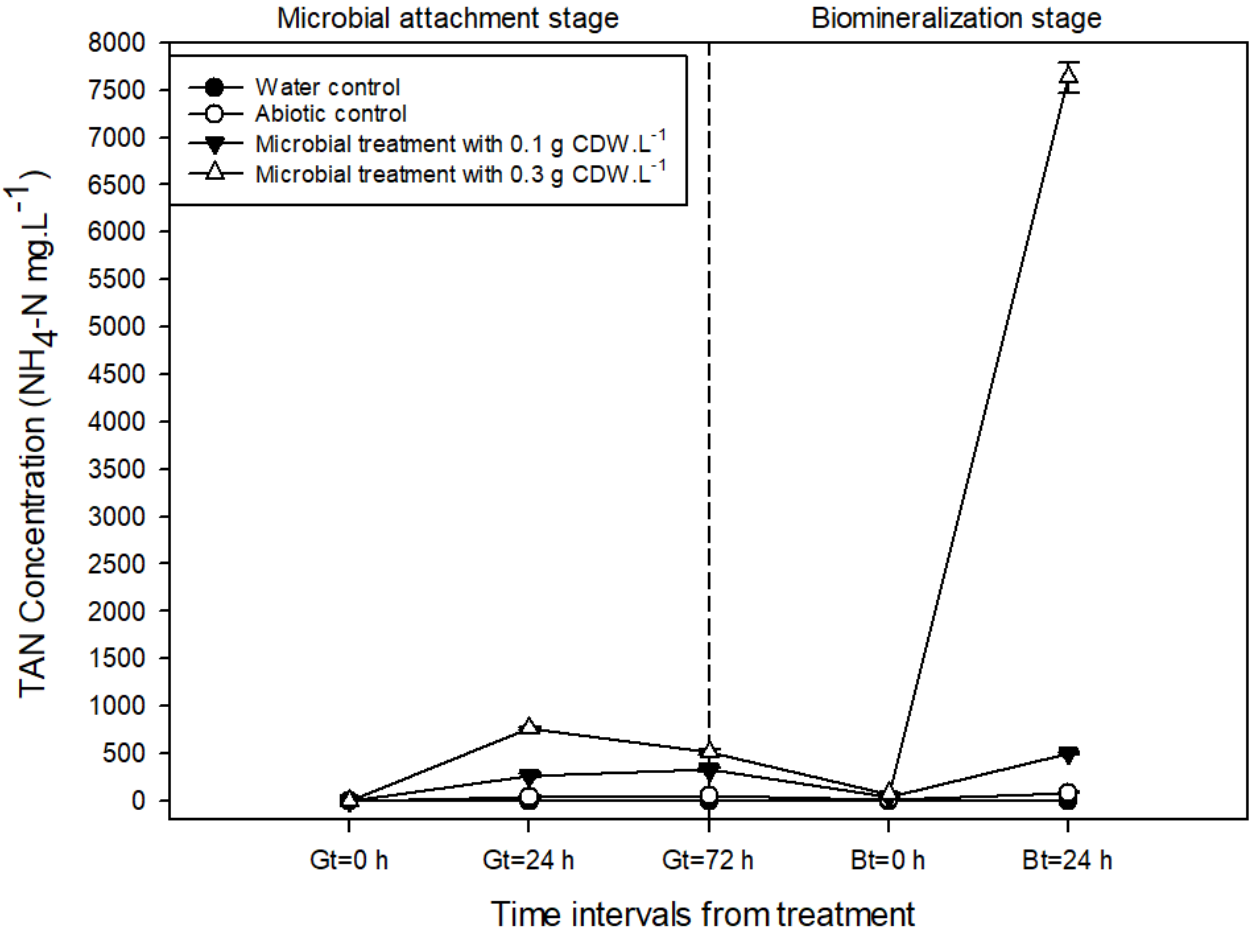

Figure 4.5. Comparison of TAN concentrations during treatments with 0.1 g $CDW.L^{-1}$ and 0.3 g $CDW.L^{-1}$; Gt=0 h) 0^{th} hour of microbial attachment stage, Gt=24 h) 24^{th} hour of microbial attachment stage, Gt=72 h) 72^{th} hour of microbial attachment stage, Bt=0 h) 0^{th} hour of biomineralization stage, Bt=24 h) 24^{th} hour of biomineralization stage

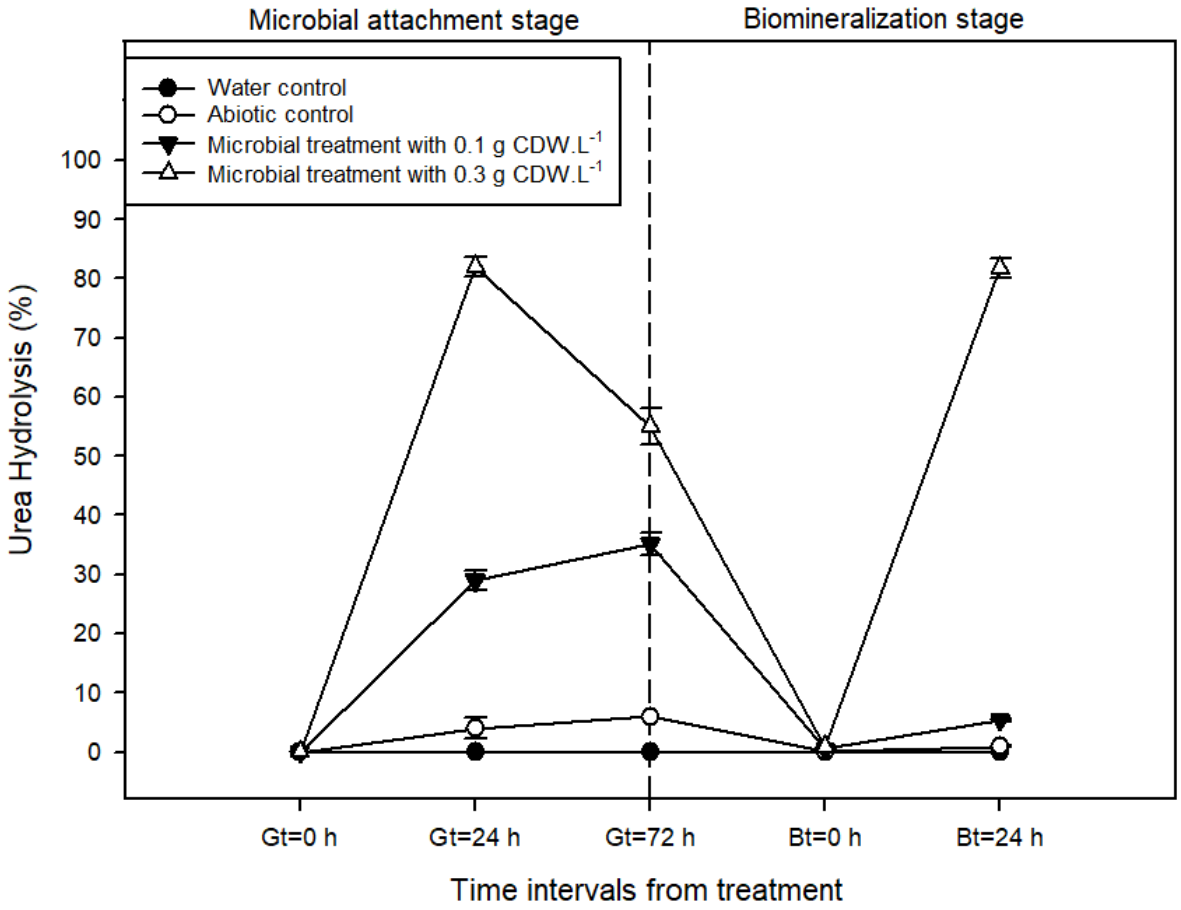

Figure 4.6. Urea hydrolysis during treatments with 0.1 g CDW.L^{-1} and 0.3 g CDW.L^{-1}

In the microbial treatment, during the biomineralization stage, TAN concentration rose from 0 mg.L^{-1} to 500.7±16.2 mg.L^{-1} after 24 hours which corresponded to 5.4±0.2% urea hydrolysis efficiency. In the treatment test containing 0.3 g CDW.L^{-1}, at the end of 24 hours in microbial attachment stage, TAN concentration of 765.3±16.2 mg.L^{-1} were recorded (Figure 4.5). This corresponds to 82.0±1.7% urea hydrolysis efficiency (Figure 4.6). A decrease in TAN concentration was observed at the end of the microbial attachment stage, and the TAN concentration recorded after 72 hours was 513.3±29.1 mg.L^{-1}. In the treatment with 0.3 g CDW.L^{-1}, the TAN concentration was 7629.0±162.0 mg.L^{-1} after 24 hours of the biomineralization stage which corresponded to 81.7±1.7% urea hydrolysis efficiency.

The observed decrease in NH_4^+ concentration at the end of 72 hours of the microbial attachment stage in treatment with 0.3 g CDW.L^{-1}, might be attributed to the conversion of ammonium nitrogen into free ammonia due to elevated pH levels. In aqueous solutions,

ammonia nitrogen consists of two main forms, ammonium ion (NH_4^+) and free ammonia (NH_3).Ammonium is an ionized form that remains soluble in water, whereas free ammonia is a gaseous chemical. The relationship between ammonium ion and free ammonia is reversible as expressed in Equation 4.1.

$$NH_4^+ + OH^- \leftrightharpoons NH_3 + H_2O \quad \text{(Equation 4.1)}$$

The concentrations of NH_3 and NH_4^+ in a solution are influenced by the pH and temperature of the solution. Among these factors, pH has a greater impact on NH_3 concentration than temperature. At higher pH levels, the equilibrium shifts to the right, favoring the formation of NH_3, whereas at lower pH levels, the equilibrium shifts to the left, favoring the formation of NH_4^+. The concentration of free ammonia nitrogen (FAN) can be calculated using the dissociation constant of ammonium, as provided in Equation 4.2 [164–166]

$$FAN\ \left(\frac{mg}{L}\right) = \frac{\text{TAN}}{1+\frac{[H^+]}{Ka}} = \frac{\text{TAN}\ (\frac{\text{mg}}{\text{L}})}{1+10^{(pKa-pH)}} \quad \text{(Equation 4.2)}$$

The rise in pH levels during treatment leads to a decrease in the pKa value, resulting in a decrease in NH_4^+ concentration and an increase in FAN concentration over time. The pH values at microbial treatment with 0.3 g CDW.L^{-1} were given in Table 4.3.

Table 4.3. The pH values during microbial treatment

Stages of microbial treatment	pH values
Microbial attachment, t=0 h	7.8±0.1
Microbial attachment, t=24 h	9.3±0.1
Microbial attachment, t=72 h	9.5±0.1
Biomineralization, t=0 h	8.3±0.1
Biomineralization, t=24 h	9.1±0.1

In the system where 2.0 g.L^{-1} of urea is supplied, the variation in NH_3 and NH_4^+ concentrations according to pH at room temperature (20 °C) is illustrated in Figure 4.7. At a pH of 7.5, NH_3 constitutes 1.2% of the total ammonia nitrogen, and as the pH increases to 9.5, this NH_3 ratio escalates to 55.7%, consequently reducing the NH_4^+ concentration to 414 mg.L^{-1}. The decrease in TAN concentration obtained as a result of the microbial treatment experiment is compatible with the illustrated FAN concentration

in Figure 4.7. These results indicate that NH_4^+ converts to free ammonia due to high pH, supporting the possibility that NH_3, in its gaseous form, may have escaped from the aqueous solution over time.

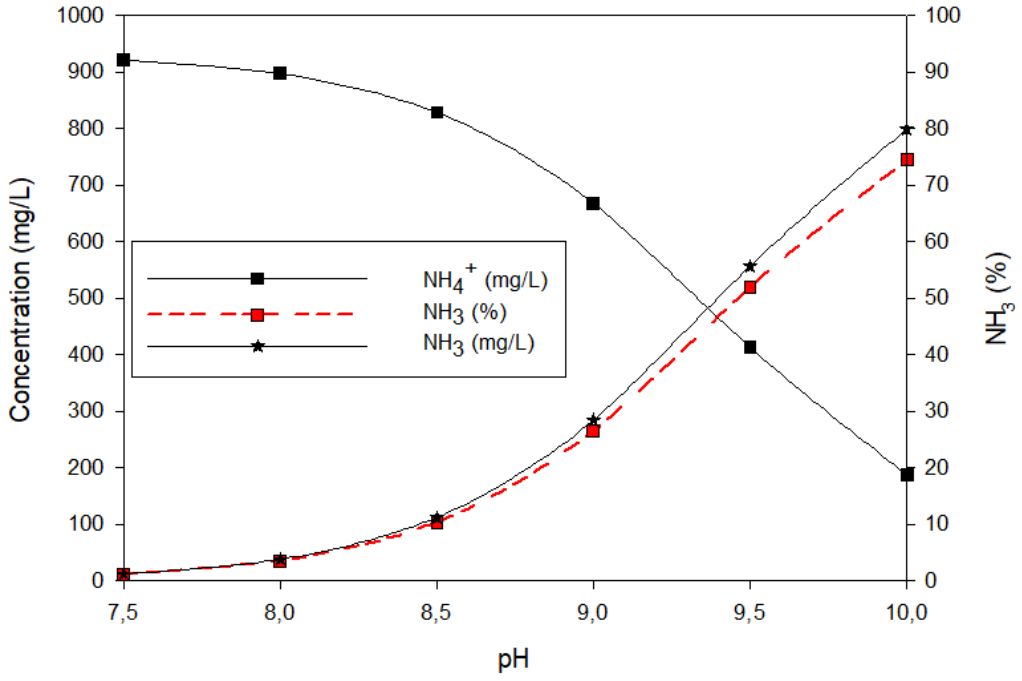

Figure 4.7. NH_4^+-NH_3 relationship according to pH

In the results of two microbial treatments using different bacterial concentrations, 29.0±1.7% and 82.0±1.7% urea hydrolysis was obtained at the end of 24 hours in the microbial attachment stage of the treatment with 0.1 g CDW.L^{-1} and 0.3 g CDW.L^{-1}, respectively. Findings with 0.1 g CDW.L^{-1} suggested the occurrence of urea hydrolysis during microbial treatment, albeit at values lower than anticipated. This lower urea hydrolysis was attributed to the insufficient bacterial concentration of 0.1 g CDW.L^{-1}. The significant increase in urea hydrolysis in the microbial attachment stage, achieved by increasing the concentration from 0.1 g CDW.L^{-1} to 0.3 g CDW.L^{-1}, underscores the effect of bacterial concentration. The impact of bacterial concentration on urea hydrolysis, MICP kinetics, and $CaCO_3$ precipitation was shown in previous studies. Tobler et al. [167] reported that when the inoculum density of *S. Pasteurii* was 0.07 OD (2.3×10^6 cells ml^{-1}), complete urea hydrolysis occurred within 2 days in MICP process. In contrast, using an inoculum density of 0.03 OD (7.2×10^5 cells ml^{-1}) resulted in only one-third of

the urea being hydrolyzed within the same time [167]. Similarly, Wen et al. [168] demonstrated that increasing the initial bacteria concentration increased both urea hydrolysis and $CaCO_3$ precipitation. At the end of biomineralization stage with 0.1 g CDW.L^{-1}, the urea hydrolysis was only 5.4±0.2% and insufficient attached bacteria to the aggregates during biomineralization stage likely contributed to this. This inference was supported by the decrease in urea hydrolysis from 29.0±1.7% at the end of 24 hours in the microbial attachment stage to 5.4±0.2% in the biomineralization stage, indicating a transfer limitation of bacteria from the growth media to the biominerilization stage.

In both stages of the microbial treatment with 0.3 g CDW.L^{-1}, significantly higher hydrolysis were obtained compared to the treatment with 0.1 g CDW.L^{-1}. In the microbial treatment with 0.3 g CDW.L^{-1}, the urea hydrolysis performance at the 24 hours of the microbial attachment stage and at the 24 hours of the biomineralization stage were 82.0±1.7% and 81.7±1.7%, respectively. These close urea hydrolysis results obtained in both stages suggested that the aggregates progressed to biomineralization stage by absorbing most of the bacteria provided in growth media. During the biomineralization stage, initial Ca^{2+} concentration of 2.2 g.L^{-1} had no negative effect on the urea hydrolysis activity. There were previous studies reporting that high Ca^{2+} concentration could negatively affect the activity of bacteria or even inhibit it [169,170]. Ouyang et al. determined the optimum Ca^{2+} concentration to be 0.3 mol.L^{-1} and reported that higher Ca^{2+} concentrations than 0.3 mol.L^{-1} reduced the urea activity and mineralization activity. [169]. In addition, Zhu et al. [171] reported that an initial 10 g.L^{-1} Ca^{2+} concentration had no negative effect on the activity of ureolytic bacteria in MICP, while Tobler et al. [167] reported that Ca^{2+} concentration between 50–500 mM (2–20 g.L^{-1}) did not inhibit the ureolytic activity of *S. pasteurii* and did not significantly affect the rate constants of urease activity. Since the Ca^{2+} concentration used in this thesis was low as 2.2 g.L^{-1}, no obvious negative effect was observed on urea hydrolysis and the urea hydrolysis was 81.7±1.7% at the end of biomineralization stage with 0.3 g CDW.L^{-1}.

Consequently, a urea hydrolysis rate of 81.7±1.7% was obtained using 0.3 g CDW.L^{-1}, indicating the significant presence of microbial activity through urea hydrolysis in the MICP process. The urea consumption in MICP were associated with bacterial concentration. Subtracting the bacterial concentration used in microbial treatment from 0.1 g CDW.L^{-1} to 0.3 g CDW.L^{-1} improved the MICP improvement process by increasing the urea hydrolysis performance.

4.4.2. Changes in Ca^{2+} Concentrations During Biodeposition

The precipitation of $CaCO_3$ during treatment was determined by monitoring the changes in Ca^{2+} concentrations. Time-dependent Ca^{2+} concentrations for the water control, abiotic control, and microbial treatments with 0.1 g CDW.L^{-1} and 0.3 g CDW.L^{-1} were given in Figure 4.8.

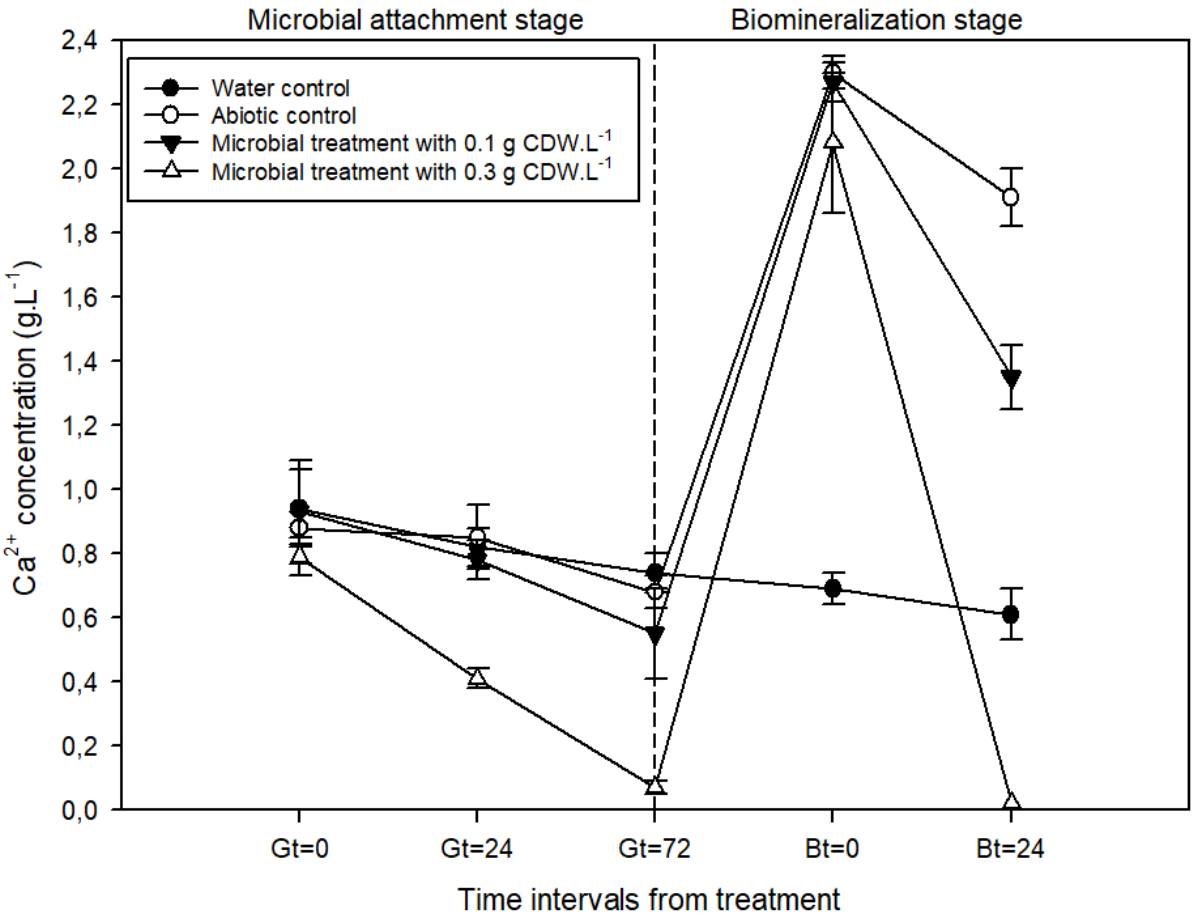

Figure 4.8. Change in Ca^{2+} concentrations in treatment groups

Ca^{2+} concentrations decreased by the end of the microbial attachment and biomineralization stages in all treatment groups. In the water control group, no significant decrease in Ca^{2+} concentration was observed. Total decrease in the Ca^{2+} concentration at the end of the microbial attachment stage was 0.2±0.1 g.L^{-1} (from 0.94±0.88 g.L^{-1} to 0.74±0.68 g.L^{-1}) and at the end of the biomineralization stage, it was only 0.1±0.1 g.L^{-1}. In abiotic control group, Ca^{2+} concentration decreased by 0.2±0 g.L^{-1} at the end of the microbial attachment stage which was similar to the results obtained in water control group. In biomineralization stage, due to the Ca^{2+} concentration of the biomineralization

media (2.2 $g.L^{-1}$) initial Ca^{2+} concentration at Bt = 0 was 2.3±0.1 $g.L^{-1}$ for abiotic control group, while for the water control it was 0.7±0.1 $g.L^{-1}$. At the end of the biomineralization stage, Ca^{2+} concentration decreased from 2.3±0.1 $g.L^{-1}$ to 1.9±0.1 $g.L^{-1}$ in abiotic control group, decreasing by 0.4±0.1 $g.L^{-1}$ in total calcium concentration. The decrease in Ca^{2+} concentration in the microbial treatment groups were greater compared to the both abiotic and water control groups. In the microbial treatment group with 0.1 g $CDW.L^{-1}$, the decrease in the initial Ca^{2+} concentration was 0.4±0 $g.L^{-1}$ (from 0.9±0.1 $g.L^{-1}$ to 0.5±0.1 $g.L^{-1}$) at the end of the microbial attachment stage and it was 0.9±0.2 $g.L^{-1}$ (from 2.3±0.1 $g.L^{-1}$ to 1.4±0.1 $g.L^{-1}$) at the end of the biomineralization stage. In the microbial treatment group with 0.3 g $CDW.L^{-1}$, the decrease in the initial Ca^{2+} concentration was 0.7±0.1 $g.L^{-1}$ (from 0.8±0.1 $g.L^{-1}$ to 0.1±0 $g.L^{-1}$) at the end of the microbial attachment stage and it was 2.1±0.2 $g.L^{-1}$ (from 2.1±0.2 $g.L^{-1}$ to 0±0 $g.L^{-1}$) at the end of the biomineralization stage.

The decreases in calcium concentration observed in the control groups can be explained by the reaction of calcium ions formed by dissolving $Ca(OH)_2$ of recycled aggregates in water with CO_2 in the ambient environment. As demonstrated in Equation 4.3, carbonation takes place subsequent to the reaction, leading to the precipitation responsible for the observed minor decreases in calcium concentration.

$$Ca(OH)_2 + CO_2 \rightarrow H_2O + CaCO_3 \qquad \text{(Equation 4.3)}$$

A higher decrease in Ca^{2+} was observed in the biomineralization stage of the abiotic control group (0.4±0.1 $g.L^{-1}$) compared to the water control group (0.1±0.1 $g.L^{-1}$). This could be due to the initial different calcium concentrations between the two groups. The abiotic control group had a higher calcium content due to the addition of media containing $Ca(NO_3)_2.4H_2O$ and $Ca(HCOO)_2$, potentially leading to more $CaCO_3$ precipitation through carbonation and a greater decrease in Ca^{2+}. Additionally, despite the treatment process occurring under clean conditions, the lack of sterile conditions may have allowed for the presence of some microorganisms in abiotic group and the activity of this microorganisms (Figure 4.5) could have contributed to the decrease in Ca^{2+} concentration with some precipitation.

When all groups were compared, the Ca^{2+} decrease was greater in the microbial treatment groups than in the control groups, indicating that more $CaCO_3$ precipitated in the microbial groups than in the control groups. This more $CaCO_3$ deposition was attributed

to microbial pathways. As a result of metabolic activities of bacteria, carbonate (CO_3^{2-}) was precipitated together with Ca^{2+} attracted to the negatively charged cell surface. As the metabolic activity obtained in the microbial treatment groups was higher than the other control groups (Figure 4.6), more $CaCO_3$ precipitation was achieved. When the microbial treatment groups were compared among themselves, Ca^{2+} concentration decreased by 0.4±0 $g.L^{-1}$ g corresponding to 40.8±5.2% decrease and 0.7±0.1 $g.L^{-1}$ corresponding to 90.6±2.6% decrease at the end of the microbial attachment stage in the treatment with 0.1 g $CDW.L^{-1}$ and 0.3 g $CDW.L^{-1}$, respectively. In the biomineralization stage, Ca^{2+} concentration decreased by 0.9±0.2 $g.L^{-1}$ corresponding to 40.2±5.8% decrease and 2.1±0.2 $g.L^{-1}$ corresponding to 99.2±0.2% decrease at the end of the stage in the treatment with 0.1 g $CDW.L^{-1}$ and 0.3 g $CDW.L^{-1}$, respectively. In the microbial treatment with 0.3 g $CDW.L^{-1}$, almost all calcium ions present in the media precipitated as $CaCO_3$. This results indicated a more effective MICP process that resulted in higher microbially induced $CaCO_3$ precipitation in the treatment with 0.3 g $CDW.L^{-1}$ than 0.1 g $CDW.L^{-1}$. This increased efficiency of MICP could be attributed to the more efficient microbial activity, as demonstrated by the urea hydrolysis results in Figure 4.6. The performance of microbial activity positively impacted the MICP process, leading to the formation of more CO_3^{2-} ions and the precipitation of more microbial-induced $CaCO_3$.

4.4.3. Weight Increase on f-RCA Sand Mixes

The weight changes of f-RCA sand mixes after treatments were presented in Figure 4.9. While a weight increase was achieved in the f-RCA sand mixes in the abiotic control group and microbial treatment groups, on the contrary, a weight decrease was achieved in the water control group. This weight decrease obtained in the water control group showed that there were aggregates losses during the treatment procedure. Similarly, in the improvement tests of f-RCA according to their size, it was also discussed that some losses were observed in the aggregates smaller than 0.075 mm and this likely was resulted in less weight increase on the f-RCA smaller than 0.075 mm (Figure 4.3). In the two-stage MICP treatment, procedures such as separating the aggregates from the growth media and transferring them into biomineralization media and during the weight increase analysis transferring the aggregates between containers can caused the loss of very small-sized of aggregates. Therefore, the loss of some small aggregates might be inevitable during the improvement process of f-RCA.

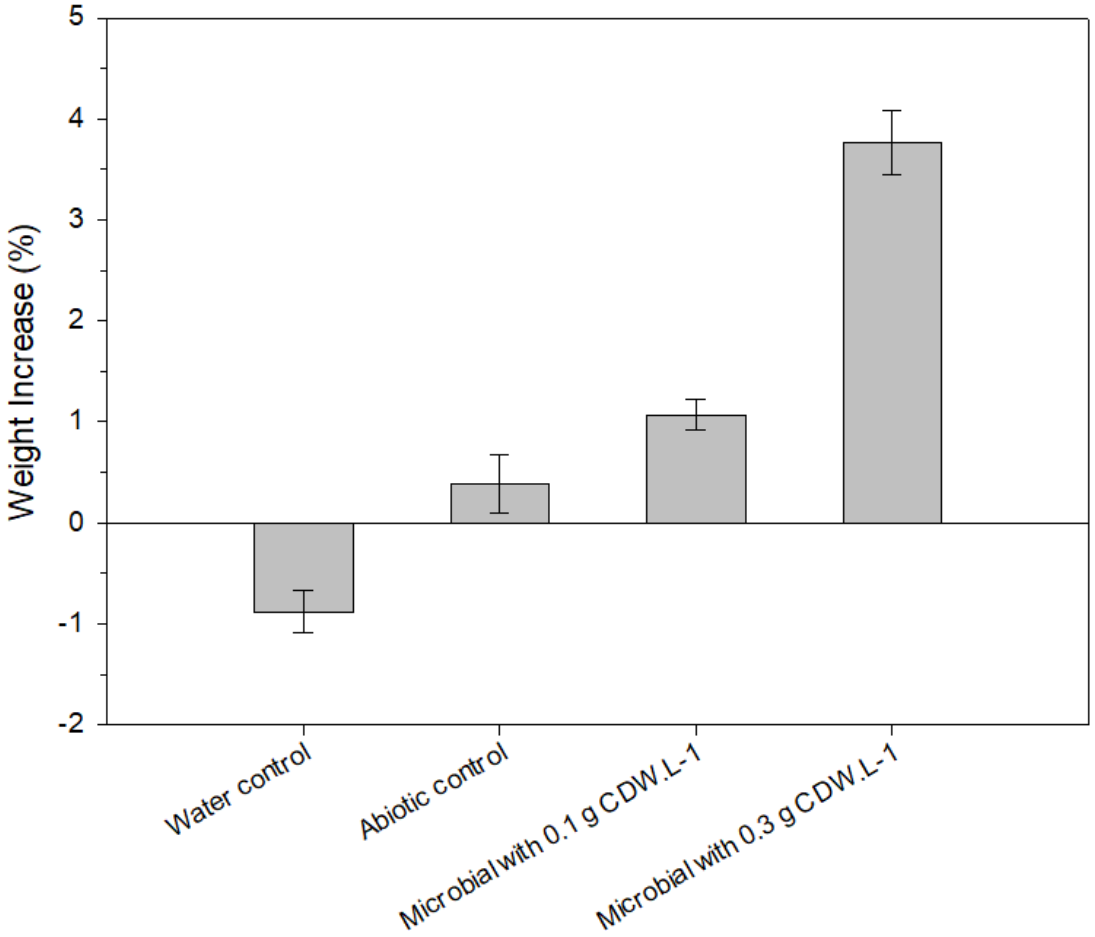

Figure 4.9. Weight increase in f-RCA sand mixes after treatments

A weight increase of 0.4±0.3%, 1.1±0.2% and 3.8±0.3% was achieved in abiotic control treatment, microbial treatment with 0.1 g CDW.L^{-1} and 0.3 g CDW.L^{-1} respectively, and 0.9±0.2% weight decrease was achieved in the water control group (Figure 4.9). Considering the aggregates losses during the treatment procedure, correction was made to the weight increases by using the formula in the Equation 4.4.

$$WI\ (\%)_{correction} = \frac{(W_{treated} + W_{loss}) - W_{initial}}{W_{initial}}\ x\ 100 \qquad \text{(Equation 4.4)}$$

$W_{treated}$ = Weight of dried RCA sand mix after treatment (g)

W_{loss} = Weight losses during procedure (g), equal to weight decrease in the water control group (g)

$W_{initial}$ = Initial weight of dried RCA sand mix before treatment (g), equal to 450 g

After correction, there was no weight increase in water control group. The weight increase in the abiotic control group, microbial treated group with 0.1 g CDW.L^{-1} and 0.3 g CDW.L^{-1} were 1.3±0.4%, 2.0±0.2% and 4.6±0.1%, respectively. Corrected weight increases of f-RCA sand mixes after treatments were presented in Figure 4.10.

The excess weight in the abiotic control group can be attributed to carbonation, as showed by calcium analysis (Figure 4.8). Additionally, non-consumed chemicals remaining from the growth media and/or biomineralization media might contribute to the weight increase in this group.

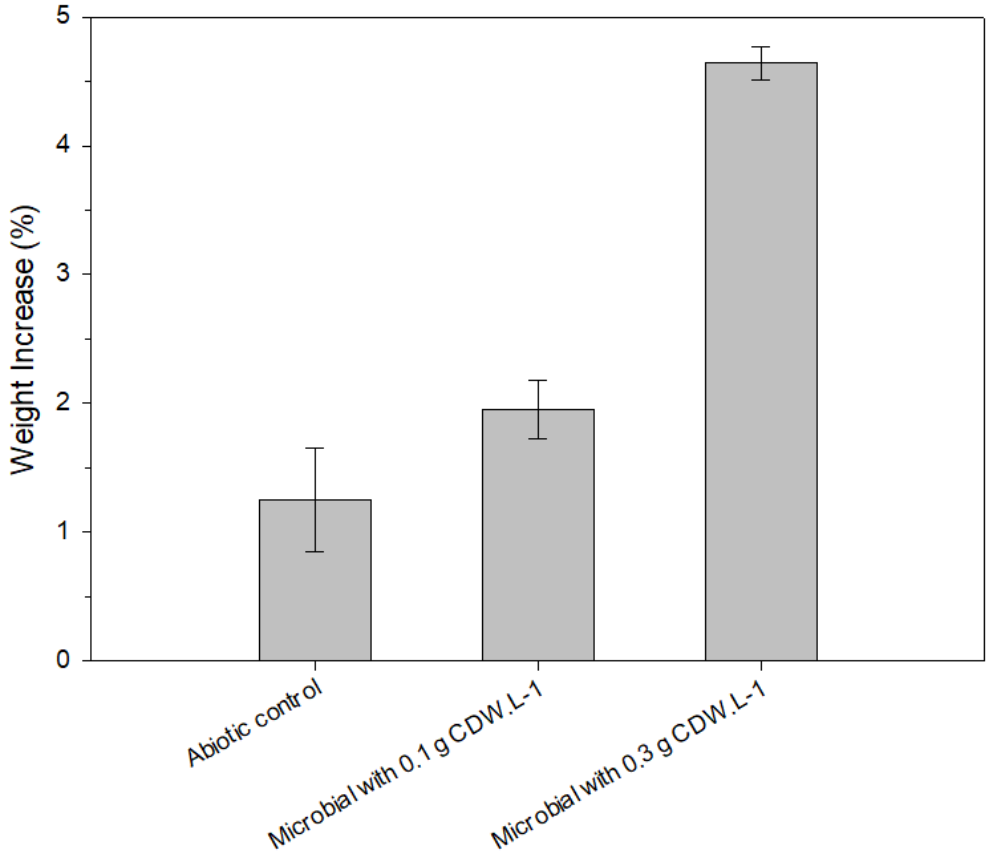

Figure 4.10. Corrected weight increase in f-RCA sand mixes after treatments

Weight increase in the microbial treated groups were higher than the abiotic control group. The reason for this higher weight increases in microbial groups was the precipitation of higher microbial-based $CaCO_3$ compared to abiotic group. This was directly related to better microbial activity performances of bacteria during microbial treatments as also shown in Figure 4.6. Specifically, 0.7±0.2% higher weight increase obtained in the microbial treatment group with 0.1 g CDW.L^{-1} compared to the abiotic

control group and this suggested that at least 3.1±0.7 g more microbial-induced $CaCO_3$ precipitated in every 450 g of f-RCA sand mix. The weight differences observed between the microbial treatment group and the abiotic control group revealed the impact of the MICP process. When microbial treatments were compared among themselves, microbial treatment with 0.3 g CDW.L^{-1} resulted in a 2.7±0.3% greater weight increase than treatment with 0.1 g CDW.L^{-1}. This difference in weight increase indicated a higher microbial-induced $CaCO_3$ precipitate with the MICP process in the treatment with 0.3 g CDW.L^{-1}. Specifically, in the treatment with 0.3 g CDW.L^{-1}, an extra 36.4±3.9 g of microbial $CaCO_3$ precipitate was formed in the 1350 g f-RCA sand mix compared to the treatment with 0.1 g CDW.L^{-1}. This additional precipitation was further supported by the observed higher decrease in calcium ions in the treatment with 0.3 g CDW.L^{-1} than treatment with 0.1 g CDW.L^{-1} (Figure 4.8). In addition, the view of the dried f-RCA sand mixes (each was 450 g) after the microbial treatment with 0.3 g CDW.L^{-1} was presented in Figure 4.11. As illustrated in Figure 4.11, the f-RCA sand mixes were covered with white precipitates. These whites were also confirmed the $CaCO_3$ precipitated on the aggregate surface during the MICP process.

Figure 4.11. Obtained $CaCO_3$ in f-RCA sand mixes after the microbial treatment with 0.3 g CDW.L^{-1}

As a result, more $CaCO_3$ precipitate was obtained with microbial treatments compared to control treatments and these precipitates were shown to be of microbial origin by urea hydrolysis, Ca^{2+} concentration and weight increase tests (Figure 4.6, 4.8 and 4.10). Furthermore, more effective MICP process was achieved in the microbial treatment with 0.3 g CDW.L^{-1} compared with 0.1 g CDW.L^{-1}. In the treatment with 0.3 g CDW.L^{-1}, almost all the initial Ca^{2+} was precipitated by high urea hydrolysis performance of non-axenic culture. In line with these findings, the optimized microbial treatment method with 0.3 g CDW.L^{-1} was selected for the further tests of thesis.

4.5. Quality Improvement of Commercially Available fRCA Sand Mixes

This section pertains to the MICP treatment of commercially available fRCA (c-fRCA) sand mixes. The successful MICP process achieved with the optimized treatment on f-RCA sand mixes was subsequently applied to c-fRCA sand mixes obtained from industry. Throughout the evaluation of the MICP process, nitrate reduction activity of the used culture was also monitored together with urea hydrolysis.

4.5.1. Nitrate Reduction Performance During Microbial Treatment

Within the scope of this thesis, the MICP process was conducted using two metabolic pathways simultaneously: nitrate reduction and urea hydrolysis. The capacity of nitrate-reducing bacteria to execute the MICP process under anoxic conditions and their ability to endure in nutrient-deficient environments provides a significant advantage. Nitrate reduction during treatment with MICP was investigated by analyzing the change in NO_3-N concentration. The changes in NO_3-N concentration during the microbial attachment and biomineralization stages were given in Figure 4.12. Furthermore, nitrate reduction efficiencies (%) were outlined in Table 4.4.

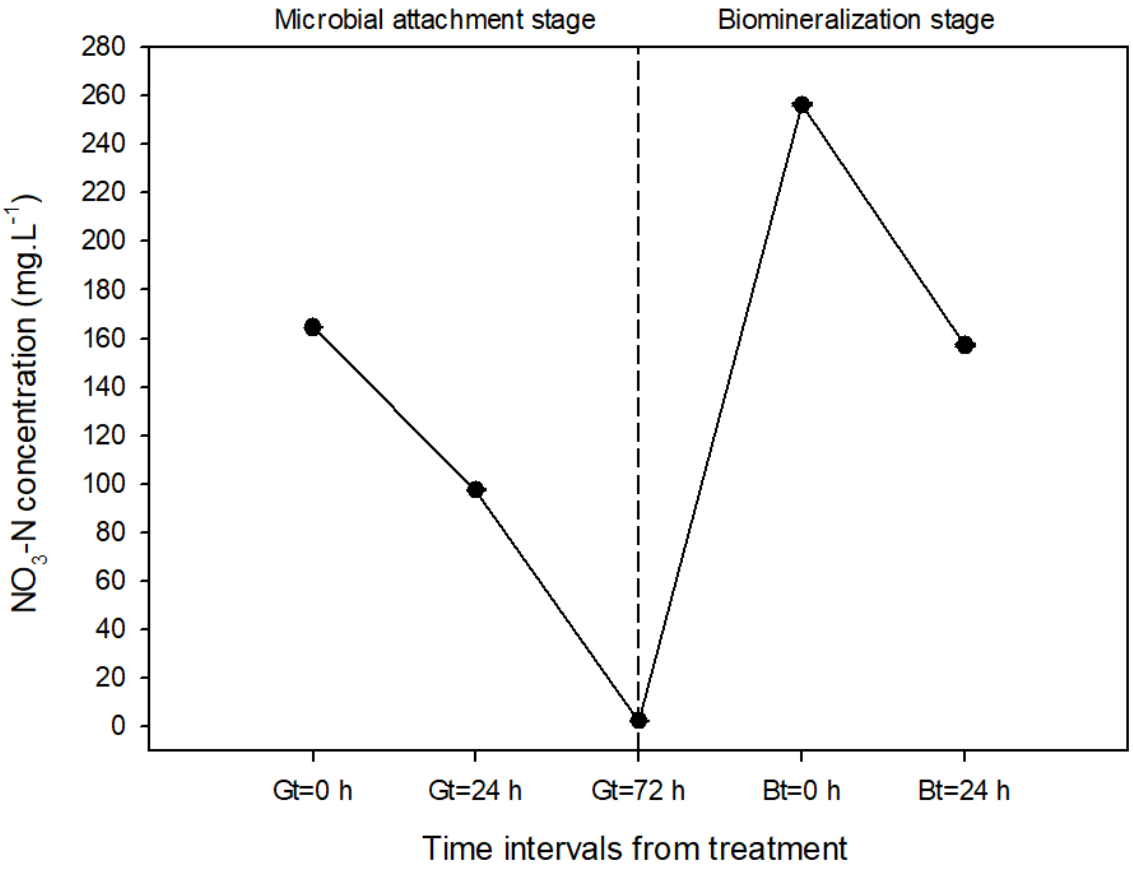

Figure 4.12. Change in NO_3-N concentration during microbial treatment

Table 4.4. Nitrate reduction (%) achieved during microbial treatment

Time intervals from treatment	NO_3-N concentration ($mg.L^{-1}$)	Decrease NO_3-N concentration ($mg.L^{-1}$)	Nitrate reduction (%)
Gt=0 h	164.5±0.2	0±0	0±0
Gt=24 h	97.4±0.4	67.1±0.4	40.8±0.2
Gt=72 h	2.4±0.1	162.1±0.2	98.6±0.1
Bt=0 h	256.2±0.4	0±0	0±0
Bt=24 h	157.1±0.6	99.1±0.3	38.7±0.2

During the microbial attachment stage, the initial NO_3-N concentration of 164.5±0.2 $mg.L^{-1}$ decreased to 97.4±0.4 $mg.L^{-1}$ at the end of 24 hours, corresponding to a decrease of 67.1±0.4 $mg.L^{-1}$ NO_3-N concentration with a 40.8±0.2% nitrate reduction. By the end of 72 hours, almost all nitrate had been reduced and the remaining NO_3-N concentration was 2.4±0.1 $mg.L^{-1}$. The nitrate reduction efficiency by non-axenic culture after 72 hours reached a high level of 98.6±0.1%. At the initial of the biomineralization stage, the NO_3-N concentration was 256.2±0.4 $mg.L^{-1}$. Following the 24-hour biomineralization process, 38.7±0.2% of the nitrate was reduced, resulting in a decrease of 99.1±0.3 $mg.L^{-1}$ NO_3-N concentration from 256.2±0.4 $mg.L^{-1}$ to 157.1±0.6 $mg.L^{-1}$. The 98.6±0.1% reduction achieved during the microbial attachment stage and the 38.7±0.2% reduction obtained in the biomineralization stage revealed the existence and effectiveness of nitrate reduction during bacterial treatment.

The variation in nitrate reduction rates during different times of the microbial attachment stage indicated that the reduction of nitrate was influenced by the duration of the process. Specifically, while nearly all nitrate was reduced within 72 hours during the microbial attachment stage, the reduction rate was 40.8±0.2% after the first 24 hours of microbial attachment stage. This suggested that extending the process time could result in further nitrate reduction. It is hypothesized that the 38.7±0.2% efficiency achieved at the end of biomineralization could potentially be increased with a longer biomineralization period. Nitrate reduction is a slower process than urea hydrolysis [171]. Therefore, in the MICP process combined with nitrate reduction and urea hydrolysis, it was likely that $CaCO_3$ precipitation via urea hydrolysis was occured faster than $CaCO_3$ precipitation via nitrate reduction. This might had caused of nitrate reduction to slowed down further by limiting the uptake of nutrient for nitrate-reducing bacteria. Zhu et al. [171] reported that the presence of Ca^{2+} did not negatively affect urea hydrolysis activity in MICP, but inhibited nitrate reduction activity. They also reported that after urea hydrolysis was completed and the NH_4-N concentration in the solution reached a steady state, nitrate reduction continued effectively in the MICP [171]. Furthermore, studies had shown that repetitive $CaCO_3$ precipitation could be achieved through nitrate reduction activity [138]. This indicated that bacteria, whose nitrate reduction activity was inhibited by precipitations around their cells, could re-establish their activity over time by getting rid of the precipitated minerals [138].

The results revealed the nitrate reduction activity in the MICP process combined with urea hydrolysis and nitrate reduction, and demonstrated the efficiency of nitrate reduction. Culture exhibited a positive performance in reducing nitrate during the treatment process. In the microbial attachment stage at the end of 24 hours, 40.8±0.2% nitrate reduction achieved. It was possible that nitrate reduction activity was affected by urea hydrolysis and $CaCO_3$ formation during MICP. It was observed that the non-axenic culture reduced almost all of the nitrate with 98.6±0.1% activity performance with the completion of urea hydrolysis at the end of 3 days of microbial attachment stage. In the biomineralization stage, the nitrate reduction was 38.7±0.2% at the end of 24 hours which was similar with the reduction rate at 24 hours of microbial attachment stage.

The results showed that MICP improvement of recycled aggregates is possible using both urea hydrolysis and denitrification metabolic activities. In the MICP process, where two metabolisms were utilized, it appeared feasible to further enhance nitrate reduction performance by extending the process time.

4.5.2. Urea Hydrolysis Performance During Microbial Treatment

Urea hydrolysis was monitored through TAN analysis in regular intervals. TAN concentrations obtained in the water control, abiotic control, and microbial treatment groups were presented in Figure 4.13. In the water control group, the TAN concentration remained consistently at 0±0 $mg.L^{-1}$ across all time intervals. In the abiotic control group, 32.7±21.4 $mg.L^{-1}$ and 46.7±16.2 $mg.L^{-1}$ TAN concentrations were achieved at the microbial attachment stage of 24^{th} and 72^{nd} hours, respectively. In the biomineralization stage of abiotic control group, 93.3±8.1 $mg.L^{-1}$ TAN concentration was achieved, indicating that minor urea hydrolysis occurred due to the non-sterile conditions.

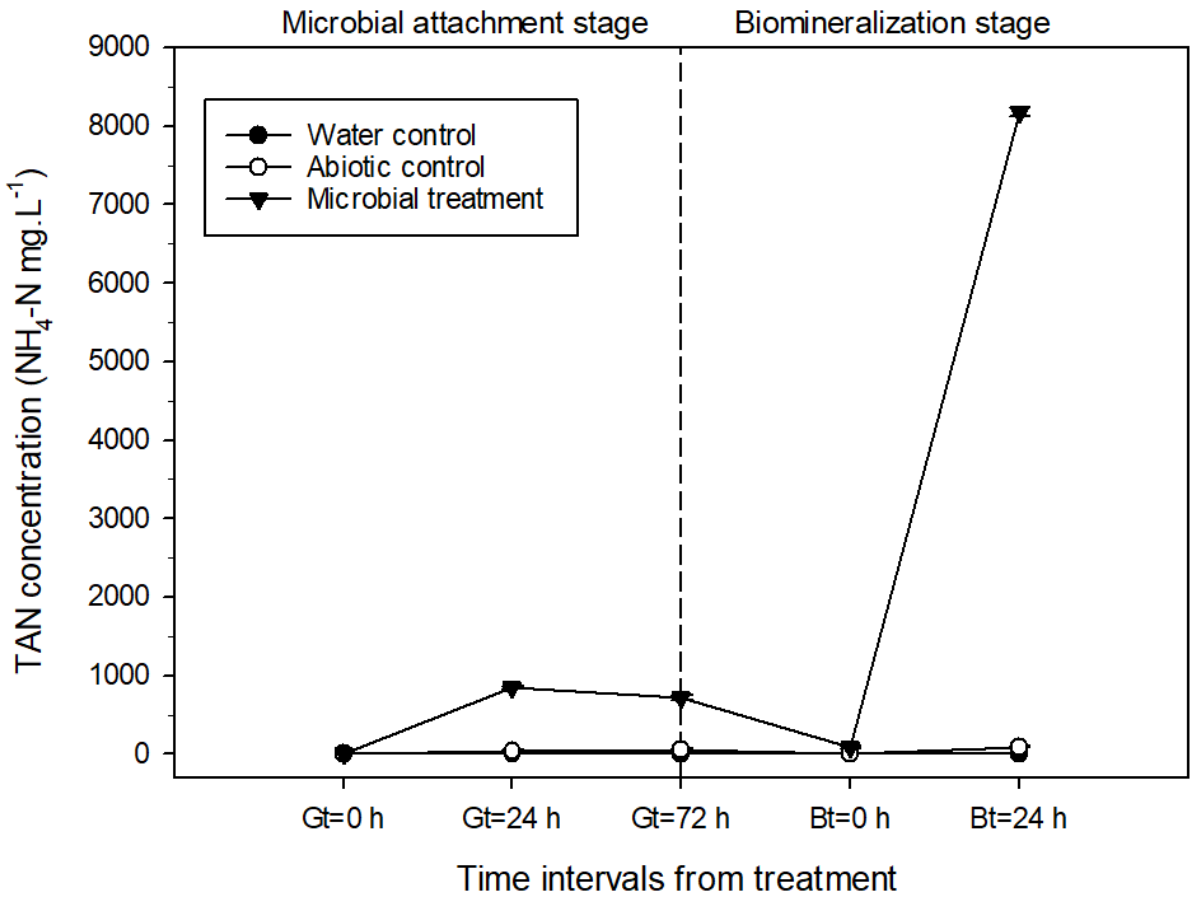

Figure 4.13. TAN concentration during treatments

Substantial urea hydrolysis was evident in the microbial treatment group. The TAN concentration, initially 0±0 $mg.L^{-1}$ of the microbial attachment stage, rose to 854.0±14.0 $mg.L^{-1}$ TAN concentration after 24 hours. The urea hydrolysis efficiency attained within the initial 24 hours was 91.5±1.5%. Subsequently, by the end of the 72 hours in the microbial attachment stage, a decline in TAN concentration was observed, with the TAN concentration achieving at 718.7±32.3 $mg.L^{-1}$. In the biomineralization stage, a high urea hydrolysis performance of 87.6±0.6% was achieved, resulting in TAN concentration of 8176.0±56.0 $mg.L^{-1}$.

The decrease in NH_4-N concentration at the 72 hours of microbial attachment stage was attributed to the conversion of ammonium nitrogen into free ammonia due to elevated pH levels. The pH values at microbial treatment stages were provided in Table 4.5. Increasing the pH to 9.1 led to an increase in the NH_3 ratio in the total ammonia nitrogen to 33.3%, resulting in a decrease in NH_4^+ concentration to 622 $mg.L^{-1}$. It is plausible that gas escape occurred over time as NH_4^+ transformed into NH_3 in its gaseous form.

Table 4.5. The pH values during microbial treatment

Stages of microbial treatment	pH values
Microbial attachment, t=0 h	7.8±0.1
Microbial attachment, t=24 h	8.9±0.1
Microbial attachment, t=72 h	9.1±0.1
Biomineralization, t=0 h	7.8±0.1
Biomineralization, t=24 h	8.4±0.1

The pH values observed in the treatment of c-fRCA sand mixes (Table 4.5) differed from pH values obtained during the treatment of f-RCA sand mixes (Table 4.3), despite utilizing the same MICP process and adjusting the same initial pH at the microbial attachment stage. This variation also influenced the extent of NH_4-N concentration decrease at the end of 72 hours of microbial attachment phase in both treatments. During the treatment of c-fRCA mixes, the pH values (Table 4.5) in the microbial attachment and biomineralization stages were lower compared to the pH values obtained in the treatment of f-RCA mixes (Table 4.3). The f-RCA was more alkaline than c-fRCA, with the pH of f-RCA was around 12.5 before treatment process while the pH of c-fRCA was below 8. The alkalinity of RCA might vary depending on the properties of the waste concrete, such as CaO content, whether it is freshly crushed or not, its age, and the weathering conditions it has been exposed to [172]. Generally, the pH of RCA varies between 8-13 [172]. An RCA sample with 17% CaO content (by weight) exhibits a pH of 11.8, while a sample with 13% CaO content has a pH of 10.4 [149]. In addition, the pH of RCA varies depending on the age of the concrete from which it is obtained [150]. The pH in the pore water of freshly cured concrete with a binder containing Portland cement is around 13-14 [173]. Even whether the waste concrete is sub-surface or surface concrete affects its pH due to the weathering. Long-term contact of waste concrete with atmospheric CO_2 may cause carbonation of the cement. On the other hand, exposure of waste concrete to rainwater might result in the removal of more soluble cement phase and a decrease in portlandite content. While RCA obtained from surface concrete may have lower pH due to weather conditions such as carbonation or rainwater, RCA obtained from subsurface concrete or freshly crushed concrete may have higher pH [172]. The f-RCA used in the thesis was the freshly crushed concrete aggregates, and with its higher alkalinity, it

increased the pH of the solutions it was immersed in in the treatment tests more than c-fRCA.

The TAN concentration results revealed the existence of urea hydrolysis pathway in addition to nitrate reduction pathway (Figure 4.12) in the MICP process for improvement of c-fRCA sand mixes. The urea hydrolysis efficiency of ureolytic bacteria in the non-axenic culture was reached up to 87.6±0.6%, and this also revealed the high performance of ureolytic bacteria under anoxic conditions. Figure 4.12 and Figure 4.13 showed that the MICP process operates simultaneously with both denitrification and urea hydrolysis metabolism, and the achieved 38.7±0.2% nitrate reduction with 87.6±0.6% urea hydrolysis revealed the activity performance of the culture.

4.5.3. Decrease in Ca^{2+} Concentrations During MICP Treatment

Ca^{2+} concentrations during water control, abiotic control and microbial treatment of c-fRCA sand mixes were given in Table 4.6.

Similar Ca^{2+} concentrations were observed in the water control and abiotic control groups at the end of the microbial attachment stage. The initial Ca^{2+} concentration of 0.29±0.01 $g.L^{-1}$ decreased to 0.15±0.01 $g.L^{-1}$ at the end of 72 hours in the water control group and to 0.12±0.01 $g.L^{-1}$ in the abiotic control group. In the microbial treatment group, all Ca^{2+} was decreased by the end of the microbial attachment stage, resulting in a remaining Ca^{2+} concentration of 0 $mg.L^{-1}$, which differed from the Ca^{2+} decrease observed in both control groups. All Ca^{2+} in the microbial treatment group was precipitated as $CaCO_3$. While there was still Ca^{2+} concentration remaining to precipitate in the control groups, the fact that the microbial group precipitated all the calcium indicated that MICP occurred through microbial activity.

The effect of MICP was also evident in the biomineralization stage. In the abiotic control group, at the end of biomineralization, the Ca^{2+} concentration decreased from 2.2±0 $g.L^{-1}$ to 1.9±0.1 $g.L^{-1}$, indicating a decrease of 0.3±0.1 $g.L^{-1}$. In contrast, in the microbial treatment group, the entire 2.2±0.1 $g.L^{-1}$ Ca^{2+} concentration was consumed within 24 hours, resulting in a remaining Ca^{2+} concentration of 0 $mg.L^{-1}$. The higher decrease of Ca^{2+} concentration (1.9±0.1 $g.L^{-1}$) in the microbial treatment group than abiotic control group showed the effect of microbial activities. This 1.9±0.1 $g.L^{-1}$ Ca^{2+} precipitated directly as biological $CaCO_3$ as a result of the metabolism of nitrate reduction and urea

hydrolysis. Consequently, all calcium ions in the microbial treatment group were precipitated as $CaCO_3$, leading to the successful realization of the MICP process combined with nitrate reduction and urea hydrolysis.

Table 4.6. Ca^{2+} concentrations during treatments

Group of treatment	Time interval from treatment	Ca^{2+} concentration ($g.L^{-1}$)
Water control	Gt=0	0.29±0
	Gt=24	0.21±0.01
	Gt=72	0.15±0.01
	Bt=0	0.11±0.01
	Bt=24	0.05±0.01
Abiotic control	Gt=0	0.30±0.01
	Gt=24	0.19±0.01
	Gt=72	0.12±0.01
	Bt=0	2.21±0.03
	Bt=24	1.87±0.06
Microbial treatment	Gt=0	0.28±0.01
	Gt=24	0.01±0.01
	Gt=72	0±0
	Bt=0	2.18±0.05
	Bt=24	0±0

4.5.4. Weight Increase of c-fRCA Sand Mixes after MICP Treatment

The weight increase (%) in microbial treatment of c-fRCA sand mixes by applying correction (Equation 4.4) was given in Figure 4.14 with comparing with the microbial treatment of f-RCA sand mixes and abiotic control.

In the microbial treatment of c-fRCA sand mixes, higher weight increase achieved than abiotic control and the weight increase was 3.8±0.2% after the microbial treatment of c-fRCA sand mixes. This indicates that, after microbial treatment, 2.6±0.2% (equivalent to 34.4±3.1 g) more $CaCO_3$ precipitated on c-fRCA sand mixes compared to the abiotic control group. The extra 34.4±3.1 g of precipitate obtained in the microbial group compared to the abiotic control group was due to the nitrate reduction and urea hydrolysis activities of the bacteria in culture. Therefore, the 34.4±3.1 g of extra precipitation was revealed the microbially induced $CaCO_3$. The difference in weight increases obtained in the abiotic control and microbial group revealed the effect of the microbial pathways used in the MICP process.

After the microbial treatment, the weight increase attained in c-fRCA sand was lower than weight increase attained in f-RCA sand. A 4.6±0.1% weight increase was observed in f-RCA sand mixes, whereas a 3.8±0.2% weight increase was observed in c-fRCA sand mixes. Although the same MICP process was employed in both treatments, the difference in weight increase originated from the variance in total calcium ions during the process. The initial Ca^{2+} concentration in MICP treatment of f-RCA sand was higher than in MICP treatment of c-fRCA sand. This distinction was also evident from the calcium analysis of the two aggregates sand mixes (Figure 4.8 and Table 4.6). While the initial Ca^{2+} concentration of f-RCA sand mixes during the microbial attachment stage was 0.8±0.1 $g.L^{-1}$, the initial Ca^{2+} concentration of c-fRCA sand mixes was 0.3±0 $g.L^{-1}$. This alteration affected the amount of calcium ion that could precipitate during the microbial treatment of the two different types of aggregates, resulting in less $CaCO_3$ precipitation in c-fRCA sand mixes than in f-RCA sand mixes.

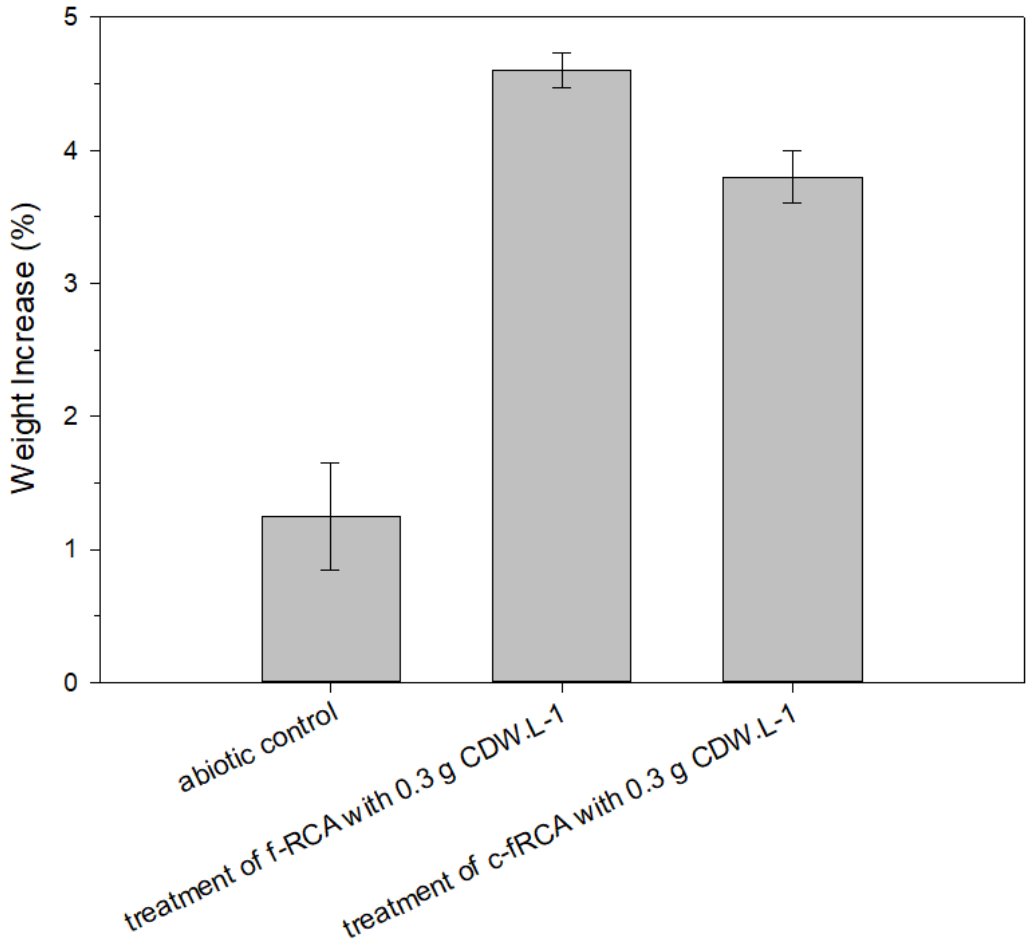

Figure 4.14. Comparison of weight increases of f-RCA and c-fRCA after microbial treatment with 0.3 g CDW.L^{-1}

The results revealed additional weights incurred during MICP. The weight differences that occurred during microbial treatments and abiotic control treatment demonstrated the effect of the MICP process. In the microbial treatment of f-RCA sand mixes, 3.4±0.4% more microbial $CaCO_3$ (45.8±5.8 g of $CaCO_3$ for 1350 g) was precipitated than in the abiotic control treatment. In the microbial treatment of c-fRCA sand mixes, 2.6±0.2% more microbial $CaCO_3$ (34.4±3.1 g of $CaCO_3$ for 1350 g) was precipitated compared to the abiotic control treatment. Positive results were achieved in both the microbial treatment of f-RCA and c-fRCA sand mixes, could leading to an improve in the quality of the aggregates due to precipitated $CaCO_3$.

4.6. Change in Mortar Properties Containing Treated fRCA and Improved Surface Properties of fRCA

4.6.1. Change in Quality of MICP Treated f-RCA Sand Mixes

Mortar specimens containing f-RCA sand mixes (fRAM) were prepared and the change in the mechanical properties of f-RCA sand mixes improved with optimized MICP (microbial treatment with 0.3 g CDW.L^{-1}) were examined. Additionally, the surface properties of f-RCA sand mixes were analyzed with SEM.

4.6.1.1. Compressive Strength of Mortar Specimens

The effect of f-RCA improved with optimized MICP treatment on mortar properties was evaluated on 7 and 28-days compressive strength. The strength results of MICP treated fRAM and untreated fRAM specimens were given in Figure 4.15.

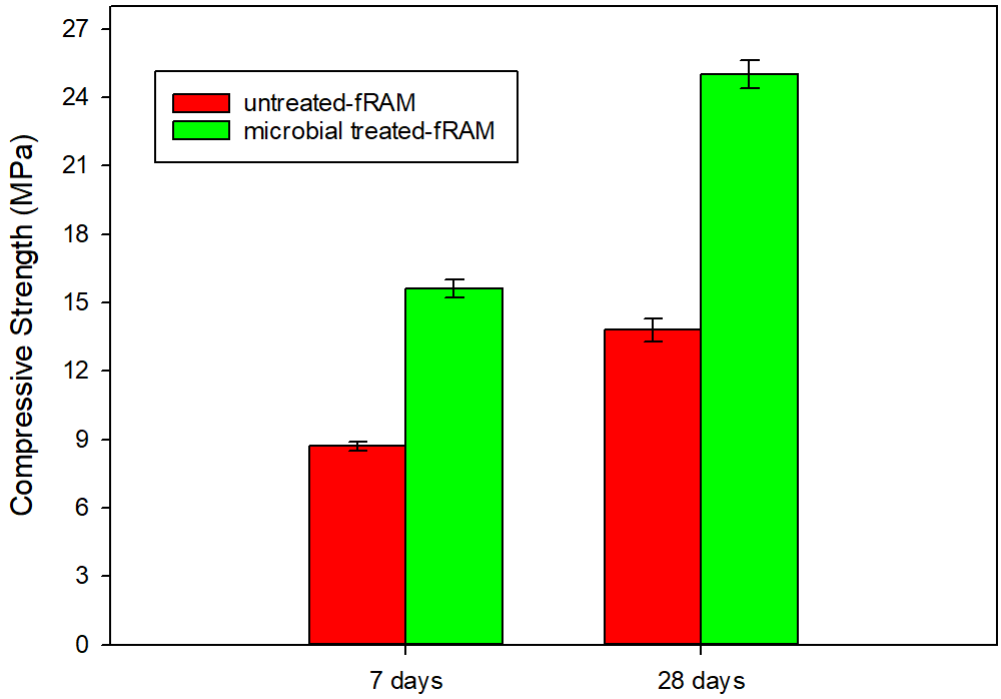

Figure 4.15. Compressive strength of fRAM specimens

It was observed from the compressive strength test results that the utilization of microbially treated f-RCA sand mixes had a positive influence on the mortar properties. The 7 and 28-days compressive strengths of microbial treated-fRAM were notably higher compared to those of untreated-fRAM. Specifically, the 7-day compressive strength of untreated-fRAM noted as 8.7±0.2 MPa, while the 7-day compressive strength of

microbial treated-fRAM reached to 15.6±0.4 MPa. Remarkably, the 7-day compressive strength of microbial treated-fRAM even surpassed the 28-day strength of untreated-fRAM, which was 13.8±0.5 MPa. Microbial treated-fRAM at the 7-day registered a compressive strength 13.4±1.4% higher than the 28-day compressive strength of untreated-fRAM. Moreover, the 28-day compressive strength of the microbial treated-fRAM reached 25.0±0.6 MPa. These findings underscored the significant impact of improved f-RCA on mortar performance.

The impact of the MICP process on fRAM was also demonstrated by the Figure 4.16, which belonged to the mortar mixtures during casting. Despite using the same amount of water in preparing both mortar mixtures, the mixtures prepared with microbially treated f-RCA sand mixes were wetter and more water-saturated (Figure 4.16a), whereas the mixture prepared with untreated f-RCA sand mixes were drier (Figure 4.16b). This difference observed in mortar mixtures originated from the reduced water absorption of f-RCA sand mixes after MICP treatment.

Figure 4.16. Mortar mixtures with (a) microbially treated f-RCA sand mixes; (b) untreated f-RCA sand mixes

Microbial treated-fRAM exhibited a significant 81.5±2.2% increase in compressive strength at 28 days, compared to untreated-fRAM. The results highlighted the substantial positive influence of MICP on the performance of fRAM. The number of studies

examining the mechanical properties of fRA was quite limited in literature. Feng et al. [145] researched the improvement of fRA, had a 24.5% water absorption, by MICP treatment and they achieved a 14.3% increase in 28th days compressive strength of mortar containing improved fRA compared to the mortar containing unimproved fRA. Wu et al. [174] researched the mechanical properties of cRCA after biodeposition and the compressive strength at 28 days of the mortar containing improved cRCA with a w/c ratio of 0.5 was approximately 36% higher than the mortar with untreated cRCA. Wang et al. [18] obtained 40% compressive strength increase in concrete containing MICP-treated cRCA (76 MPa) compared to concrete containing untreated cRCA (54 MPa). Even more, the compressive strength of concrete containing improved cRCA was higher than the concrete containing NA. The compressive strength of concrete with improved cRCA (76 MPa) was 20% higher than the concrete with NA (61 MPa) [18].

The better strength results obtained compared to previous studies might be attributed to an effective MICP process. Different from the previous studies, the use of a the two metabolic MICP mechanism was effective in these positive outcomes. The existence of both nitrate reduction and urea hydrolysis metabolisms during MICP treatment was revealed by the changes in TAN and NO_3-N concentrations. By utilizing two metabolisms simultaneously, it was possible to obtain greater amount of CO_3^{2-} than in MICP that used only a single metabolism. The bacterial concentration used in the MICP process was critical for the quality of improvement [145,167,168]. Therefore, a concentration of 0.3 g CDW.L^{-1} was selected with the optimized method, as it provided better bacterial activity. This bacterial concentration facilitated the formation of more precipitates on the aggregates during the two-metabolism MICP process. The calcium ions were also highly effective in MICP process [145]. In this thesis, the provided Ca^{2+} for the improvement of 1350 g of RCA sand mixes was approximately 20 g totally and almost all precipitated during process. The weight increase (%) obtained on the RCA sand mixes was 4.6%, which corresponded to approximately 62 g of precipitation in 1350 g of RCA sand mixes. When compared to other studies, the weight increases achieved in this study were higher [18,145]. The high $CaCO_3$ precipitation obtained on the surface/pores of the aggregates significantly reduced the high water absorption of the aggregates. This significantly reduced water absorption of aggregates was revealed from the difference between the mortar mixtures containing improved f-RCA sand mixes and those containing untreated f-RCA sand mixes (Figure 4.16). Moreover, as reported by Wu et al. [174], the decrease

in water absorption could have influenced the crushing value, leading to its decrease. Additionally, the formed $CaCO_3$ particles can enhance the density of the ITZ by promoting the hydration reaction [174]. The above-mention factors could contributed to a significant increase in compressive strength.

4.6.1.2. SEM Analysis of MICP Treated f-RCA Sand Mixes

Microstructure and properties of microbially treated f-RCA sand mixes were analyzed by SEM. Micrographs of microbially treated f-RCA sand mixes were given in Figures 4.17-4.18.

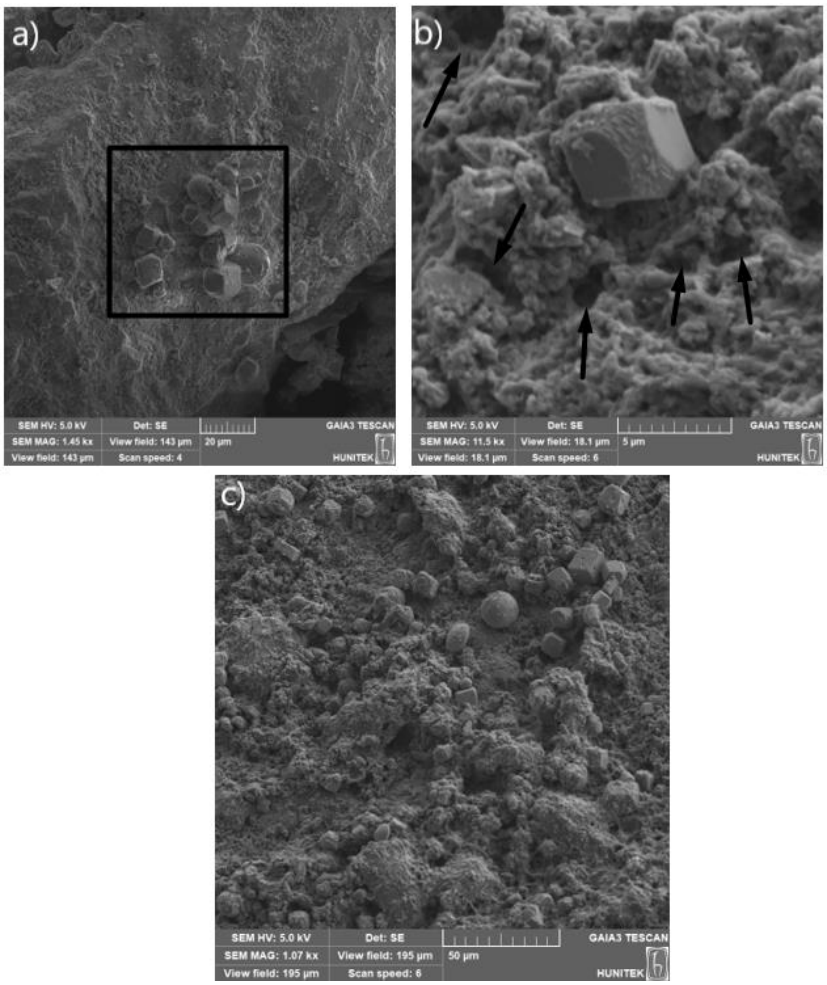

Figure 4.17. SEM micrographs of microbially treated f-RCA sand mixes (a) showing $CaCO_3$ crystals on the aggregate surface; (b) showing pores on the aggregates; (c) showing significant amount of precipitated rhombic calcite and vaterite

The $CaCO_3$ crystals formed on the surface of the f-RCA sand mixes after MICP treatment were clearly revealed in Figures 4.17a and 4.17c. The numerous precipitated crystals confirmed an effective MICP process. The structure of these precipitated crystals was generally rhombic calcite, although some spherical vaterite were also observed (Figure 4.17c). This diversity in the structure of the $CaCO_3$ crystals formed might be attributed to a pH difference between the aggregates surface surrounding the media and the inner parts of the aggregates. Figure 4.17c shows that the surface of f-RCA sand mixes was densely covered with $CaCO_3$ crystals. However, as indicated by the arrows in Figure 4.17b, some pores were still unfilled.

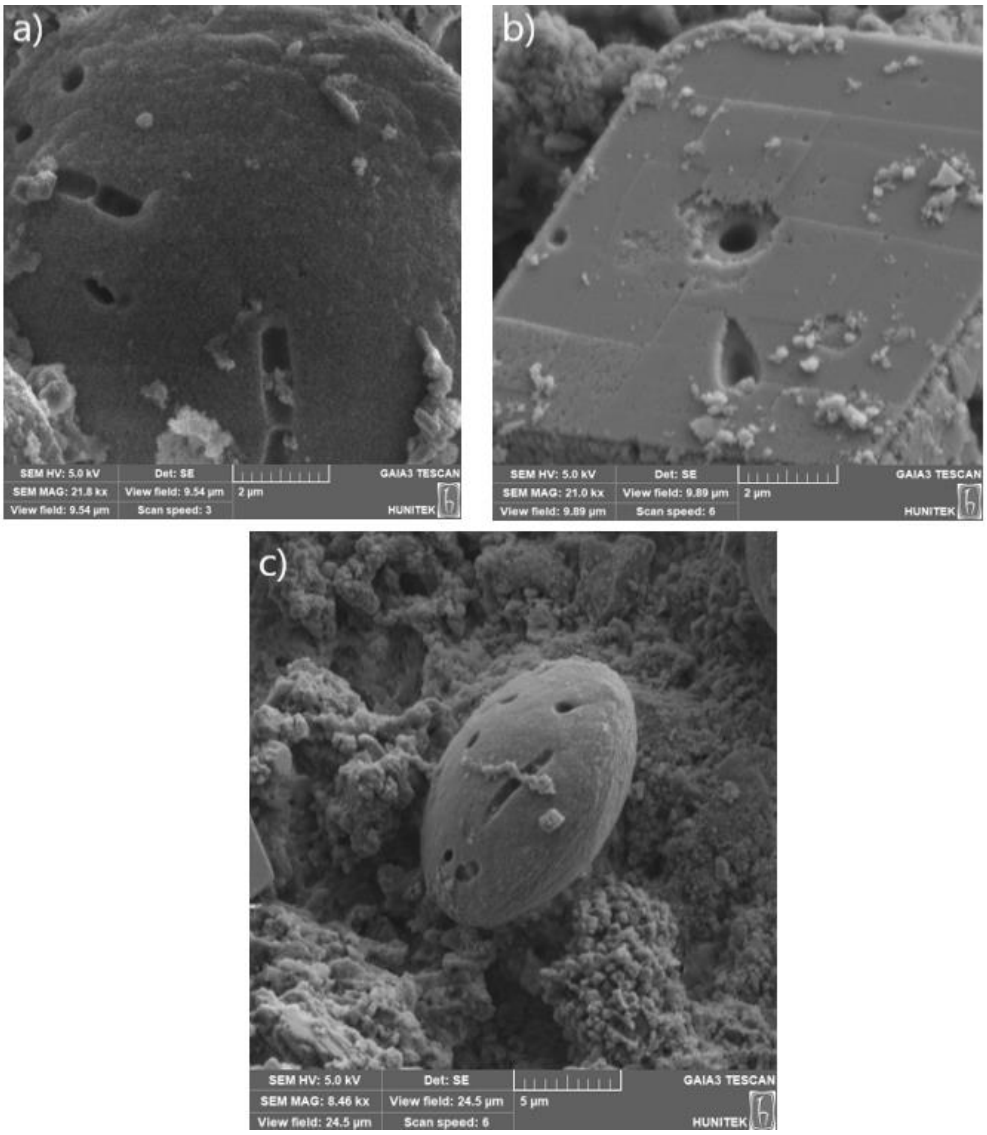

Figure 4.18. SEM micrographs of the MICP treated aggregate surface (a) showing bacterial footprint on a precipitate; (b) showing holes on a calcite crystal; (c) showing vaterite with a bacterial footprint and mineralized bacteria

Figure 4.18 clearly demonstrated that the MICP process and the precipitated $CaCO_3$ crystals were of microbial origin. The imprints of bacterial culture on the precipitated crystals was illustrated by Figure 4.18a-c. Moreover, Figure 4.18c showed the residual bacteria existed on the $CaCO_3$ crystal. All these SEM micrographs showed that the MICP process and the improvement of the f-RCA sand mixes occurred through microbial metabolism.

4.6.2. Change in Quality of MICP Treated c-fRCA Sand Mixes

Mortar specimens containing c-fRCA sand mixes (cfRAM) were prepared and the change in the mechanical properties of c-fRCA sand mixes improved with optimized MICP were examined. Additionally, the surface and chemical properties of c-fRCA sand mixes were analyzed with SEM coupled with EDX and FTIR.

4.6.2.1. Compressive Strength of Mortar Specimens

The effect of MICP on the mechanical properties of c-fRCA sand mixes was evaluated through compressive strength. For this evaluation, six different types of cfRAM were prepared as untreated-cfRAM, water control-cfRAM, abiotic control-cfRAM, microbial treated-cfRAM, reference 0.65-NAM, and reference 0.50-NAM. Reference NAMs formed the basis for comparing the properties of mortar specimens containing standard sand with those containing c-fRCA sand mixes. Untreated-cfRAM allowed to investigate the properties of mortar including c-fRCA sand mixes without treatment, and water control, abiotic control, and microbial treated-cfRAM enabled the investigation of the effect of treatment methods on mortar properties. Compressive strength tests were applied to the mortar specimens cured in water of 3, 7, and 28 days. The results of compressive strenght for mortar specimens were presented in Figure 4.19.

It is noteworthy that treatments increased the compressive strength of 3 days for mortar specimens (Figure 4.19a). Water control, abiotic control, and microbial treatment led to a statistically significant increase in compressive strength ($p < 0.05$). The 3-day compressive strength of untreated-cfRAM was 3.48±0.33 MPa, while the 3-day compressive strengths of water control-cfRAM, abiotic control-cfRAM, and microbial treated-cfRAM were 5.70±0.47, 5.65±0.70, and 9.98±0.69 MPa, respectively. It was observed that water control and abiotic control did not exhibit statistically different strengths from each other after 3 days ($p > 0.05$). The compressive strength of reference 0.50-NAM after 3 days was 10.98±2.11 MPa. This was interestingly indicated that there

was no statistically significant difference between the reference 0.50-NAM and the microbial treated-cfRAM in terms of 3-days compresive strength ($p>0.05$). This finding suggested that the 3-day strengths of specimens prepared with standard sand and microbial treated c-fRCA sand mixes were similar.

There was no statistically significant difference in 3-day strength between reference 0.65-NAM and untreated-cfRAM ($p>0.05$). Increasing the water content in the reference specimen caused a decrease in 3-day compressive strength, and reference 0.65-NAM showed similar properties to the untreated-cfRAM, with a compressive strength of 3.50±0.27 MPa. According to the 3-day tests result, the highest compressive strength among the specimens was observed in microbial treated-cfRAM and reference 0.50-NAM. This increase in compressive strength seen in microbial treated-cfRAM shows the improvement by the MICP process on mortar.

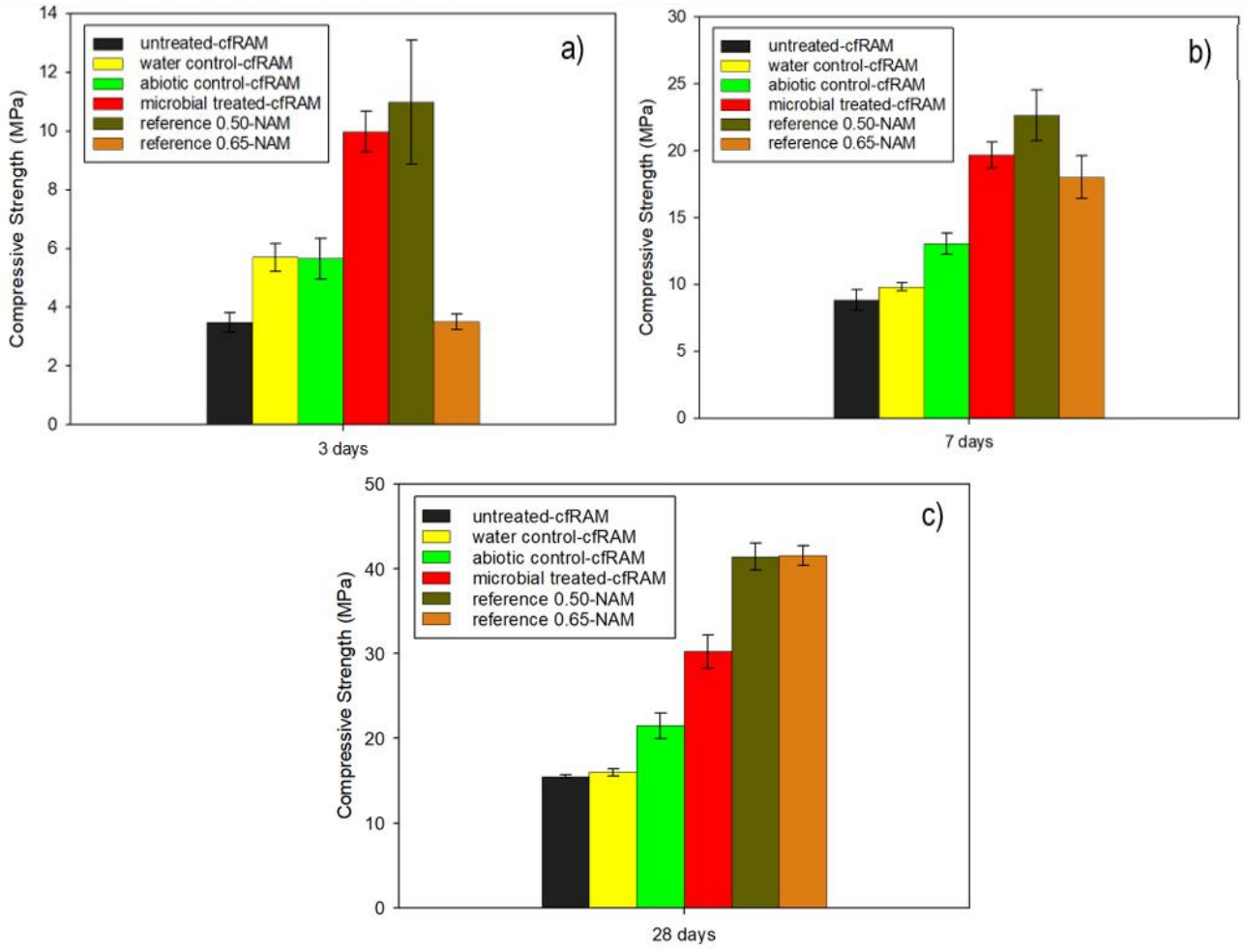

Figure 4.19. Compressive strength of mortar specimens (a) for 3 days; (b) for 7 days; (c) for 28 days

The 7-day compressive strength of the specimens was presented in Figure 4.19b. At the end of 7 days, there was no significant difference between the compressive strengths of untreated-cfRAM and water control-cfRAM ($p>0.05$) and the compressive strength values obtained for these two groups were 8.83±0.77 MPa and 9.83±0.30 MPa, respectively. On the other hand, the abiotic control-cfRAM showed significantly better compressive strength than the water control group at 7 days, with a 13.05±0.81 MPa. At the end of 7 days, the specimens showing the highest compressive strength among the treatment groups was microbial treated-cfRAM, with a compressive strength of 19.68±0.99 MPa. Microbial treated-cfRAM showed 122.95%, 100.25% and 50.77% more strength than untreated-cfRAM, water control-cfRAM and abiotic control-cfRAM, respectively. As anticipated, the highest compressive strength among all groups at 7 days belonged to the reference 0.50-NAM, with a strength of 22.65±1.89 MPa. It was observed that reference 0.65-NAM achieved a compressive strength similar to microbial treated-cfRAM at 7 days, unlike the 3-day test results. Reference 0.65-NAM exhibited a statistically similar compressive strength to microbial treated-cfRAM, with 18.03±1.58 MPa ($p>0.05$). In the 7-day test results, reference 0.50-NAM showed the highest compressive strength, followed by microbial treated and reference 0.65-NAM as the second highest compressive strengths in all groups.

The 28-day compressive strength results obtained from the mortar specimens were presented in Figure 4.19c. At the end of 28 days, the specimens with the highest compressive strength were the reference groups. There was no significant difference in the strength of reference 0.50-NAM and reference 0.65-NAM; they exhibited similar strength ($p>0.05$). The compressive strengths of reference 0.50-NAM and reference 0.65-NAM after 28 days were 41.43 ± 1.60 MPa and 41.53 ± 1.16 MPa, respectively. Following the reference specimens, the best 28-day compressive strength among treatment groups was observed in the microbial treated-cfRAM, consistent with the 3- and 7-day strengths. This indicates the consistent positive impact of MICP on the strength of cfRAM.

The MICP-treated cfRAM showed significant improvement, reaching 30.23±2.00 MPa, which corresponded to a remarkable 95.0% improvement over untreated-cfRAM. The increases in compressive strength at 3, 7 and 28 days in microbial treated-cfRAM compared to untreated-cfRAM were given in Table 4.7.

Table 4.7. Compressive strength increase in microbial treated specimens compared to untreated specimens

Days of test	Compressive strength of untreated-cfRAM (MPa)	Compressive strength of microbial treated-cfRAM (MPa)	Compressive strength increase (%) in microbial treated-cfRAM compared to untreated-cfRAM
3	3.48±0.33	9.98±0.69	187.78±14.65
7	8.83±0.77	19.68±0.99	123.66±13.22
28	15.50±0.18	30.23±2.00	95.11±14.80

Compared to untreated-cfRAM, the compressive strengths of microbial treated-cfRAM at 3, 7, and 28 days increased by 188%, 124%, and 95%, respectively. The decrease in the compressive strength increase over time was due to the lower early strength gains of untreated specimens compared to MICP-treated specimens. Untreated specimens gained 22% of their 15.50 MPa strength in 3 days and 57% in 7 days. In contrast, MICP-treated specimens gained 33% of their 30.23 MPa strength in 3 days and 65% in 7 days. Since the early strength gains of the untreated specimens were lower compared to the MICP-treated specimens, the early strength increases obtained in the MICP-treated specimens were higher and they decreased with the increases in strength gain in untreated specimens after 7 days. The slower early strength development of the untreated specimens may be attributed to the slowdown in hydration of cement, resulting from less water content in mortar due to the high water absorption of untreated c-fRCA. Similarly, Gong et al. [175] observed a decrease in the increase in compressive strength of the concrete containing MICP-improved RA compared to concrete containing untreated RA after 28 days.

Water control treatment had no significant effect on compressive strength, as seen in the similarity (Figure 4.19c) between untreated-cfRAM and water control-cfRAM after 28 days ($p>0.05$). However, abiotic treatment showed a notable improvement, with abiotic-cfRAMs achieving a strength of 21.5±1.52 MPa, representing a 38.71% improvement over untreated-cfRAMs. The improvement observed in abiotic-cfRAM might be due to two reasons. The first reason might be that the chemicals used during the abiotic treatment (calcium formate and calcium nitrate tetrahydrate) cannot be completely separated from

the c-fRCA sand mixes after the treatment, resulting in the chemicals remaining on the sand mixes and its surfaces. The biomineralization media used during abiotic treatment, wherein each 450 g of c-fRCA sand mixes were immersed, contained 19.5 g of calcium formate and 3.6 g of calcium nitrate tetrahydrate. Even though the c-fRCA sand mixes were filtered through the biomineralization media, some chemical particles were likely remained attached on the sand mixes. Studies in the literature indicated that calcium formate and calcium nitrate had an improving effect on compressive strength [176,177]. There are also studies, which show that calcium formate and calcium nitrate were used as chemical additives to improve the early strength of concrete [178]. In this case, the chemicals remaining on the c-fRCA sand mixes might explain the improvement seen in the abiotic control-cfRAM. Another reason could be the positive effect of $CaCO_3$ precipitation within the c-fRCA after abiotic control treatment. There was a greater weight increase in c-fRCA sand mixes after abiotic treatment compared to water control treatment, and more Ca^{2+} decreased during abiotic treatment. This is associated with a higher level of $CaCO_3$ precipitation in the abiotic treatment compared to the water control treatment. These precipitated $CaCO_3$ particles might have a positive effect on the strength of mortar containing abiotically treated c-fRCA sand mixes.

The results indicated that water control treatment did not enhance concrete properties, whereas both abiotic control treatment and microbial treatment led to improvements. At the end of 28 days, abiotic control-cfRAM displayed a 38.7% increase in compressive strength compared to untreated-cfRAM, while microbial treated-cfRAM exhibited a remarkable improvement of 95.0%. The possible reasons for the high compressive strength were previously discussed and attributed to several factors. These were included the simultaneous two metabolism in MICP, optimized bacterial concentration, high initial calcium ion concentration and effective declined of these calcium ions, significant weight increased in aggregates, decreased water absorption and reduced crushing value [174]. All these improvement contributed to the enhanced quality of c-fRCA sand mixes and its mechanical properties.

The compressive strength of non-structural concrete should be at least 15 MPa [179]. In this thesis, MICP-treated cfRAM showed a compressive strength of 30.23 MPa, which is well above the limit strength determined for non-structural concrete. Therefore, MICP-treated c-fRCA are suitable for use in non-structural concrete. According to the legislation in various countries that limit the use of RCA in concrete (as shown in Table 4.1), Italy

uses cRCA with a 60% replacement for the production of C25/30 class structural concrete. In this study, it was demonstrated that it is also possible to produce C25/30 class concrete with 100% replacement of fine fraction with MICP-treated c-fRCA.

4.6.2.2. Flexural Strength of Mortar Specimens

The flexural strength test results of mortar specimens at 3-day, 7-day, and 28-day were presented in Figure 4.20.

It was observed that treatment applications increased the flexural strength of cfRAM of 3 days (Figure 4.20a). The flexural strength of untreated-cfRAM was 0.75±0.07 MPa, while the strengths of water control, abiotic control, and microbial treated-cfRAM were 1.35 MPa±0.07, 1.25±0.18 MPa, and 2.25±0.06 MPa, respectively. There was no statistical difference in the 3-day flexural strength between water control-cfRAM and abiotic control-cfRAM ($p>0.05$).

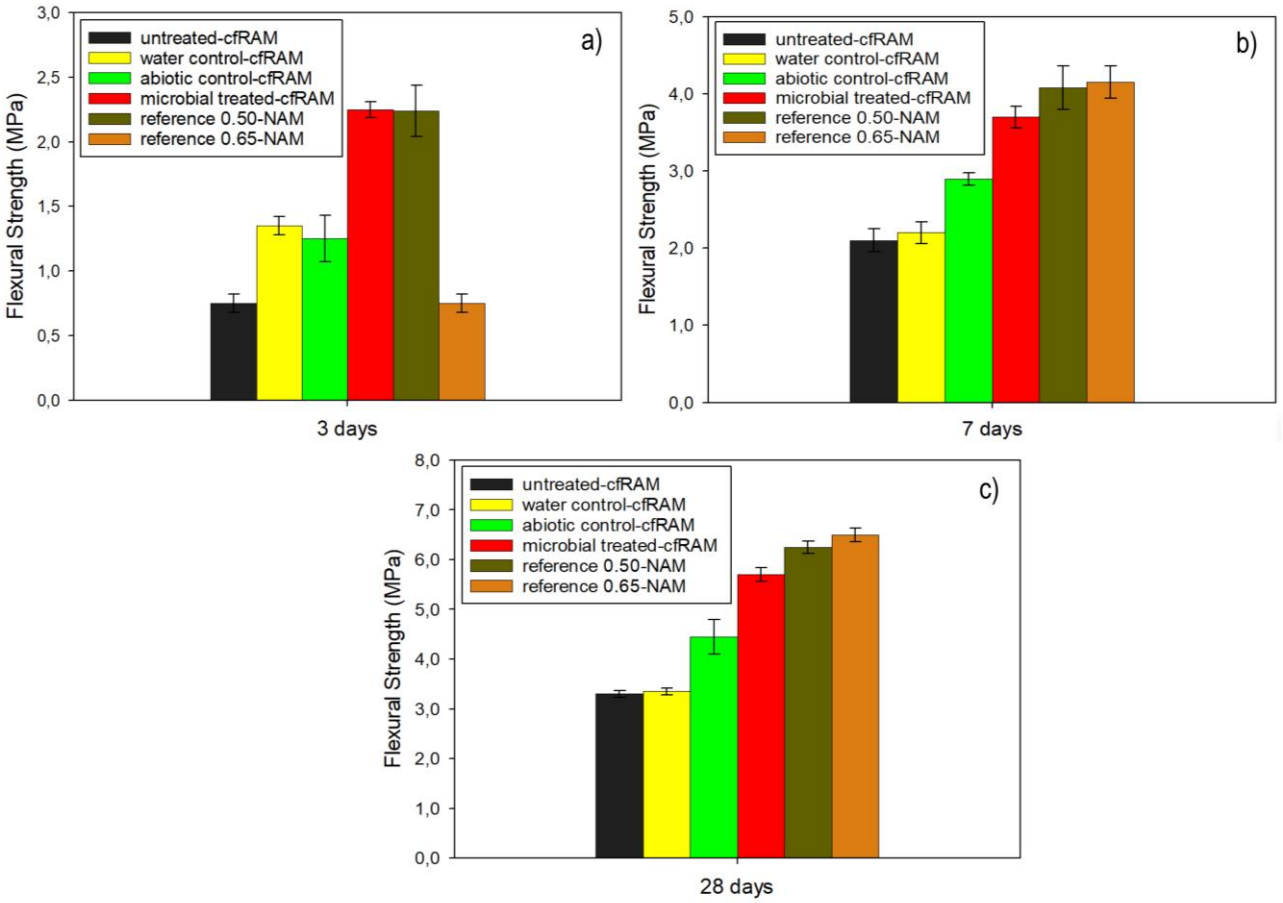

Figure 4.20. Flexural strength of mortar specimens (a) for 3 days; (b) for 7 days; (c) for 28 days

The flexural strength of the reference 0.50-NAM was statistically similar to flexural strength of the microbial treated-cfRAM with 2.24±0.20 MPa ($p>0.05$). The 3-day flexural strength of reference 0.65-NAM was close to the performance of untreated-cfRAM with 0.75±0.07 MPa ($p>0.05$). The fact that reference 0.65-NAM showed such low 3-day strength despite being prepared with standard sand was due to the negative effect created by the excess water content in the mortar. Among the 3-day test results, the highest flexural strength was observed in microbial treated-cfRAM and reference 0.50-NAM.

At the end of 7 days (Figure 4.20b), the flexural strengths of untreated-cfRAM and water control-cfRAM reached 2.10±0.15 MPa and 2.20±0.14 MPa, respectively, with no statistical difference observed between these two strengths. The flexural strength of abiotic control-cfRAM showed a statistical difference compared to untreated and water control, increasing to 2.90±0.08 MPa at the end of 7 days. In the 7-day results, the highest flexural strength was observed in reference 0.50-NAM, reference 0.65-NAM, and microbial treated-cfRAM, with no statistically significant difference between these three groups. The strengths observed in these three groups were 4.08±0.28 MPa, 4.15±0.21 MPa, and 3.7±0.14 MPa, respectively. The 7-day flexural strength of microbial treated-cfRAM was 76.35% higher than untreated-cfRAM. According to the 7-day results, the flexural strengths of the reference specimens and microbial treated specimens were similar ($p>0.05$).

At the end of 28 days, the highest flexural strength was observed among the reference specimens (Figure 4.20c). The strengths of reference 0.50-NAM and reference 0.65-NAM were 6.25±0.12 MPa and 6.50±0.14 MPa, respectively, at the end of 28-days. In the reference 0.65 group, it was noted that the excess water content had a negative impact on the early strength; however, this adverse effect disappeared over time, leading to flexural strength similar to reference 0.50-NAM in terms of both 7-day and 28-day strengths. The highest flexural strength among the treatment groups was observed in microbial treated-cfRAM. At the end of 28 days, the strength of microbial treated-cfRAM was statistically 28.1% higher than the abiotic control-cfRAM, with a value of 5.70±0.14 MPa. The flexural strengths of untreated and water control specimens were 3.30±0.07 and 3.35±0.07, respectively, at the 28-day and did not show a statistically significant difference. The 28-day flexural strength of abiotic control specimens was 4.45±0.35 MPa, indicating a 34.9% improvement compared to untreated-cfRAM. While the results did

not demonstrate a positive impact of water control treatment on the flexural strength of cfRAM, they did highlight the benefits of both abiotic control treatment and microbial treatment. At the end of 28 days, abiotic control-cfRAM exhibited a 34.9% increase in flexural strength compared to untreated-cfRAM, while microbial treated-cfRAM showed much more substantial improvement, with a 72.7% increase compared to untreated-cfRAM. The positive effect of the abiotic control group on flexural strength was also evident in compressive strength. This increase observed in the mechanical properties of the abiotic control group is attributed to the strengthening effect of calcium formate and calcium nitrate. Additionally, the $CaCO_3$ formed during abiotic control treatment can contributes to the improved mechanical properties of abiotic control-cfRAMs.

In previous studies, Zhao et al. [16] reported up to a 23% increase in 28-day flexural strength in mortar containing MICP-improved fine-sized RMA compared to mortar containing untreated fine-sized RCA. In another study, MICP was applied to coarse aggregates obtained from commercial concrete cured in open air for more than 500 days, an increase of 28-day flexural strenght up to 18.3% was achieved in concrete compared to concrete containing untreated RCA [180]. Moreover, Feng et al. [145] achieved a very high increase of up to 84.5% in the flexural strength of mortar with MICP-treated fRA. The results obtained in this study were close to the strength improvement results obtained by Feng et al. [145] and the 73% improvement in the flexural strength of microbial treated mortar specimens revealed the significant impact of MICP application on mortar strength. This effect on flexural strength was attributed to the biodeposition process of c-fRCA sand mixes, which improves their properties. The calcium carbonate produced by bacteria might had strengthened the weak ITZ, a problem in RCA. The increase in flexural strength of cfRAMs can be attributed to the repair of defects on the RCA surface and the development of the ITZ. Similar results were reported by Zhao et al. [16]. However, to understand in more detail the effect of MICP-improved recycled aggregates on flexural strength, further studies on the ITZ structure and concrete/mortar microstructure is needed.

4.6.2.3. SEM Analysis of MICP Treated c-fRCA

The MICP mechanism was examined in greater detail by analyzing the microstructure and properties of improved c-fRCA sand mixes. Microbially treated c-fRCA sand mixes were segregated into three distinct sizes: 2.00-1.00 mm, 1.00-0.50 mm, and 0.50-0.075 mm, and visualised under SEM. The surface microstructure and morphology of microbially treated c-fRCA were illustrated in Figures 4.21-4.23 according to the three distinct sizes.

After treatment, it was seen that the surfaces of c-fRCA in all size groups were coated with $CaCO_3$ crystals produced through biomineralization. In MICP treated c-fRCA with in the size between 2.00-1.00 mm, the internal microstructure and pores were shown in a black square frame in Figure 4.21a, and it was determined that a part of this pore was visibly filled with $CaCO_3$. An important advantage of MICP is the ability of bacteria to penetrate micro cavities and pores within aggregates, facilitated by their small size. This advantage was prominently showcased in Figure 4.21b, where bacteria entering the pores of aggregates initiated a substantial amount of $CaCO_3$ precipitation in the pores of c-fRCA.

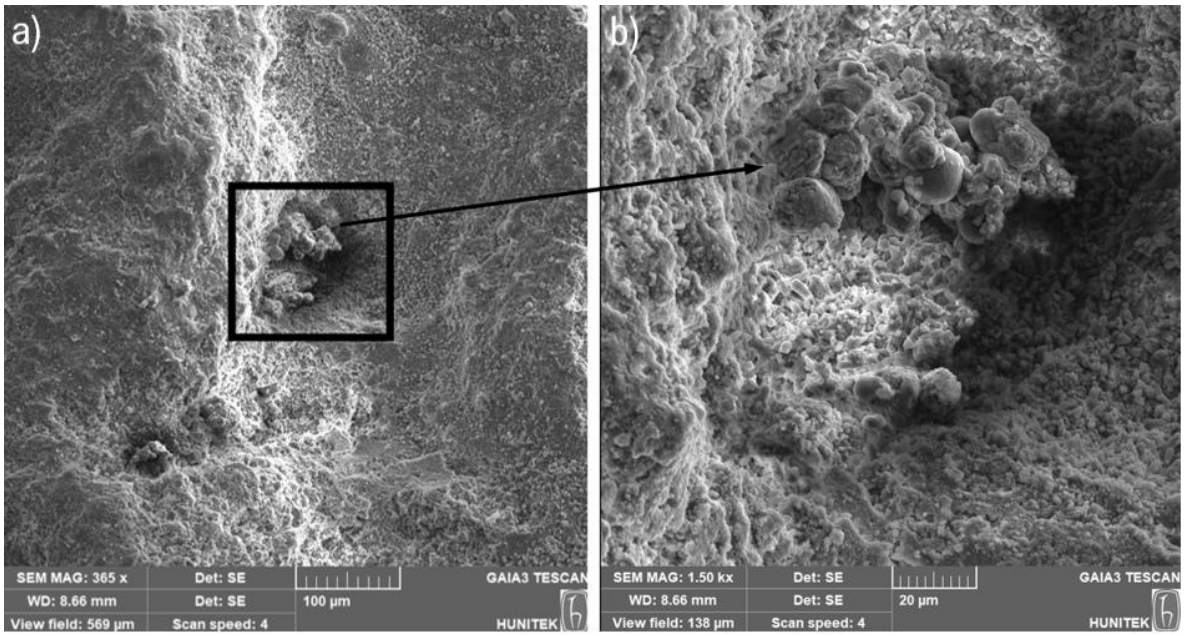

Figure 4.21. SEM micrographs of microbially treated c-fRCA in size between 2.00-1.00 mm (a) showing crystals filling the pore on the c-fRCA; (b) detailed image of $CaCO_3$ crystals

The surfaces of the MICP treated c-fRCA were filled with calcite, as depicted in Figures 4.21-4.23. These precipitated crystals consisted mostly of spherical vaterite, with some rhombohedral calcites also present, as seen in Figure 4.22b.

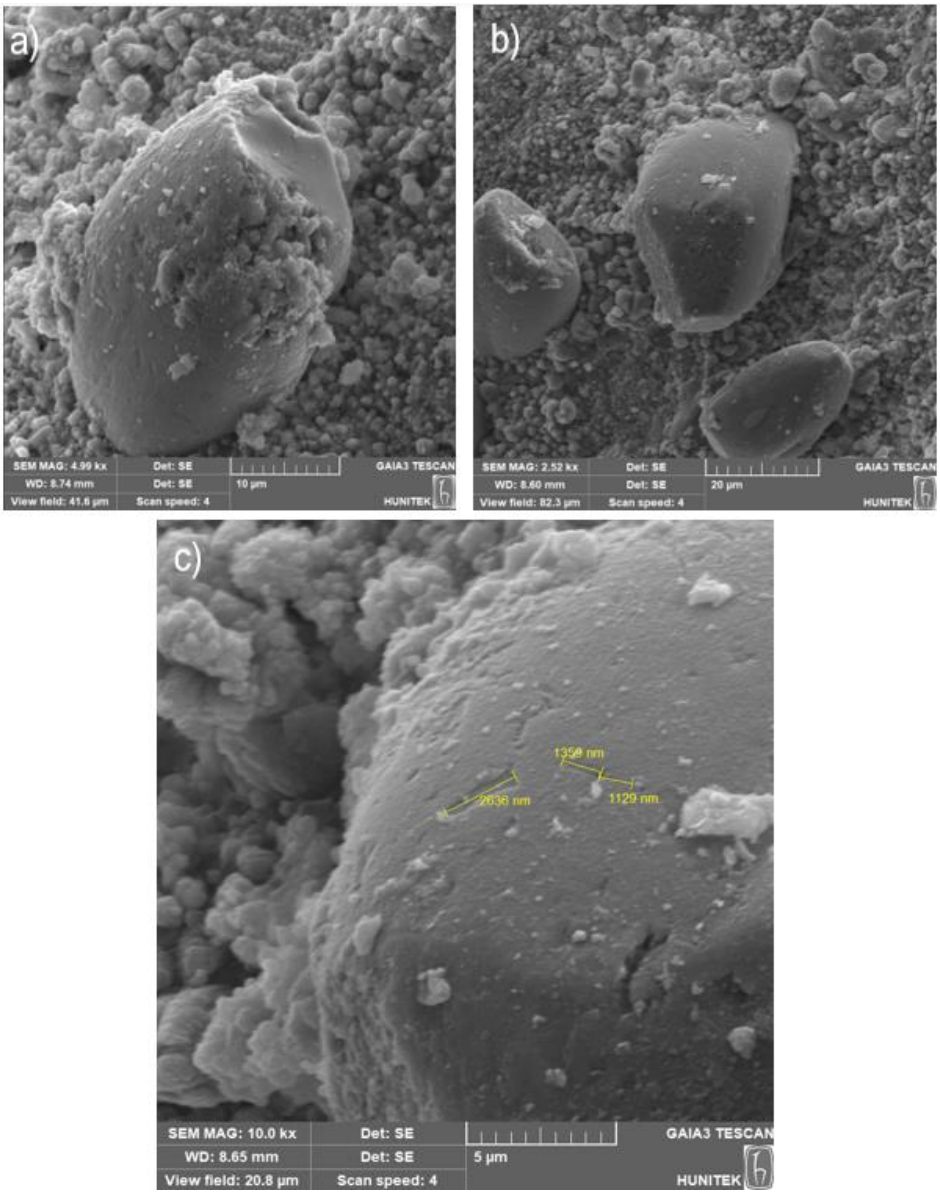

Figure 4.22. SEM micrographs of microbially treated c-fRCA in size between 1.00-0.50 mm (a) showing precipitated vaterite after MICP; (b) showing different crystal structure from vaterite as rhombohedral calcites; (c) showcasing bacterial imprints with sizes ranging between 1-2 µm

From the SEM micrographs of f-RCA (Figure 4.17), it was observed that the precipitated crystals were predominantly rhombohedral calcite, with a small amount of spherical vaterite. Conversely, for c-fRCA, the precipitated crystals were generally spherical vaterite. During the MICP process of the two fRCA mixes, the environmental pH differed, which influenced the morphology of the formed crystal. The higher pH during the treatment of the more alkaline f-RCA resulted in the precipitated crystals exhibiting a rhombohedral structure. In contrast, the lower pH in c-fRCA caused the precipitated crystals to be predominantly spherical structure.

Figure 4.22c, illustrated the bacterial imprints (with 1-2 µm size) formed on the surface of the precipitate crystal, and Figure 4.23b,c provided an enlarged detail showing residual bacteria at 1.8 µm in size. These SEM images served as evidence of bacterial involvement in the $CaCO_3$ precipitation process.

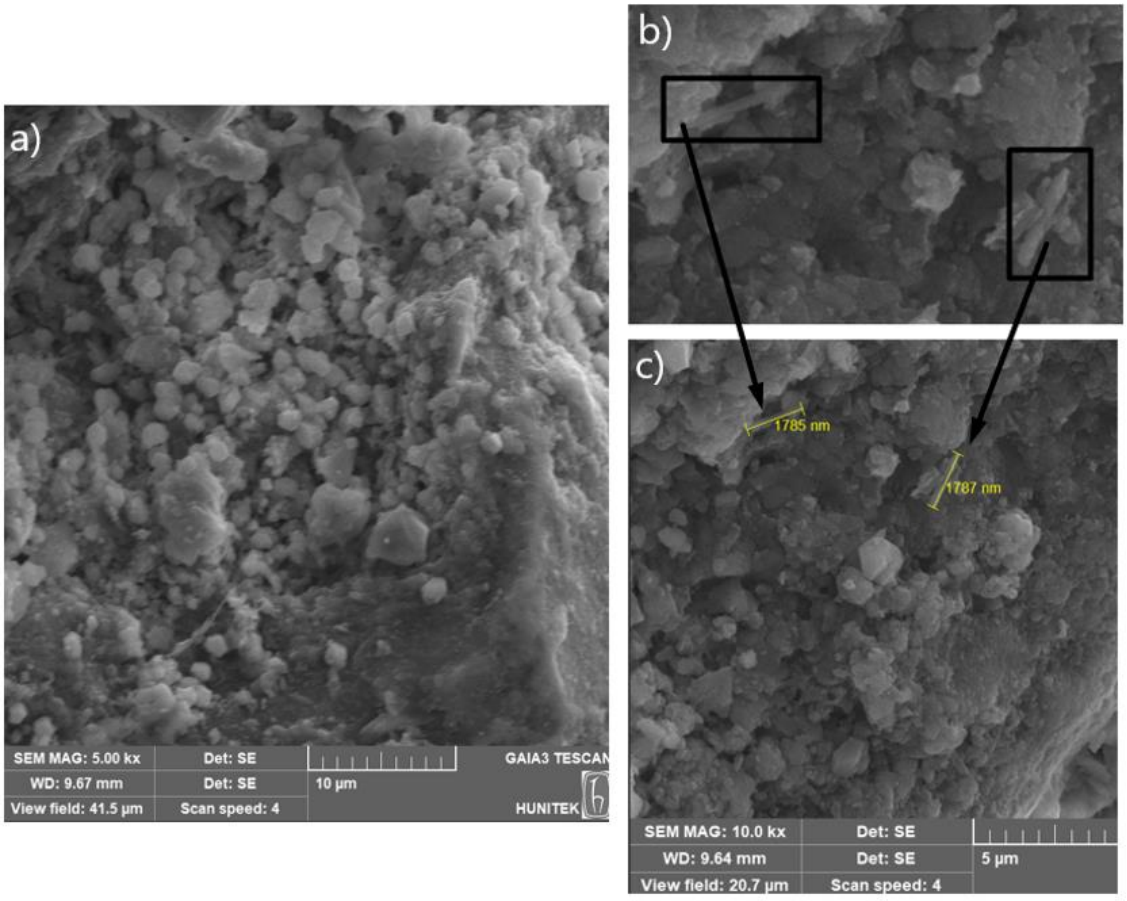

Figure 4.23. SEM micrographs of microbially treated c-fRCA in size between 0.50-0.075 mm (a) showing calcites; (b) showing bacterial residue between calcites on the c-fRCA; (c) shows the size of bacterial residues

Energy dispersive X-ray (EDX) analysis was conducted to determine the elemental composition on the surface of MICP treated c-fRCA. Results were presented in Figure 4.24. Following the analysis, the main elements detected in the 2.00-1.00 mm and 1.00-0.50 mm aggregates were Ca, O, and C, confirming the presence of a $CaCO_3$ layer above the aggregates. The total weight fraction of 3 elements, Ca, O and C, in the 2.00-1.00 mm and 1.00-0.50 mm aggregates exceeded than 96% and 98%, respectively. In contrast, for aggregates in the size range of 0.50-0.075 mm, the main elements detected by EDX were C, Si and N. This finding indicated that MICP treated c-fRCA within 0.50-0.075 mm size range were predominantly composed of the C-S-H elements typically found in untreated c-fRCA. However, upon examining the SEM analysis of the 0.50-0.075 mm MICP treated c-fRCA, it was observed that calcite crystals were present on its surface (Figure 4.23). This observation suggested that precipitated calcium carbonate by bacteria was present in specific regions of the small-sized treated c-fRCA. While certain parts of c-fRCA exhibited $CaCO_3$ crystals, other sections did not show significant $CaCO_3$ formation.

The SEM-EDX analyses revealed that the pores and surface of c-fRCA were filled with biological $CaCO_3$ crystals after MICP. The cell wall of bacteria possessed a negative zeta potential, facilitating the absorption of Ca^{2+} ions during the MICP process. Subsequent reaction of these calcium ions with CO_3^{2-} ions led to the formation of insoluble $CaCO_3$ precipitate crystals. The reduced water absorption and increased weight of microbially treated c-fRCA could be attributed to the presence of these crystal particles filling the pores and voids, effectively enhancing the structural integrity of the c-fRCA.

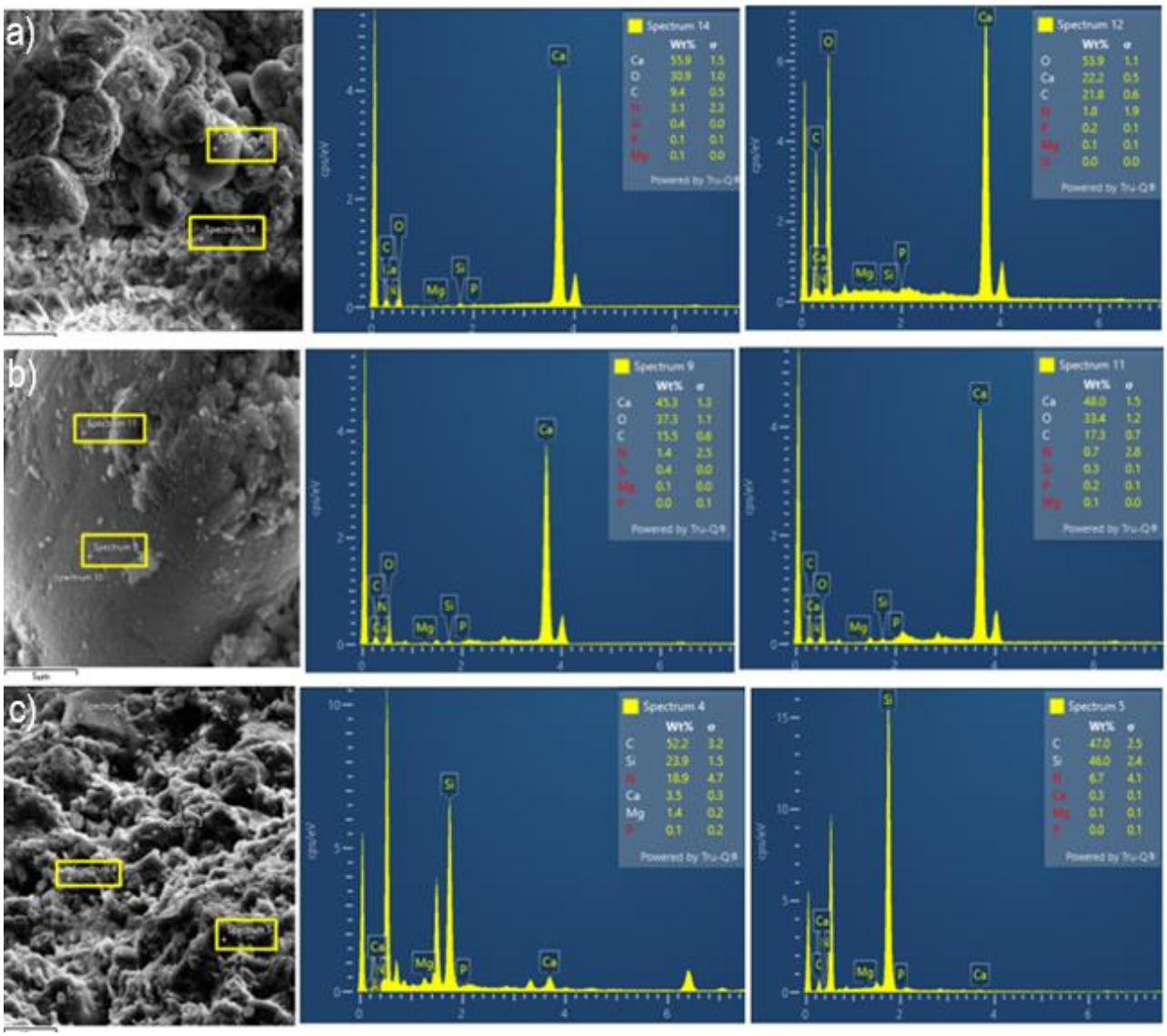

Figure 4.24. EDX micrographs of microbially treated c-fRCA for (a) 2.00-1.00 mm; (b) 1.00-0.50 mm; (c) 0.50-0.075 mm

4.6.2.4. Chemical Characterization with FTIR Analysis

The chemical composition of the powder obtained from the surface of c-fRCA sand mixes were analyzed using Fourier Transform Infrared Spectroscopy (FTIR). FTIR spectra of the powder samples obtained from untreated, abiotic control treated, and microbially treated c-fRCA sand mixes were illustrated in Figures 4.25-4.27.

The FTIR spectra obtained at 1413-1420 cm^{-1}, 873 cm^{-1} and 712 cm^{-1} in the analyzed powders indicated the presence of calcite [181,182]. Peaks observed at 1737-1747 cm^{-1} were attributed to the presence of C=O carboxyl group, similar to findings reported by Xu et al. [183]. Additionally, consistent with previous studies, the peaks at 1008 -1020 cm^{-1} could be due to abundance of C-S-H in the powder sample [181,182].

These FTIR findings corroborated the presence of calcium carbonate as the mineral precipitates observed and visualized on the surfaces of the aggregates. Furthermore, notable variations were observed in the calcite peak of the FTIR analysis for microbially treated c-fRCA sand mixes compared to untreated and abiotic control c-fRCA sand mixes (Figure 4.28). This difference could indicated higher calcium carbonate fraction in the overall powder resulting from microbial treatment.

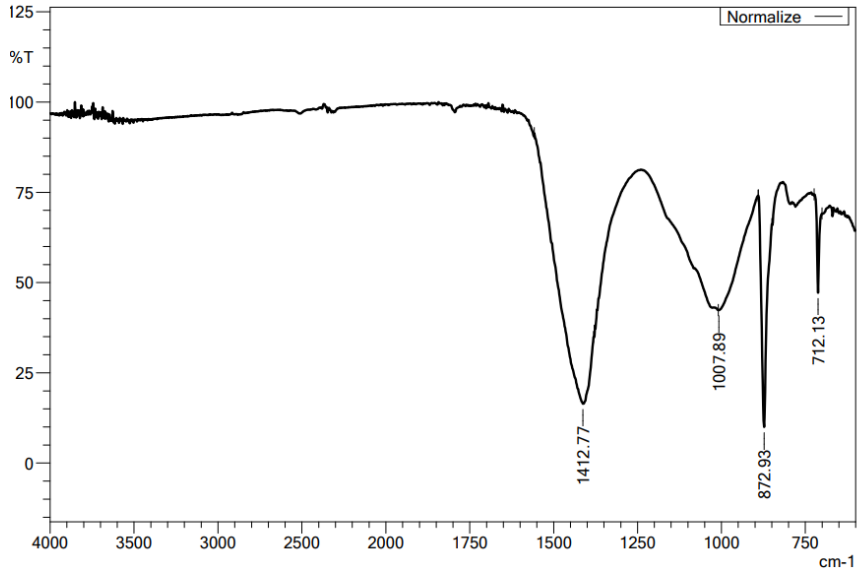

Figure 4.25. FTIR spectra of the powder samples obtained from untreated c-fRCA sand mixes

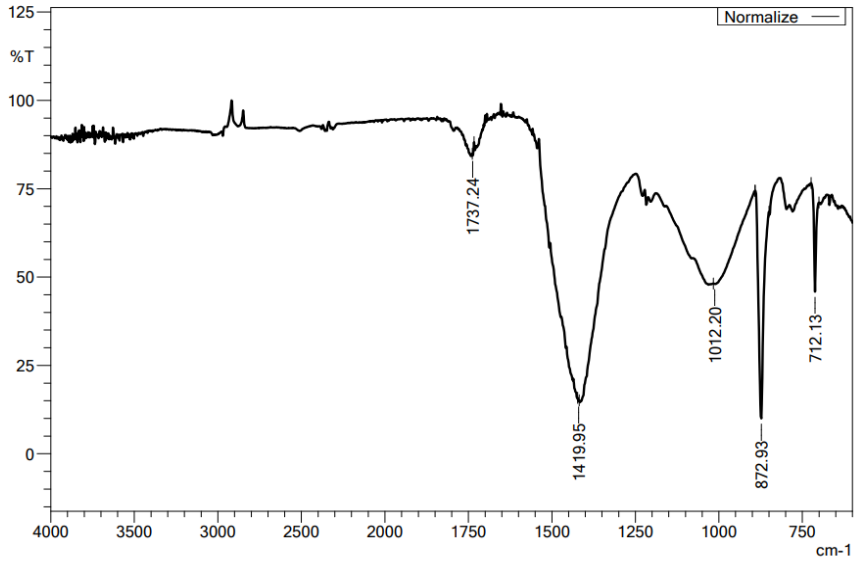

Figure 4.26. FTIR spectra of the powder samples obtained from abiotic control treated c-fRCA sand mixes

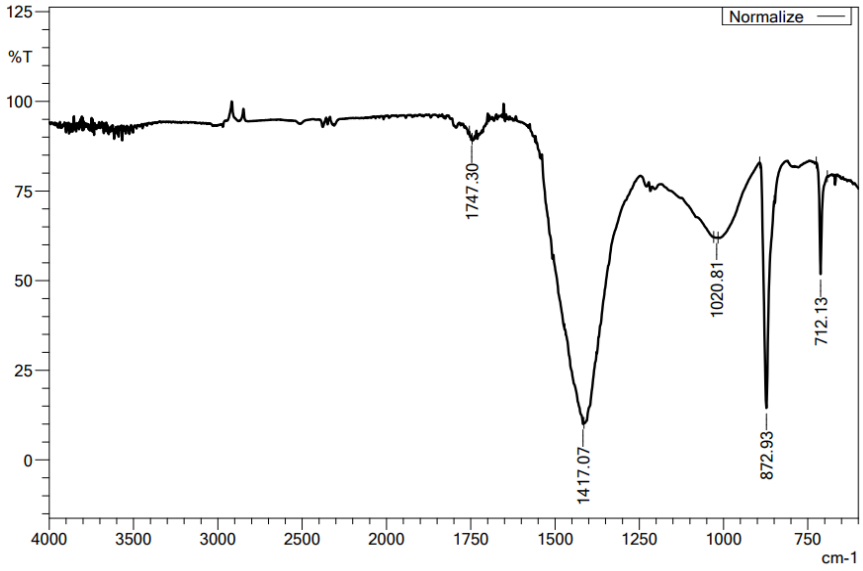

Figure 4.27. FTIR spectra of the powder samples obtained from microbially treated c-fRCA sand mixes

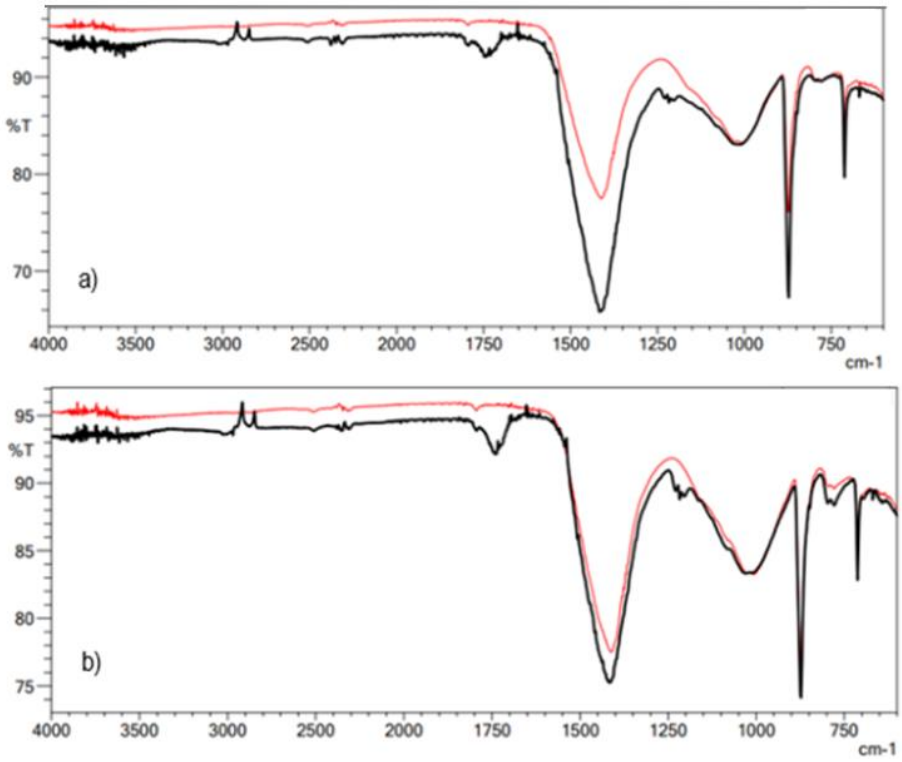

Figure 4.28. Comparison of FTIR spectra of the powder samples obtained from (a) untreated and microbially treated c-fRCA sand mixes; (b) untreated and abiotic control treated c-fRCA sand mixes

4.7. An Overview of Industrial Application and Economic Viability of Recycled Fine Aggregates Treatment with MICP

This thesis demonstrated the effect of the optimized MICP method on the enhancement of both f-RCA and c-fRCA. While the improvement method showed promising results, it was crucial to also consider the economic challenges associated with this method. This thesis study did not include a cost analysis. However, in a previous study about MICP conducted by Ersan [181], operating cost for production of 1 kg of denitrifying biogranules (ACDC) was reported as 17.4 €.kg^{-1}. Additionally, in Sonmez et al. study [146], which involved the enhancement of fRA with MICP using ACDCs, the total cost was calculated to be approximately 225 € per ton of aggregate. In this thesis, the total bacterial mass used to treat 1350 g of fRCA sand mixes was 2.7 g (0.3 g CDW.L^{-1}), indicating that the bacterial mass required to improve 1.0 ton of aggregates is 2.0 kg. Considering that microbial culture growth is the cost-determining factor and that bacterial growth is not expected to be more expensive than biogranule growth, it is estimated that

the MICP method used in this thesis would be approximately 3-4 times cheaper than the costs described in the study of Sonmez et al [146]. It is possible to reduce the cost more with future studies.

MICP method explored in this thesis, holds potential for application within the concrete production industry. Experimental treatments conducted on fRCA sand mixes using the immersion method demonstrated its applicability in large immersion baths in concrete production plant. However, a significant constraint to widespread adoption lies in the procurement of bacteria, a process that not only escalates costs but also entails time-intensive procedures. Within the scope of this thesis, an attempt was made to use 0.67 g bacteria/kg fRCA to reduce bacterial production costs and time but successful improvement could not be achieved. In the optimized treatment procedure 2 g bacteria/kg fRCA were used. It is believed that studies can further optimize the process to decrease the total treatment costs. The latter will pave the way for upscaling of this approach in construction sector.

5. CONCLUSION

In this thesis, the quality improvement of fRCA was investigated by applying a two-metabolism MICP treatment involving nitrate reduction and urea hydrolysis. Significant decrease in water absorption and increase in weight could be obtained in all f-RCA size groups upon MICP treatment. Obtained decreases in water absorption were changing between 7.3-23.5% and increases in weight were changing between 0.7-7.0% depending on the size groups of the f-RCA. In water control and abiotic control setups, no significant changes in water absorption and weight were observed, highlighting the positive effect of the microbial process. The suitability of the MICP method was confirmed through the decrease in water absorption and weight increase of all sizes of f-RCA.

The optimum MICP treatment for f-RCA sand mixes was determined as 72 hours microbial attachment stage with 2.0 g bacteria/kg aggregate application at initial urea and NO_3-N concentrations of 2.0 $g.L^{-1}$ and 0.16 $g.L^{-1}$ respectively, followed by 24 hours of biomineralization stage with initial urea, NO_3-N and Ca^{2+} concentrations of 20.0 $g.L^{-1}$, 0.26 $g.L^{-1}$ and 2.2 $g.L^{-1}$, respectively. It was found that yeast extract positively affected the urea hydrolsis performance, thus use of 2.0 $g.L^{-1}$ of yeast extract concentration in both stages is recommended. In optimized treatment conditions, urea hydrolysis efficiency of 82% was achieved at the end of biomineralization stage leading to complete precipitation of the Ca^{2+} in the media. The weight increase after the optimized MICP process of f-RCA sand mixes, having similar size distribution with standard sand, was 4.6±0.1%.

The optimized MICP method was used to treat c-fRCA sand mixes. The nitrate reduction and urea hydrolysis efficiencies obtained at the end of biomineralization of c-fRCA sand mixes were 39% and 88%, respectively. After MICP, all calcium ions were precipitated as $CaCO_3$, and the resulting weight increase was 3.8±0.2%. These findings highlighted the efficiency of bacterial activity in the MICP process through nitrate reduction and urea hydrolysis, indicating the microbial origin of the precipitated $CaCO_3$ and the simultaneous occurrence of MICP with nitrate reduction and urea hydrolysis.

The changes in the mechanical properties of the MICP-treated f-RCA and c-fRCA sand mixes were examined by casting mortar specimens. The 28-day compressive strength of the mortar containing microbially treated f-RCA sand mixes was 25.0±0.6 MPa which was 82% higher than the mortar containing untreated f-RCA sand mixes. Significant

improvement was also demonstrated for the mortar with microbially treated c-fRCA sand mixes and 95% higher 28-day compressive strength along with 75% higher flexural strength than mortar with untreated c-fRCA sand mixes were achieved. These outcomes highlighted the effectiveness of MICP technology in improving recycled aggregate quality, thus presenting a promising approach for potential applications in the ready-mixed concrete industry.

Presence and abundance of $CaCO_3$ on microbially treated f-RCA and c-fRCA sand mixes were confirmed by SEM, EDX and FTIR analysis. Microbial fingerprints on precipitated $CaCO_3$ minerals also confirmed that the $CaCO_3$ precipitation on aggregate surfaces were solely due to microbial activity.

Consequently, this study demonstrated enhanced surface and mechanical properties of recycled fine aggregates upon MICP treatment. The positive results obtained in this thesis might be promising for future research on recycled fine aggregates' improvement and their utilization in the concrete industry. It is possible to achieve more $CaCO_3$ precipitation and greater improvement in fRCA by researching different calcium concentrations in MICP in future studies. Additionally, in the MICP process utilizing both urea hydrolysis and nitrate reduction, it is anticipated that nitrate reduction performance can be increased by extending the biomineralization duration. Further research is required to understand the alterations in mortar containing MICP-treated fRCA and to examine its long-term effects. Long-term strength gain assessments of mortar through 56-day or 90-day compressive strength tests, along with durability tests to evaluate the mortar's resistance to deterioration are recommended. Analyzing changes in water absorption and porosity properties of the mortar would also contribute to a comprehensive evaluation.

6. REFERENCES

[1] V.W.Y. Tam, M. Soomro, A.C.J. Evangelista, A review of recycled aggregate in concrete applications (2000–2017), Constr Build Mater 172 (2018) 272–292. https://doi.org/10.1016/j.conbuildmat.2018.03.240.

[2] P. Peduzzi, Sand, Rarer Than One Thinks., Global Environmental Alert Service (GEAS), United Nations Environment Programme. 11 (2014) 208–218. https://doi.org/10.1016/j.envdev.2014.04.001.

[3] Hazır Beton Sektör Raporu 2021, Türkiye Hazır Beton Birliği, İstanbul, 2022. https://www.thbb.org/media/563130/2021-haz%C4%B1r-beton-sekt%C3%B6r-raporu-28-subat-2022.pdf (accessed June 14, 2024).

[4] A. Omar, K. Muthusamy, Concrete Industry, Environment Issue, and Green Concrete: A Review, Construction 2 (2022) 01–09. https://doi.org/https://doi.org/10.15282/construction.v2i1.7188.

[5] Md.U. Hossain, C.S. Poon, I.M.C. Lo, J.C.P. Cheng, Comparative environmental evaluation of aggregate production from recycled waste materials and virgin sources by LCA, Resour Conserv Recycl 109 (2016) 67–77. https://doi.org/10.1016/j.resconrec.2016.02.009.

[6] M. Bendixen, L.L. Iversen, J. Best, D.M. Franks, C.R. Hackney, E.M. Latrubesse, L.S. Tusting, Sand, gravel, and UN Sustainable Development Goals: Conflicts, synergies, and pathways forward, One Earth 4 (2021) 1095–1111. https://doi.org/10.1016/j.oneear.2021.07.008.

[7] C.P. Ginga, J.M.C. Ongpeng, Ma.K.M. Daly, Circular Economy on Construction and Demolition Waste: A Literature Review on Material Recovery and Production, Materials 13 (2020) 2970. https://doi.org/10.3390/ma13132970.

[8] G.F. Banias, C. Karkanias, M. Batsioula, L.D. Melas, A.E. Malamakis, D. Geroliolios, S. Skoutida, X. Spiliotis, Environmental Assessment of Alternative Strategies for the Management of Construction and Demolition Waste: A Life Cycle Approach, Sustainability 14 (2022) 9674. https://doi.org/10.3390/su14159674.

[9] K. Kabirifar, M. Mojtahedi, C. Wang, V.W.Y. Tam, Construction and demolition waste management contributing factors coupled with reduce, reuse, and recycle strategies for effective waste management: A review, J Clean Prod 263 (2020) 121265. https://doi.org/10.1016/j.jclepro.2020.121265.

[10] B. Suhendro, Toward Green Concrete for Better Sustainable Environment, Procedia Eng 95 (2014) 305–320. https://doi.org/10.1016/j.proeng.2014.12.190.

[11] M. Behera, S.K. Bhattacharyya, A.K. Minocha, R. Deoliya, S. Maiti, Recycled aggregate from C&D waste & its use in concrete – A breakthrough towards sustainability in construction sector: A review, Constr Build Mater 68 (2014) 501–516. https://doi.org/10.1016/j.conbuildmat.2014.07.003.

[12] C. Shi, Y. Li, J. Zhang, W. Li, L. Chong, Z. Xie, Performance enhancement of recycled concrete aggregate – A review, J Clean Prod 112 (2016) 466–472. https://doi.org/10.1016/J.JCLEPRO.2015.08.057.

[13] L. Li, C.S. Poon, J. Xiao, D. Xuan, Effect of carbonated recycled coarse aggregate on the dynamic compressive behavior of recycled aggregate concrete, Constr Build Mater 151 (2017) 52–62. https://doi.org/10.1016/j.conbuildmat.2017.06.043.

[14] V. Spaeth, A. Djerbi Tegguer, Improvement of recycled concrete aggregate properties by polymer treatments, International Journal of Sustainable Built Environment 2 (2013) 143–152. https://doi.org/10.1016/j.ijsbe.2014.03.003.

[15] A.M. Grabiec, J. Klama, D. Zawal, D. Krupa, Modification of recycled concrete aggregate by calcium carbonate biodeposition, Constr Build Mater 34 (2012) 145–150. https://doi.org/10.1016/j.conbuildmat.2012.02.027.

[16] Y. Zhao, L. Peng, Z. Feng, Z. Lu, Optimization of microbial induced carbonate precipitation treatment process to improve recycled fine aggregate, Cleaner Materials 1 (2021) 100003. https://doi.org/10.1016/j.clema.2021.100003.

[17] J. Qiu, D.Q.S. Tng, E.-H. Yang, Surface treatment of recycled concrete aggregates through microbial carbonate precipitation, Constr Build Mater 57 (2014) 144–150. https://doi.org/10.1016/j.conbuildmat.2014.01.085.

[18] J. Wang, B. Vandevyvere, S. Vanhessche, J. Schoon, N. Boon, N. De Belie, Microbial carbonate precipitation for the improvement of quality of recycled

aggregates, J Clean Prod 156 (2017) 355–366. https://doi.org/10.1016/j.jclepro.2017.04.051.

[19] Sustainability of Construction Materials (Second Edition), Woodhead Publishing Series in Civil and Structural Engineering, 2016, Pages 181-207.

[20] M. Aşık, Structural lightweight concrete with natural perlite aggregate and perlite powder, Master of Science, Middle East Technical University , 2006. https://open.metu.edu.tr/handle/11511/15945.

[21] S. Ismail, K.W. Hoe, M. Ramli, Sustainable Aggregates: The Potential and Challenge for Natural Resources Conservation, Procedia Soc Behav Sci 101 (2013) 100–109. https://doi.org/10.1016/J.SBSPRO.2013.07.183.

[22] I.A. Rahman, H. Hamdam, A.M.A. Zaidi, Assessment of Recycled Aggregate Concrete, Mod Appl Sci 3 (2009) 47–54. https://doi.org/10.5539/mas.v3n10p47.

[23] Aggregate-Cement, Mining Turkey Journal (2018) 92–96. https://madencilikturkiye.com/madencilik-turkiye-dergisinin-72-sayisi-cikti/ (accessed June 14, 2024).

[24] Hazır Beton Sektör Raporu 2022, Türkiye Hazır Beton Birliği, İstanbul, 2023. https://www.thbb.org/media/661866/2022-haz%C4%B1r-beton-sekt%C3%B6r-raporu-04052023.pdf (accessed June 14, 2024).

[25] A. Tuğrul, M. Yilmaz, İ. Sönmez, S. Hasdemir, Sustainable management of aggregate resources in İstanbul, Geological Society, London, Engineering Geology Special Publications 27 (2016) 55–61. https://doi.org/https://doi.org/10.1144/EGSP27.5.

[26] G.S. dos Reis, M. Quattrone, W.M. Ambrós, B. Grigore Cazacliu, C. Hoffmann Sampaio, Current Applications of Recycled Aggregates from Construction and Demolition: A Review, Materials 14 (2021) 1700. https://doi.org/10.3390/ma14071700.

[27] C. Llatas, A model for quantifying construction waste in projects according to the European waste list, Waste Management 31 (2011) 1261–1276. https://doi.org/10.1016/j.wasman.2011.01.023.

[28] W. Lu, C. Webster, Y. Peng, X. Chen, X. Zhang, Estimating and calibrating the amount of building-related construction and demolition waste in urban China,

International Journal of Construction Management 17 (2017) 13–24. https://doi.org/10.1080/15623599.2016.1166548.

[29] Eurostat Statistics for Waste Flow Generation 2016, European Commision (2018), http://epp.eurostat.ec.europa.eu/portal/page/portal/eurostat/home/

[30] Advancing Sustainable Materials Management. 2014 Fact Sheet United States Environmental Protection Agency Office of Land and Emergency Management (5306P) Washington, DC , 2016.

[31] B. Lei, L. Yu, Z. Chen, W. Yang, C. Deng, Z. Tang, Carbon Emission Evaluation of Recycled Fine Aggregate Concrete Based on Life Cycle Assessment, Sustainability 14 (2022) 14448. https://doi.org/10.3390/su142114448.

[32] Ministry of Environment and Urbanization (2017), National Waste Management and Action Plan 2023, Ankara, Turkey.

[33] R.F. de Magalhães, Â. de M.F. Danilevicz, T.A. Saurin, Reducing construction waste: A study of urban infrastructure projects, Waste Management 67 (2017) 265–277. https://doi.org/10.1016/j.wasman.2017.05.025.

[34] T. Esin, N. Cosgun, A study conducted to reduce construction waste generation in Turkey, Build Environ 42 (2007) 1667–1674. https://doi.org/10.1016/j.buildenv.2006.02.008.

[35] S. Ulubeyli, A. Kazaz, V. Arslan, Construction and Demolition Waste Recycling Plants Revisited: Management Issues, Procedia Eng 172 (2017) 1190–1197. https://doi.org/10.1016/j.proeng.2017.02.139.

[36] W. Lu, Y. Peng, C. Webster, J. Zuo, Stakeholders' willingness to pay for enhanced construction waste management: A Hong Kong study, Renewable and Sustainable Energy Reviews 47 (2015) 233–240. https://doi.org/10.1016/j.rser.2015.03.008.

[37] R.V. Silva, J. de Brito, R.K. Dhir, Availability and processing of recycled aggregates within the construction and demolition supply chain: A review, J Clean Prod 143 (2017) 598–614. https://doi.org/10.1016/j.jclepro.2016.12.070.

[38] T. Vincent, M. Guy, P. Louis-César, B. Jean-François, M. Richard, Physical process to sort construction and demolition waste (C&DW) fines components using process water, Waste Management 143 (2022) 125–134. https://doi.org/10.1016/j.wasman.2022.02.012.

[39] Hafriyat Toprağı, İnşaat ve Yıkıntı Atıklarının Kontrolü Yönetmeliği, Turkish Ministry of Environment and Forestry, Directorate General of Environmental Management, Ankara, Turkey, 2004.

[40] B.N. Şen, Z. Eren, Döngüsel Ekonomi Modeli Kapsamında Erzurum İli Hafriyat Toprağı, İnşaat ve Yıkıntı Atıklarının Yol Yapımında Kullanılabilirliğinin İncelenmesi, Sürdürülebilir Çevre Dergisi 1 (2021) 41–52. https://dergipark.org.tr/tr/pub/cevder/issue/67695/986363 (accessed May 28, 2024).

[41] A.B. Ayan, A. Dalı, H. Mühendislik, B. Programı, H. Program, Dekonstrüksiyon İçin Tasarım Tekniklerinin Türkiye'de Uygulanabilirliği, Yüksek Lisans Tezi, İstanbul Teknik Üniversitesi, 2013.

[42] N. Tojo, Europe as a Recycling Society, Working Paper 6, European Topic Centre on Sustainable Consumption and Production, Copenhagen, 2010.

[43] M.O. Federle, Overview of building construction waste and the potential for materials recycling, Build. Res. J. 2 (1993) 31–37.

[44] European Union. Directive 2008/98/EC of the European Parliament and of the Council of 19 November 2008 on waste and repealing certain directives. 2008. doi:2008/98/EC. 32008L0098].

[45] N. Hamdi, I. Ben Messaoud, E. Srasra, Production of geopolymer binders using clay minerals and industrial wastes, Comptes Rendus. Chimie 22 (2018) 220–226. https://doi.org/10.1016/j.crci.2018.11.010.

[46] E. Kravchenko, G. Lazorenko, X. Jiang, Z. Leng, Alkali-activated materials made of construction and demolition waste as precursors: A review, Sustainable Materials and Technologies 39 (2024) e00829. https://doi.org/10.1016/j.susmat.2024.e00829.

[47] M. Alhawat, A. Ashour, G. Yildirim, A. Aldemir, M. Sahmaran, Properties of geopolymers sourced from construction and demolition waste: A review, Journal of Building Engineering 50 (2022) 104104. https://doi.org/10.1016/j.jobe.2022.104104.

[48] Y. Jani, W. Hogland, Waste glass in the production of cement and concrete – A review, J Environ Chem Eng 2 (2014) 1767–1775. https://doi.org/10.1016/j.jece.2014.03.016.

[49] S. Chandra Paul, B. Šavija, A.J. Babafemi, A comprehensive review on mechanical and durability properties of cement-based materials containing waste recycled glass, J Clean Prod 198 (2018) 891–906. https://doi.org/10.1016/j.jclepro.2018.07.095.

[50] Waste and Supplementary Cementitious Materials in Concrete, Characterisation, Properties and Applications, A volume in Woodhead Publishing Series in Civil and Structural Engineering, book, 2018, Pages 79-120.

[51] R.V. Silva, J. de Brito, R.K. Dhir, Properties and composition of recycled aggregates from construction and demolition waste suitable for concrete production, Constr Build Mater 65 (2014) 201–217. https://doi.org/10.1016/j.conbuildmat.2014.04.117.

[52] M. Menegaki, D. Damigos, A review on current situation and challenges of construction and demolition waste management, Curr Opin Green Sustain Chem 13 (2018) 8–15. https://doi.org/10.1016/j.cogsc.2018.02.010.

[53] P.B. Cachim, Mechanical properties of brick aggregate concrete, Constr Build Mater 23 (2009) 1292–1297. https://doi.org/10.1016/j.conbuildmat.2008.07.023.

[54] J.R. Jiménez, J. Ayuso, F. Agrela, M. López, A.P. Galvín, Utilisation of unbound recycled aggregates from selected CDW in unpaved rural roads, Resour Conserv Recycl 58 (2012) 88–97. https://doi.org/10.1016/J.RESCONREC.2011.10.012.

[55] A. Neville, The confused world of sulfate attack on concrete, Cem Concr Res 34 (2004) 1275–1296. https://doi.org/10.1016/j.cemconres.2004.04.004.

[56] C.S. Poon, S.C. Kou, L. Lam, Use of recycled aggregates in molded concrete bricks and blocks, Constr Build Mater 16 (2002) 281–289. https://doi.org/10.1016/S0950-0618(02)00019-3.

[57] Schoon, J.; Van Der Heyden, L.; Eloy, P.; Gaigneux, E.M.; De Buysser, K.; Van Driessche, I.; De Belie, N. Waste fibrecement: An interesting alternative raw material for a sustainable Portland clinker production. Constr. Build. Mater. 2012.

[58] Allahverdi, A.; Kani, E. Use of Construction and Demolition Waste (CDW) for Alkali-Activated or Geopolymer Cements. Handbook of Recycled Concrete and Demolition Waste; Woodhead publishing: Cambridge, UK, 2013.

[59] Z. Sun, H. Cui, H. An, D. Tao, Y. Xu, J. Zhai, Q. Li, Synthesis and thermal behavior of geopolymer-type material from waste ceramic, Constr Build Mater 49 (2013) 281–287. https://doi.org/10.1016/j.conbuildmat.2013.08.063.

[60] T. Luukkonen, Z. Abdollahnejad, J. Yliniemi, P. Kinnunen, M. Illikainen, One-part alkali-activated materials: A review, Cem Concr Res 103 (2018) 21–34. https://doi.org/10.1016/j.cemconres.2017.10.001.

[61] R.-U.-D. Nassar, P. Soroushian, Strength and durability of recycled aggregate concrete containing milled glass as partial replacement for cement, Constr Build Mater 29 (2012) 368–377. https://doi.org/10.1016/j.conbuildmat.2011.10.061.

[62] Study on Recycled Aggregate and Recycled Concrete, Concrete Journal 16 (1978) 18–31. https://doi.org/10.3151/coj1975.16.7_18.

[63] C.S. Poon, Z.H. Shui, L. Lam, Effect of microstructure of ITZ on compressive strength of concrete prepared with recycled aggregates, Constr Build Mater 18 (2004) 461–468. https://doi.org/10.1016/j.conbuildmat.2004.03.005.

[64] S. Nagataki, A. Gokce, T. Saeki, M. Hisada, Assessment of recycling process induced damage sensitivity of recycled concrete aggregates, Cem Concr Res 34 (2004) 965–971. https://doi.org/10.1016/J.CEMCONRES.2003.11.008.

[65] G. Bai, C. Zhu, C. Liu, B. Liu, An evaluation of the recycled aggregate characteristics and the recycled aggregate concrete mechanical properties, Constr Build Mater 240 (2020) 117978. https://doi.org/10.1016/j.conbuildmat.2019.117978.

[66] V.W.Y. Tam, H. Wattage, K.N. Le, A. Buteraa, M. Soomro, Methods to improve microstructural properties of recycled concrete aggregate: A critical review, Constr Build Mater 270 (2021) 121490. https://doi.org/10.1016/j.conbuildmat.2020.121490.

[67] R. Wang, N. Yu, Y. Li, Methods for improving the microstructure of recycled concrete aggregate: A review, Constr Build Mater 242 (2020) 118164. https://doi.org/10.1016/j.conbuildmat.2020.118164.

[68] British Standards Institution, Tests for mechanical and physical properties of aggregates. Part 6, Determination of particle density and water absorption.

[69] T.C. Hansen, H. Narud, Strength of Recycled Concrete Made From Crushed Concrete Coarse Aggregate, Concrete International 5 (1983) 79–83.

[70] K. McNeil, T.H.-K. Kang, Recycled Concrete Aggregates: A Review, Int J Concr Struct Mater 7 (2013) 61–69. https://doi.org/10.1007/s40069-013-0032-5.

[71] A. Ajdukiewicz, A. Kliszczewicz, Influence of recycled aggregates on mechanical properties of HS/HPC, Cem Concr Compos 24 (2002) 269–279. https://doi.org/10.1016/S0958-9465(01)00012-9.

[72] J. Xiao, W. Li, Y. Fan, X. Huang, An overview of study on recycled aggregate concrete in China (1996–2011), Constr Build Mater 31 (2012) 364–383. https://doi.org/10.1016/j.conbuildmat.2011.12.074.

[73] V.W.Y. Tam, X.F. Gao, C.M. Tam, Microstructural analysis of recycled aggregate concrete produced from two-stage mixing approach, Cem Concr Res 35 (2005) 1195–1203. https://doi.org/10.1016/j.cemconres.2004.10.025.

[74] H.-J. Chen, T. Yen, K.-H. Chen, Use of building rubbles as recycled aggregates, Cem Concr Res 33 (2003) 125–132. https://doi.org/10.1016/S0008-8846(02)00938-9.

[75] J. Xiao, W. Li, C. Poon, Recent studies on mechanical properties of recycled aggregate concrete in China—A review, Sci China Technol Sci 55 (2012) 1463–1480. https://doi.org/10.1007/s11431-012-4786-9.

[76] N.K. Bairagi, K. Ravande, V.K. Pareek, Behaviour of concrete with different proportions of natural and recycled aggregates, Resour Conserv Recycl 9 (1993) 109–126. https://doi.org/10.1016/0921-3449(93)90036-F.

[77] A. Katz, Properties of concrete made with recycled aggregate from partially hydrated old concrete, Cem Concr Res 33 (2003) 703–711. https://doi.org/10.1016/S0008-8846(02)01033-5.

[78] M. Chakradhara Rao, S.K. Bhattacharyya, S. V. Barai, Influence of field recycled coarse aggregate on properties of concrete, Mater Struct 44 (2011) 205–220. https://doi.org/10.1617/s11527-010-9620-x.

[79] V.W.Y. Tam, C.M. Tam, Y. Wang, Optimization on proportion for recycled aggregate in concrete using two-stage mixing approach, Constr Build Mater 21 (2007) 1928–1939. https://doi.org/10.1016/j.conbuildmat.2006.05.040.

[80] C.S. Poon, Z.H. Shui, L. Lam, H. Fok, S.C. Kou, Influence of moisture states of natural and recycled aggregates on the slump and compressive strength of concrete, Cem Concr Res 34 (2004) 31–36. https://doi.org/10.1016/S0008-8846(03)00186-8.

[81] J. Li, J. Xiao, J. Huang, Influence of recycled coarse aggregate replacement percentages on compressive strength of concrete, Journal of Building Materials 9 (2006) 297–301.

[82] M. Malešev, V. Radonjanin, S. Marinković, Recycled Concrete as Aggregate for Structural Concrete Production, Sustainability 2 (2010) 1204–1225. https://doi.org/10.3390/su2051204.

[83] A.K. Padmini, K. Ramamurthy, M.S. Mathews, Influence of parent concrete on the properties of recycled aggregate concrete, Constr Build Mater 23 (2009) 829–836. https://doi.org/10.1016/j.conbuildmat.2008.03.006.

[84] S.W. Tabsh, A.S. Abdelfatah, Influence of recycled concrete aggregates on strength properties of concrete, Constr Build Mater 23 (2009) 1163–1167. https://doi.org/10.1016/j.conbuildmat.2008.06.007.

[85] M. Etxeberria, E. Vázquez, A. Marí, M. Barra, Influence of amount of recycled coarse aggregates and production process on properties of recycled aggregate concrete, Cem Concr Res 37 (2007) 735–742. https://doi.org/10.1016/j.cemconres.2007.02.002.

[86] R.B.E. Salem, Role of Chemical and Mineral Admixtures on the Physical Properties and Frost-Resistance of Recycled Aggre-gate Concrete, ACI Mater J 95 (1998). https://doi.org/10.14359/398.

[87] N. Deshpande, S. Kulkarni, N. Patil, Effectiveness of using coarse recycled concrete aggregate in concrete, International Journal of Earth Sciences and Engineering 4 (2011) 913–919.

[88] W.H. Kwan, M. Ramli, K.J. Kam, M.Z. Sulieman, Influence of the amount of recycled coarse aggregate in concrete design and durability properties, Constr Build Mater (2011). https://doi.org/10.1016/j.conbuildmat.2011.06.059.

[89] Waste Concrete as Aggregate for New Concrete, ACI Journal Proceedings 74 (1977). https://doi.org/10.14359/11019.

[90] K. Rahal, Mechanical properties of concrete with recycled coarse aggregate, Build Environ 42 (2007) 407–415. https://doi.org/10.1016/j.buildenv.2005.07.033.

[91] T.C. Hansen, Recycling of Demolished Concrete and Masonry, Recycling of Demolished Concrete and Masonry (1992). https://doi.org/10.1201/9781482267075.

[92] C.; Yang, C. Hs, A.F. Ashour, Influence of Type and Replacement Level of Recycled Aggregates on Concrete Properties, ACI Mater J 105 (2008) 289–296. http://hdl.handle.net/10454/7768 (accessed May 28, 2024).

[93] T.R. Sonawane, S. Pimplikar, Use Of Recycled Aggregate In Concrete, International Journal of Engineering Research and Technology (2013).

[94] L. Butler, J.S. West, S.L. Tighe, Effect of recycled concrete coarse aggregate from multiple sources on the hardened properties of concrete with equivalent compressive strength, Constr Build Mater 47 (2013) 1292–1301. https://doi.org/10.1016/j.conbuildmat.2013.05.074.

[95] S.-C. Kou, C.-S. Poon, Mechanical properties of 5-year-old concrete prepared with recycled aggregates obtained from three different sources, Magazine of Concrete Research 60 (2008) 57–64. https://doi.org/10.1680/macr.2007.00052.

[96] İ.B. Topçu, S. Şengel, Properties of concretes produced with waste concrete aggregate, Cem Concr Res 34 (2004) 1307–1312. https://doi.org/10.1016/j.cemconres.2003.12.019.

[97] M. Tavakoli, P. Soroushian, Drying shrinkage behavior of recycled aggregate concrete, Concrete International (1996).

[98] S. Han, S. Zhao, D. Lu, D. Wang, Performance Improvement of Recycled Concrete Aggregates and Their Potential Applications in Infrastructure: A Review, Buildings 13 (2023) 1411. https://doi.org/10.3390/buildings13061411.

[99] H. Tateyashiki, H. Shima, Y. Matsumoto, Y. Koga, Properties of concrete with high quality recycled aggregate by heat and rubbing method, Proc. JCI 23 (2001) 61–66.

[100] A. Mistri, S.K. Bhattacharyya, N. Dhami, A. Mukherjee, S. V. Barai, A review on different treatment methods for enhancing the properties of recycled aggregates for sustainable construction materials, Constr Build Mater 233 (2020) 117894. https://doi.org/10.1016/j.conbuildmat.2019.117894.

[101] A. Katz, Treatments for the Improvement of Recycled Aggregate, Journal of Materials in Civil Engineering 16 (2004) 597–603. https://doi.org/10.1061/(ASCE)0899-1561(2004)16:6(597).

[102] V.W.Y. Tam, C.M. Tam, K.N. Le, Removal of cement mortar remains from recycled aggregate using pre-soaking approaches, Resour Conserv Recycl 50 (2007) 82–101. https://doi.org/10.1016/j.resconrec.2006.05.012.

[103] S. Ismail, M. Ramli, Engineering properties of treated recycled concrete aggregate (RCA) for structural applications, Constr Build Mater 44 (2013) 464–476. https://doi.org/10.1016/j.conbuildmat.2013.03.014.

[104] H.-S. Ryu, D.-M. Kim, S.-H. Shin, S.-M. Lim, W.-J. Park, Evaluation on the Surface Modification of Recycled Fine Aggregates in Aqueous H2SiF6 Solution, Int J Concr Struct Mater 12 (2018). https://doi.org/10.1186/s40069-018-0256-5.

[105] S.C. Kou, C.S. Poon, Enhancing the durability properties of concrete prepared with coarse recycled aggregate, Constr Build Mater 35 (2012) 69–76. https://doi.org/10.1016/j.conbuildmat.2012.02.032.

[106] N. Kisku, H. Joshi, M. Ansari, S.K. Panda, S. Nayak, S.C. Dutta, A critical review and assessment for usage of recycled aggregate as sustainable construction material, Constr Build Mater 131 (2017) 721–740. https://doi.org/10.1016/j.conbuildmat.2016.11.029.

[107] M. Zajac, J. Skocek, Ł. Gołek, J. Deja, Supplementary cementitious materials based on recycled concrete paste, J Clean Prod 387 (2023) 135743. https://doi.org/10.1016/j.jclepro.2022.135743.

[108] D. Lu, Z. Tang, L. Zhang, J. Zhou, Y. Gong, Y. Tian, J. Zhong, Effects of Combined Usage of Supplementary Cementitious Materials on the Thermal

Properties and Microstructure of High-Performance Concrete at High Temperatures, Materials 13 (2020) 1833. https://doi.org/10.3390/ma13081833.

[109] D. Lu, Y. Wang, Z. Leng, J. Zhong, Influence of ternary blended cementitious fillers in a cold mix asphalt mixture, J Clean Prod 318 (2021) 128421. https://doi.org/10.1016/j.jclepro.2021.128421.

[110] K. Cui, D. Lau, Y. Zhang, J. Chang, Mechanical properties and mechanism of nano-CaCO3 enhanced sulphoaluminate cement-based reactive powder concrete, Constr Build Mater 309 (2021) 125099. https://doi.org/10.1016/j.conbuildmat.2021.125099.

[111] X. Jiang, Y. Zhang, Y. Zhang, J. Ma, R. Xiao, F. Guo, Y. Bai, B. Huang, Influence of size effect on the properties of slag and waste glass-based geopolymer paste, J Clean Prod 383 (2023) 135428. https://doi.org/10.1016/j.jclepro.2022.135428.

[112] R. Xiao, B. Huang, H. Zhou, Y. Ma, X. Jiang, A state-of-the-art review of crushed urban waste glass used in OPC and AAMs (geopolymer): Progress and challenges, Cleaner Materials 4 (2022) 100083. https://doi.org/10.1016/j.clema.2022.100083.

[113] B. Wang, L. Yan, Q. Fu, B. Kasal, A Comprehensive Review on Recycled Aggregate and Recycled Aggregate Concrete, Resour Conserv Recycl 171 (2021) 105565. https://doi.org/10.1016/j.resconrec.2021.105565.

[114] V. Spaeth, M.P. Delplancke-Ogletree, J.P. Lecomte, Hydration Process and Microstructure Development of Integral Water Repellent Cement Based Materials, (2008) 245–254.

[115] W.M. Shaban, J. Yang, H. Su, K.H. Mo, L. Li, J. Xie, Quality Improvement Techniques for Recycled Concrete Aggregate: A review, Journal of Advanced Concrete Technology 17 (2019) 151–167. https://doi.org/10.3151/jact.17.151.

[116] L.-X. Yang, Y.-L. QIAN, Q.-Q. Fang, Y.-T. Han, Effects of Recycled Coarse Aggregate Reinforcing Treated by Water-Glass on the Performance of Recycled Concrete, in: Proceedings of the 3rd International Conference on Material Engineering and Application (ICMEA 2016), Atlantis Press, Paris, France, 2016. https://doi.org/10.2991/icmea-16.2016.29.

[117] A. Shayan, A. Xu, Performance and Properties of Structural Concrete Made with Recycled Concrete Aggregate, Materials Journal 100 (2003) 371–380. https://doi.org/10.14359/12812.

[118] S. Lee, W. Park, H. Lee, Life cycle CO2 assessment method for concrete using CO2 balance and suggestion to decrease LCCO2 of concrete in South-Korean apartment, Energy Build 58 (2013) 93–102. https://doi.org/10.1016/j.enbuild.2012.11.034.

[119] O. Rahmani, An experimental study of accelerated mineral carbonation of industrial waste red gypsum for CO2 sequestration, Journal of CO2 Utilization 35 (2020) 265–271. https://doi.org/10.1016/j.jcou.2019.10.005.

[120] D. Sharma, S. Goyal, Accelerated carbonation curing of cement mortars containing cement kiln dust: An effective way of CO2 sequestration and carbon footprint reduction, J Clean Prod 192 (2018) 844–854. https://doi.org/10.1016/j.jclepro.2018.05.027.

[121] G. Cultrone, F.J. Carrillo Rosua, Growth of metastable phases during brick firing: Mineralogical and microtextural changes induced by the composition of the raw material and the presence of additives, Appl Clay Sci 185 (2020) 105419. https://doi.org/10.1016/j.clay.2019.105419.

[122] M. Castellote, L. Fernandez, C. Andrade, C. Alonso, Chemical changes and phase analysis of OPC pastes carbonated at different CO2 concentrations, Mater Struct 42 (2009) 515–525. https://doi.org/10.1617/s11527-008-9399-1.

[123] N. Hosseini Balam, D. Mostofinejad, M. Eftekhar, Use of carbonate precipitating bacteria to reduce water absorption of aggregates, Constr Build Mater 141 (2017) 565–577. https://doi.org/10.1016/j.conbuildmat.2017.03.042.

[124] N.K. Dhami, M.S. Reddy, A. Mukherjee, Biomineralization of calcium carbonates and their engineered applications: a review, Front Microbiol 4 (2013). https://doi.org/10.3389/fmicb.2013.00314.

[125] J. Xiao, Recycled Aggregate Concrete Structures, Springer Berlin Heidelberg, Berlin, Heidelberg, 2018. https://doi.org/10.1007/978-3-662-53987-3.

[126] Y. Li, S. Zhang, R. Wang, Y. Zhao, C. Men, Effects of carbonation treatment on the crushing characteristics of recycled coarse aggregates, Constr Build Mater 201 (2019) 408–420. https://doi.org/10.1016/j.conbuildmat.2018.12.158.

[127] C. Shi, M. Liu, P. He, Z. Ou, Factors affecting kinetics of CO2 curing of concrete, J Sustain Cem Based Mater 1 (2012) 24–33. https://doi.org/10.1080/21650373.2012.727321.

[128] Y. Ding, J. Wu, P. Xu, X. Zhang, Y. Fan, Treatment Methods for the Quality Improvement of Recycled Concrete Aggregate (RCA) - A Review, Journal of Wuhan University of Technology-Mater. Sci. Ed. 36 (2021) 77–92. https://doi.org/10.1007/s11595-021-2380-3.

[129] E. Boquet, A. Boronat, A. Ramos-Cormenzana, Production of Calcite (Calcium Carbonate) Crystals by Soil Bacteria is a General Phenomenon, Nature 1973 246:5434 246 (1973) 527–529. https://doi.org/10.1038/246527a0.

[130] C. Bu, X. Lu, D. Zhu, L. Liu, Y. Sun, Q. Wu, W. Zhang, Q. Wei, Soil improvement by microbially induced calcite precipitation (MICP): a review about mineralization mechanism, factors, and soil properties, Arabian Journal of Geosciences 15 (2022). https://doi.org/10.1007/S12517-022-10012-W.

[131] F. Hammes, W. Verstraete*, Key roles of pH and calcium metabolism in microbial carbonate precipitation, Rev Environ Sci Biotechnol 1 (2002) 3–7. https://doi.org/10.1023/A:1015135629155.

[132] C. Feng, B. Cui, Y. Huang, H. Guo, W. Zhang, J. Zhu, Enhancement technologies of recycled aggregate – Enhancement mechanism, influencing factors, improvement effects, technical difficulties, life cycle assessment, Constr Build Mater 317 (2022) 126168. https://doi.org/10.1016/j.conbuildmat.2021.126168.

[133] A. Bandyopadhyay, A. Saha, D. Ghosh, B. Dam, A.K. Samanta, S. Dutta, Microbial repairing of concrete & its role in CO2 sequestration: a critical review, Beni Suef Univ J Basic Appl Sci 12 (2023) 7. https://doi.org/10.1186/s43088-023-00344-1.

[134] Y. Zhao, L. Peng, W. Zeng, C. sun Poon, Z. Lu, Improvement in properties of concrete with modified RCA by microbial induced carbonate precipitation, Cem

Concr Compos 124 (2021) 104251. https://doi.org/10.1016/j.cemconcomp.2021.104251.

[135] F.G. Priest, Biological control of mosquitoes and other biting flies by Bacillus sphaericus and Bacillus thuringiensis, Journal of Applied Bacteriology 72 (1992) 357–369. https://doi.org/10.1111/j.1365-2672.1992.tb01847.x.

[136] Y.Ç. Erşan, E. Hernandez-Sanabria, N. Boon, N. de Belie, Enhanced crack closure performance of microbial mortar through nitrate reduction, Cem Concr Compos 70 (2016) 159–170. https://doi.org/10.1016/j.cemconcomp.2016.04.001.

[137] E.Jr. Kavazanjian, I. Karatas, Microbiological Improvement of the Physical Properties of Soil, in: International Conference on Case Histories in Geotechnical Engineering. 1, 2008.

[138] Y.Ç. Erşan, N. de Belie, N. Boon, Microbially induced CaCO3 precipitation through denitrification: An optimization study in minimal nutrient environment, Biochem Eng J 101 (2015) 108–118. https://doi.org/10.1016/j.bej.2015.05.006.

[139] C. Feng, B. Cui, H. Ge, Y. Huang, W. Zhang, J. Zhu, Reinforcement of Recycled Aggregate by Microbial-Induced Mineralization and Deposition of Calcium Carbonate—Influencing Factors, Mechanism and Effect of Reinforcement, Crystals (Basel) 11 (2021) 887. https://doi.org/10.3390/cryst11080887.

[140] W. Zeng, Y. Zhao, C.S. Poon, Z. Feng, Z. Lu, S.P. Shah, Using microbial carbonate precipitation to improve the properties of recycled aggregate, Constr Build Mater 228 (2019) 116743. https://doi.org/10.1016/j.conbuildmat.2019.116743.

[141] L.P. Singh, V. Bisht, M.S. Aswathy, L. Chaurasia, S. Gupta, Studies on performance enhancement of recycled aggregate by incorporating bio and nano materials, Constr Build Mater 181 (2018) 217–226. https://doi.org/10.1016/j.conbuildmat.2018.05.248.

[142] W. De Muynck, K. Cox, N. De Belie, W. Verstraete, Bacterial carbonate precipitation as an alternative surface treatment for concrete, Constr Build Mater 22 (2008) 875–885. https://doi.org/10.1016/j.conbuildmat.2006.12.011.

[143] B. Vandevyvere, S. Vanhessche, Improving the quality of recycled aggregates by biodeposition of CaCO3 in the pore structure, Master of Science, Ghent University, 2016.

[144] Y. Zhu, Q. Li, P. Xu, X. Wang, S. Kou, Properties of Concrete Prepared with Recycled Aggregates Treated by Bio-Deposition Adding Oxygen Release Compound, Materials 12 (2019) 2147. https://doi.org/10.3390/ma12132147.

[145] Z. Feng, Y. Zhao, W. Zeng, Z. Lu, S.P. Shah, Using microbial carbonate precipitation to improve the properties of recycled fine aggregate and mortar, Constr Build Mater 230 (2020) 116949. https://doi.org/10.1016/j.conbuildmat.2019.116949.

[146] M. Sonmez, H. Ilcan, B. Dundar, G. Yildirim, Y.C. Ersan, M. Sahmaran, The effect of chemical- versus microbial-induced calcium carbonate mineralization on the enhancement of fine recycled concrete aggregate: A comparative study, Journal of Building Engineering 44 (2021) 103316. https://doi.org/10.1016/j.jobe.2021.103316.

[147] Z. Zhao, S. Remond, D. Damidot, W. Xu, Influence of fine recycled concrete aggregates on the properties of mortars, Constr Build Mater 81 (2015) 179–186. https://doi.org/10.1016/j.conbuildmat.2015.02.037.

[148] Y. Liu, J.-H. Tay, State of the art of biogranulation technology for wastewater treatment, Biotechnol Adv 22 (2004) 533–563. https://doi.org/10.1016/j.biotechadv.2004.05.001.

[149] Aydilek, A.H., 2015. Environmental suitability of recycled concrete aggregate in highways (Report No. MD-15- SP109B4G-2). Maryland State Highway Administration, Baltimore, MD.

[150] N. Gupta, M. Kluge, P.A. Chadik, T.G. Townsend, Recycled concrete aggregate as road base: Leaching constituents and neutralization by soil Interactions and dilution, Waste Management 72 (2018) 354–361. https://doi.org/10.1016/j.wasman.2017.11.018.

[151] W.-S. Ng, M.-L. Lee, S.-L. Hii, An Overview of the Factors Affecting Microbial-Induced Calcite Precipitation and its Potential Application in Soil Improvement, International Journal of Civil and Environmental Engineering 6 (2012) 188–194. https://doi.org/10.5281/ZENODO.1084674.

[152] S. Stocks-Fischer, J.K. Galinat, S.S. Bang, Microbiological precipitation of CaCO3, Soil Biol Biochem 31 (1999) 1563–1571. https://doi.org/10.1016/S0038-0717(99)00082-6.

[153] R.B. Baird, A.D. Eaton, E.W. Rice, Standard Methods for the Examination of Water and Wastewater, American Public Health Association, American Water Works Association, Water Environment Federation, Washington D.C. (2017).

[154] A. Djerbi Tegguer, Determining the water absorption of recycled aggregates utilizing hydrostatic weighing approach, Constr Build Mater 27 (2012) 112–116. https://doi.org/10.1016/j.conbuildmat.2011.08.018.

[155] R.L.S. Ferreira, M.A.S. Anjos, A.K.C. Nóbrega, J.E.S. Pereira, E.F. Ledesma, The role of powder content of the recycled aggregates of CDW in the behaviour of rendering mortars, Constr Build Mater 208 (2019) 601–612. https://doi.org/10.1016/j.conbuildmat.2019.03.058.

[156] P.O. Awoyera, A. Adesina, R. Gobinath, Role of recycling fine materials as filler for improving performance of concrete - a review, Australian Journal of Civil Engineering 17 (2019) 85–95. https://doi.org/10.1080/14488353.2019.1626692.

[157] Z. Ma, W. Li, H. Wu, C. Cao, Chloride permeability of concrete mixed with activity recycled powder obtained from C&D waste, Constr Build Mater 199 (2019) 652–663. https://doi.org/10.1016/j.conbuildmat.2018.12.065.

[158] P. Ren, B. Li, J.-G. Yu, T.-C. Ling, Utilization of recycled concrete fines and powders to produce alkali-activated slag concrete blocks, J Clean Prod 267 (2020) 122115. https://doi.org/10.1016/j.jclepro.2020.122115.

[159] J. Xiao, Z. Ma, T. Sui, A. Akbarnezhad, Z. Duan, Mechanical properties of concrete mixed with recycled powder produced from construction and demolition waste, J Clean Prod 188 (2018) 720–731. https://doi.org/10.1016/j.jclepro.2018.03.277.

[160] BS 8007 Design of concrete structures for retaining aqueous liquid, British Standards Institution, London, 1987.

[161] P. Plaza, I.F. Sáez del Bosque, J. Sánchez, C. Medina, Recycled Eco-Concretes Containing Fine and/or Coarse Concrete Aggregates. Mechanical Performance, Applied Sciences 14 (2024) 3995. https://doi.org/10.3390/app14103995.

[162] C. Vintimilla, M. Etxeberria, Limiting the maximum fine and coarse recycled aggregates-Type A used in structural concrete, Constr Build Mater 380 (2023) 131273. https://doi.org/10.1016/j.conbuildmat.2023.131273.

[163] A.S. Fouladi, A. Arulrajah, J. Chu, S. Horpibulsuk, Application of Microbially Induced Calcite Precipitation (MICP) technology in construction materials: A comprehensive review of waste stream contributions, Constr Build Mater 388 (2023) 131546. https://doi.org/10.1016/j.conbuildmat.2023.131546.

[164] B. Ahring, I. Angelidaki, Thermophilic anaerobic digestion of livestock waste:the effect of ammonia, Applied Microbiology and Biotechnology 38 (1993) 560–564. https://doi.org/10.1007/BF00242955.

[165] K.H. Hansen, I. Angelidaki, B.K. Ahring, ANAEROBIC DIGESTION OF SWINE MANURE: INHIBITION BY AMMONIA, Water Res 32 (1998) 5–12. https://doi.org/10.1016/S0043-1354(97)00201-7.

[166] M.J. Cuetos, X. Gómez, M. Otero, A. Morán, Anaerobic digestion of solid slaughterhouse waste (SHW) at laboratory scale: Influence of co-digestion with the organic fraction of municipal solid waste (OFMSW), Biochem Eng J 40 (2008) 99–106. https://doi.org/10.1016/j.bej.2007.11.019.

[167] D.J. Tobler, M.O. Cuthbert, R.B. Greswell, M.S. Riley, J.C. Renshaw, S. Handley-Sidhu, V.R. Phoenix, Comparison of rates of ureolysis between Sporosarcina pasteurii and an indigenous groundwater community under conditions required to precipitate large volumes of calcite, Geochim Cosmochim Acta 75 (2011) 3290–3301. https://doi.org/10.1016/j.gca.2011.03.023.

[168] K. Wen, Y. Li, F. Amini, L. Li, Impact of bacteria and urease concentration on precipitation kinetics and crystal morphology of calcium carbonate, Acta Geotech 15 (2020) 17–27. https://doi.org/10.1007/s11440-019-00899-3.

[169] J. Ouyang, K. Liu, D. Sun, W. Xu, A. Wang, R. Ma, A focus on Ca2+ supply in microbial induced carbonate precipitation and its effect on recycled aggregate, Journal of Building Engineering 51 (2022) 104334. https://doi.org/10.1016/j.jobe.2022.104334.

[170] Q. Chunxiang, W. Jianyun, W. Ruixing, C. Liang, Corrosion protection of cement-based building materials by surface deposition of CaCO3 by Bacillus pasteurii,

Materials Science and Engineering: C 29 (2009) 1273–1280. https://doi.org/10.1016/j.msec.2008.10.025.

[171] X. Zhu, J. Wang, N. De Belie, N. Boon, Complementing urea hydrolysis and nitrate reduction for improved microbially induced calcium carbonate precipitation, Appl Microbiol Biotechnol 103 (2019) 8825–8838. https://doi.org/10.1007/s00253-019-10128-2.

[172] D.C. Tompkins, D.I. Stewart, J.T. Graham, I.T. Burke, In situ disposal of crushed concrete waste as void fill material at UK nuclear sites: Leaching behavior and effect of pH on trace element release, Journal of Hazardous Materials Advances 5 (2022) 100043. https://doi.org/10.1016/J.HAZADV.2021.100043.

[173] C.J. Engelsen, H.A. van der Sloot, G. Petkovic, Long-term leaching from recycled concrete aggregates applied as sub-base material in road construction, Science of The Total Environment 587–588 (2017) 94–101. https://doi.org/10.1016/j.scitotenv.2017.02.052.

[174] C.R. Wu, Y.G. Zhu, X.T. Zhang, S.C. Kou, Improving the properties of recycled concrete aggregate with bio-deposition approach, Cem Concr Compos 94 (2018) 248–254. https://doi.org/10.1016/J.CEMCONCOMP.2018.09.012.

[175] Y. Gong, P. Chen, Y. Lin, Y. Wan, L. Zhang, T. Meng, Improvement of recycled aggregate properties through a combined method of mechanical grinding and microbial-induced carbonate precipitation, Constr Build Mater 342 (2022) 128093. https://doi.org/10.1016/j.conbuildmat.2022.128093.

[176] Y.Ç. Erşan, Y. Akın, Optimizing nutrient content of microbial self-healing concrete, 6th International Symposium on Life-Cycle Civil Engineering, (IALCCE) (2019) 2241–2246.

[177] M. Sonmez, Y.Ç. Erşan, Production and compatibility assessment of denitrifying biogranules tailored for self-healing concrete applications, Cem Concr Compos 126 (2022) 104344. https://doi.org/10.1016/j.cemconcomp.2021.104344.

[178] A. Derakhshani, A. Ghadi, S.E. Vahdat, Study of the effect of calcium nitrate, calcium formate, triethanolamine, and triisopropanolamine on compressive strength of Portland-pozzolana cement, Case Studies in Construction Materials 18 (2023) e01799. https://doi.org/10.1016/j.cscm.2022.e01799.

[179] A. López-Uceda, J. Ayuso, M. López, J. Jimenez, F. Agrela, M. Sierra, Properties of Non-Structural Concrete Made with Mixed Recycled Aggregates and Low Cement Content, Materials 9 (2016) 74. https://doi.org/10.3390/ma9020074.

[180] Y. Sun, K. Liu, D. Sun, N. Jiang, W. Xu, A. Wang, Evaluation of urea hydrolysis for MICP technique applied in recycled aggregate: Concentration of urea and bacterial spores, Constr Build Mater 419 (2024) 135366. https://doi.org/10.1016/j.conbuildmat.2024.135366.

[181] Y.C. Ersan, Microbial nitrate reduction induced autonomous self-healing in concrete, PhD thesis, Ghent University, 2016.

[182] Z. Tian, X. Tang, Z. Xiu, H. Zhou, Z. Xue, The mechanical properties improvement of environmentally friendly fly ash-based geopolymer mortar using bio-mineralization, J Clean Prod 332 (2022) 130020. https://doi.org/10.1016/j.jclepro.2021.130020.

[183] G. Xu, Y. Tang, J. Lian, Y. Yan, D. Fu, Mineralization Process of Biocemented Sand and Impact of Bacteria and Calcium Ions Concentrations on Crystal Morphology, Advances in Materials Science and Engineering 2017 (2017) 1–13. https://doi.org/10.1155/2017/5301385.

ANNEX

ANNEX 1 – Calibration Curve and Calibration Standards

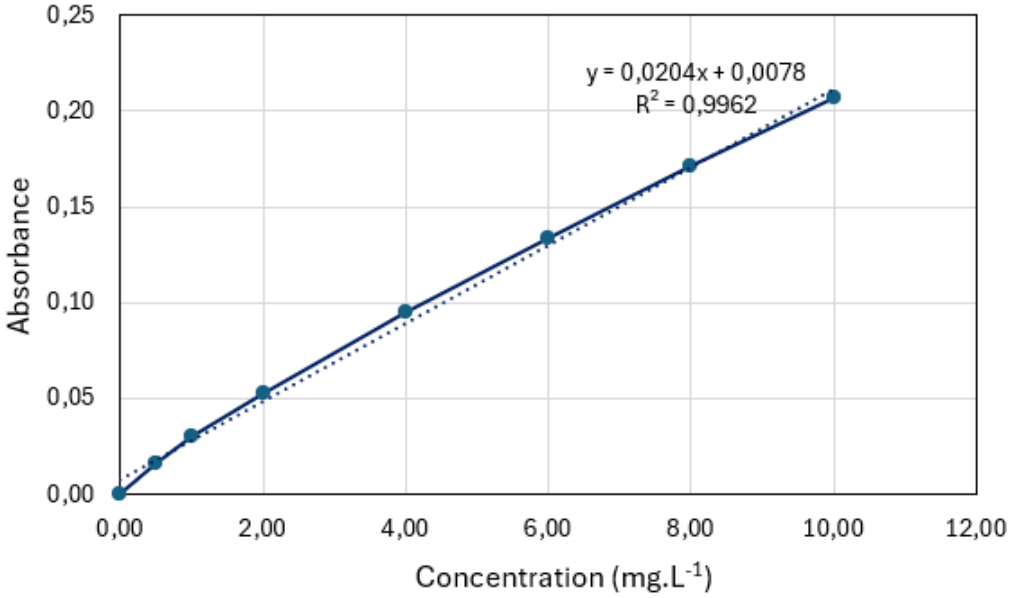

Figure Annex-1.1. Calibration curve of dissolved calcium analysis

Table Annex-1.1. Calibration standards of dissolved calcium analysis

Standards	**Absorbance**	**Entered Conc.(mg.L^{-1})**	**Calculated Conc.(mg.L^{-1})**
Calib Blank	0.000	0.0	-0.369
Calib Std 1	0.016	0.5	0.411
Calib Std 2	0.030	1.0	1.075
Calib Std 3	0.053	2.0	2.208
Calib Std 4	0.095	4.0	4.263
Calib Std 5	0.134	6.0	6.164
Calib Std 6	0.171	8.0	7.982
Calib Std 7	0.207	10.0	9.766

ANNEX 2 –Purity Regression of c-fRCA by FTIR

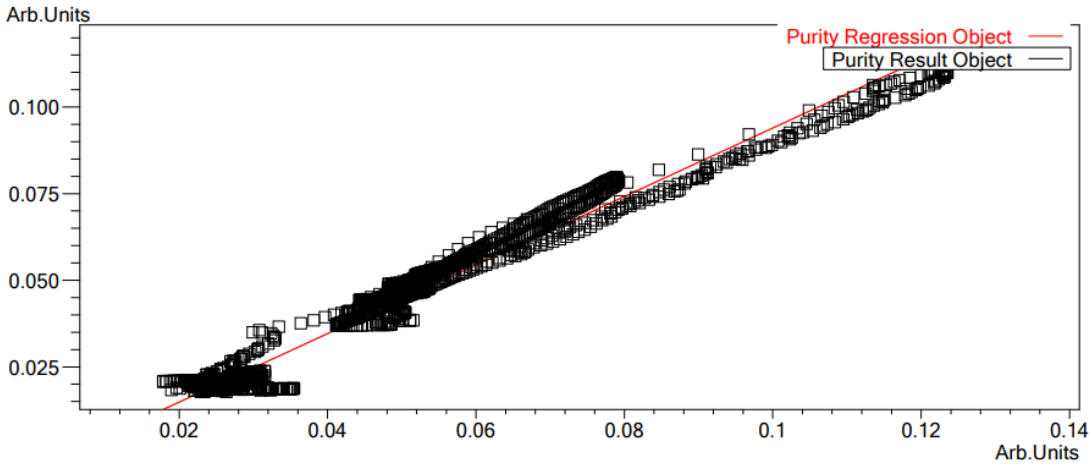

Purity index for abiotic vs. untreated

Date: 2024-04-05
Time: 12:22:09
Username: System Administrator

Normalization: None
Peak purity: Correlation
Threshold: 0.000000

Smooth: No smoothing
Purity index: 0.9905

Slope: 0.9916
Intercept: -0.0052

Figure Annex-2.1. Purity regression comparison between abiotic control treated c-fRCA and untreated c-fRCA

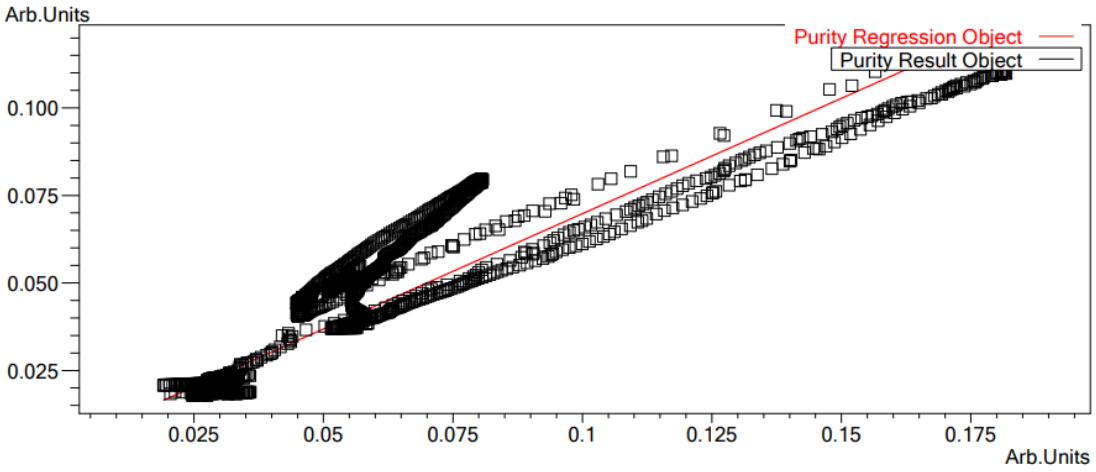

Purity index for treated vs. untreated

Date: 2024-04-05
Time: 11:50:28
Username: System Administrator

Normalization: None
Peak purity: Correlation
Threshold: 0.000000

Smooth: No smoothing
Purity index: 0.9497

Slope: 0.6764
Intercept: 0.0036

Figure Annex-2.2. Purity regression comparison between microbially treated c-fRCA and untreated c-fRCA

ANNEX 3 –Published Conference Paper Derived from Thesis

E. Arıkan et al. , "Improvement of fine recycled aggregates by microbially induced CaCO3 precipitation," *6th Eurasia Waste Management Symposium*, vol.1, İstanbul, Turkey, pp.606-613, 2022.